Neural Prosthetic Advancement: identification of circuitry in the Posterior Parietal Cortex

ALESSIA CACACE

Neural Prosthetic Advancement: identification of circuitry in the Posterior Parietal Cortex

Alessia Cacace, BSc. MSc.

Thesis submitted for the Degree of Doctor of Philosophy

Department of Psychology

Durham University

September 2019

Abstract

There are limited options for rehabilitation following an established Spinal Cord Injury (SCI) resulting in paralysis. For most of the individuals affected, SCI means a lifetime of confinement to a wheelchair and overall reduced independence.

Brain-Computer and Brain-Machine Interface (BCI and BMI) techniques may be of aid when used for assistive purposes. However, these techniques are still far from being implemented in daily rehabilitative practice.

Existing literature on the use of BCI and BMI techniques in SCI is limited and focuses on the extraction of motor control signals from the primary motor cortex (M1). However, evidence suggests that in long-term established SCI the functional activation of motor and premotor areas tends to decrease over time.

In the present project, we explore the possibility of successful implementation of assistive BCI and BMI systems using posterior parietal areas as extraction sites of motor control activity.

Firstly, we will investigate the representation of space in the posterior parietal cortex (PPC) and whether evidence of body-centered reference frames can be found in healthy individuals.

We will then proceed to extract information regarding the residual level of motor imagery activity in individuals suffering from long-term and high-level SCI. Our aim is to ascertain whether functional activation of motor and posterior areas is comparable to that of matched controls.

Finally, we will present work that was done in collaboration with the Netherlands Organisation for Applied Scientific Research that can offer an example of successful application of a BCI technique for rehabilitation purposes.

Index

List of Figures

Statement of Copyright and Declaration

I confirm that no part of the material presented in this thesis has previously been submitted by me for a degree in this or in any other institution. If material has been generated through joint work, this has been indicated where appropriate. All other sources have been referenced, and quotations suitably indicated.

Alessia Cacace

September 2019

This project was part of the European PACE innovative training network and all funding was provided under the European Union's Horizon 2020 research and innovation programme under the Marie Sklodowska-Curie grant agreement No 642961.

Publication Note

Chapter 1: the experiment reported was presented at the ESOF satellite event 2016.

Chapter 3: the experiment reported was presented at the Society for Neuroscience 2018 and included in the Neuroscience 2018 Hot Topics book.

Chapter 4: Brouwer, A. M., van der Waa, J. S., Hogervorst, M. A., Cacace, A., & Stokking, H. (2017, March). A feasible bci in real life: using predicted head rotation to improve hmd imaging. In Proceedings of the 2017 ACM Workshop on An Application-oriented Approach to BCI out of the laboratory (pp. 35-38). ACM.

Acknowledgements

I would like to give a special thanks to the current and past members of the supervisory team. Dr Jason Connolly, Dr Maria Olkkonen and Dr Lore Thaler for their help, support, time and energy. A special mention to Maria for her continuous professional guidance and emotional encouragement. Prof Charlie Heywood for teaching me how to be efficient yet compassionate. Prof Bob Kentridge for the great technical support over the years. And finally, Dr Cristiana Cavina-Pratesi for her infectious dedication and resilience who motivated me to take on this journey and continue it to the best of my abilities in her absence.

Thanks to all the amazing people from the Spinal Cord Injury Unit at the James Cook University Hospital for collaborating with me in this journey. Your dedication to help, your resilience and outlook on life will be impossible to forget and have changed me forever.

To the staff at the James Cook University Hospital, Julie, Roger, and Emmanuel especially, thank you for your assistance, knowledge, support and overall amazing personalities. Your hard work was invaluable to this project and myself.

To the technical team at Durham University, Elaine, Andy and Simon, who were able to make sense of my often confused diagrams and ideas and make them into software and hardware of the highest standards.

To all my fellow Ph.D. students from Durham University and the PACE European Network, this was very much a team effort and it would not have been as enjoyable without you. Simone, Becca, Alix, Jacob, thank you for your invaluable friendship.

To my family and friends, thanks for remaining an enthusiastic part of my life despite the distance.

To Indy, thanks for brightening up my days, everyday.

1 Introduction

The present review will investigate the possibility of introducing Brain-Computer and Brain-Machine Interface (BCI and BMI) techniques in the rehabilitation of paralysis following Spinal Cord Injury (SCI). We will focus on the assistive application of these techniques and the way they can contribute to improve the overall quality of life as perceived directly by the affected individuals.

Spinal Cord Injury (SCI) is a condition that arises as a result of damage to constitutive parts of the spinal cord (such as blood vessels, bone tissues and bone marrow) injuring both the central and peripheral nervous system. Such injury is considered irreversible at the time of writing (Schwab, 2002; Schwab and Bartoldi, 1996; Bradbury and McMahon, 2006). Incidence of SCI varies greatly worldwide, however literature reports as many as 755 incidences per million people on average (Wynadaele and Wynadaele, 2006), a number that is growing proportionally as survival rates increase (Strauss, Devivo, Paculdo, Shavelle, 2006). SCI appears to be four times more prevalent in males than females, and it can occur at any stage in life (<1 to ≥75 years of age), with an overall average age of 31.5 years old although the highest occurrence is in the age range 15-25 (Bracken, Freeman and Hellenbrand, 1981; McDonald and Sadowsky, 2002; Craig and Middleton, 2009).

The main identified causes of registered SCI are falls, accidental traumatic injuries (most commonly transport- and sport-related), and violent traumatic injuries such as gunshot and knife wounds (Ho, Wuermeser, Priebe, Chiodo, Scleza and Kirshblum, 2007; Craig and Middleton, 2009; O'Connor, 2006). According to a report published by the National Health Trust (NHS Commissioning Board, 2013), incidence in the U.K. is estimated at 12-16 per million of the population with a wide age range from

infant to elder. The leading cause of injury remains accidental trauma through falls (41.7%) and road traffic accidents (36.8%). Mortality rates immediately following SCI have decreased greatly in the last 20 years but are still dependent on prompt access to acute care (De Vivo, Krause and Lammertse, 1999; De Vivo, 1997). Upon admission to hospital, it is crucial that the injury is stabilised to minimise the risk of secondary injury and spinal shock, which can drastically diminish the chances of recovery (McDonald and Sadowsky, 2002). Once the individual is stable, standard medical procedure requires assessment of the residual motor control, sensitivity and function of the autonomic system, usually followed by specific imaging diagnostic tests to identify the location and presentation of the injury (McDonald and Sadowsky, 2002).

Classification of SCI can be quite difficult due to the traumatic nature of the injury, which results in high variability in the presentation of the condition. Nonetheless, SCIs are usually classified according to the location and severity of the injury. Proceeding caudally from the head, Cervical (C), Thoracic (T), Lumbar (L), and Sacral (S) identify the main affected area along the spine. If possible, the number of the injured vertebra/ae is also given. These are eight for the cervical, 12 for thoracic, five for lumbar and four for the sacral area. Finally, a five-level scale, the ASIA Impairment Classification, is used to assess the severity of the injury, severity here being determined by the residual connections between the tissues of the spinal cord. The ASIA score is usually proportional to the residual sensorimotor function of the affected individual and with a higher score usually representing more severe loss of sensorimotor control. Specifically, individuals are scored from A to E with the following meaning: A (*complete*), a complete loss of both motor and sensory function below the level of the injury; B (*incomplete*), motor but not sensory functions are lost below the level of the injury; C (*incomplete*), sensorimotor functions are preserved for the most part however

muscle voluntary control is severely impaired; D (*incomplete*), sensorimotor functions are preserved and muscle voluntary control is mildly impaired; E (*normal*), sensorimotor control below the injury is not affected (Maynard, Bracken, Creasey, Ditunno, Donovan, et al., 1997). Each of these classifiers will usually give a comprehensive indication on the level of sensorimotor control the individual will retain. Complete injuries of the cervical area will likely affect control over all limbs and areas of the body located below the injury, whereas the same complete injury at the sacral level might have little effect on motor control. Similarly, a complete injury of the same vertebra will have drastically different effects than an incomplete one, with complete injury bearing the highest negative impact on sensorimotor control (Maynard, Bracken, Creasey, Ditunno, Donovan, et al., 1997; McDonald and Sadowsky, 2002; Marino, Barros, Biering-Sorensen, Burns, Donovan, et al., 2002). The ASIA classification is also usually paired with a further diagnosis identifying the level and area of paralysis and distinguishing between Quadriplegia (or Tetraplegia) and Paraplegia. Quadriplegia refers to the loss of sensorimotor control of all four limbs and is usually the result of a high-level cervical SCI (commonly C4). Paraplegia occurs when the individual experiences loss of control of the lower limbs exclusively, usually following damage to lower-level SCI located on the thoracic or lumbar area of the spine (Marino et al., 2002; Kirshblum, Burns, Biering-Sorensen, Donovan, Graves, Jha et al., 2011).

During the initial acute state, spinal injuries will usually undergo a period of recovery and reorganisation that can last from at least six months to several years. Individuals may regain some of the lost sensorimotor functions, although this is less likely in the case of complete or ASIA-A lesions where the chances of spontaneous recovery are estimated at just 3% (Waters, Adkins, Yakura and Sie, 1994; McDonald and Sadowsky, 2002). Following this adjustment period, the lesion should stabilise and its

presentation will likely remain unaltered through the years. For those individuals who sustained an injury resulting in paraplegia or quadriplegia, this often means confinement to a wheelchair, severe loss of independence and a general drop in overall perceived quality of life (Kennedy, Lude and Taylor, 2005). This will likely have a substantial psychological impact on the affected individual, and related research reports prevalence of symptomatology consistent with anxiety and depression that are persistent and long-term (Kennedy and Rogers, 2000; Fuhrer, Rintala, Hart, Clearman and Young, 1993). Furthermore, the perceived lower level of control and independence following SCI has been correlated to lower self-reported levels of quality of life as well as a general tendency to withdraw from the community and one's social life which are normally identified as protective factors (Schulz and Decker, 1985). Individuals who experience psychological distress after a diagnosis of SCI have identified the severity of the injury and related loss of independence as key factors contributing to their will to withdraw, and that withdrawal correlates generally to more negative outcomes in recovery and in life (Tate, Forchheimer, Maynard and Dijkers, 1994; Bonanno, Kennedy, Galatzer-Levy, Lude and Elfstrom, 2012; Takiemski, Bergstrom, Savic and Gardner, 2000).

Based on literature reports, the lifetime cost of treating an SCI will vary on average between £2 million and £4 million (NHS England, 2013; Cao, Chen and DeVivo, 2011; McDonald and Sadowsky, 2002; Ma, Chan and Carruthers, 2014; DeVivo, 1997). This will depend on the severity of the injury and the prevalence of the condition with complete tetraplegia accounting for the highest societal and individual costs (Johnson, Brooks and Whiteneck, 1996).

Although the traumatic aspect of the aetiology of SCI suggests preventive measures should be a focal point of research and scientific debate (Cripps, Lee, Wing, Werts, Mackay et al., 2011; McDonald and Sadowsky, 2002; Wyndaele and Wyndaele, 2006), the lack of restorative options for those who have already acquired an injury means novel assistive techniques should also continue to be investigated.

Rehabilitation practice following an established SCI (i.e. an SCI that is no longer in its acute state) focuses on implementing a number of environmental adjustments and physical therapy necessary to help maintain and, where possible, improve the overall health of the individuals affected by paralysis to the point of ultimately returning the patients to the community (Behrman, Bowden and Nair, 2006; Burns and Ditunno, 2001). Although any rehabilitation plan should be tailored individually to the specific presentation of each case, assistive techniques are based on the common factor that neural pathways above and below the injury are mostly intact and can therefore still be of use. Examples include early implementation of neuroplasticity or locomotor training using treadmills such as Body Weight-Supported treadmill training (BWSTT), which has been consistently reported to improve muscle tone, minimise bone loss and promote adaptive plasticity of the spinal tissue to improve or even restore walking ability in lower-level, incomplete SCIs (ASIA C or D) (Dobkin, Barbeau, Deforge, Ditunno, Elashoff et al., 2007; Giangregorio and McCartney, 2006; Harkema, 2001; Burns and Dituno, 2001; Harkema, Schmidt-Read, Lorenz, Edgerton and Behrman, 2012). Functional Neuromuscular Stimulation (FNS) and Functional Electric Stimulation (FES) have been successful in partly restoring walking ability in low-level, incomplete SCI and grasp control in low-level incomplete cervical injuries (Chae, Kilgore, Triolo and Creasey, 2000; Burns and Ditunno, 2001; Yarkony, Roth, Cybulski and Jaeger, 1992). These techniques involve inducing electrical current to the motor neurons of paralysed

muscles either externally (through patches placed on the skin) or internally (through muscle implants) that will mimic or enhance existing muscle contraction observed when walking or grasping (Burns and Ditunno, 2001; Hamid and Hayek, 2008). The current in both FES and FNS, however, is externally generated and therefore does not provide individuals with the ability to directly control the movement. Pain resulting from the electrical stimulation as well as muscle fatigue incurring after prolonged used are additional factors limiting the effective application of these techniques in rehabilitative practice (Yarkony, Roth, Cybulski and Jaeger, 1992; Graupe and Kohn, 1997; Ragnarsson, 2008). The surgical transfer of intact tendons to areas only partially affected by SCI is another option aiming to restore hand and arm control, however again this technique has been shown to work best on low-level and incomplete SCI (Keith, Kilgore, Peckham, Wuolle, Creasey et al., 1996; Freehafer, Kelly and Peckham, 1984; Freehafer, 1991). Options in common rehabilitative practice for C4 injuries and above, and complete injuries overall, are quite limited to this date and do not offer the possibility of actually restoring voluntary motor control.

In the last few decades, rehabilitation of motor disabilities has explored the implementation of techniques that are able to enhance or redirect brain activity in an attempt to assist individuals in regaining control over voluntary movement. Brain-Computer Interface (BCI) and Brain-Machine Interface (BMI) techniques share the common basic principle of connecting the brain to an external device that gives the individual the ability to control and act in the surrounding environment through said assistive device in place of the brain's standard neural pathways (Wolpaw, Birbaumer, Heetderks, McFarland, Peckham et al., 2000). Typically, both systems make use of three main components: a sensor to record brain signals; a translator to convert brain activity into signal for the actuator; and the actuator or output device which carries out the

specified action (Hochberg and Donoghue, 2006). Although the terms BCI and BMI are at times used interchangeably, BCI systems are usually those involving the use of a computer as the actuator and work by recording whole brain activity by using more diffuse (i.e., extracting information from a larger portion of, or the whole, brain as compared to more localised acquisition methods used in BMI systems) and non-invasive recording devices such as Electroencephalograms (EEG). Previous research in the application of EEG-based BCI has successfully applied the detection of a number of brain potentials to produce on-screen spellers, drive wheelchairs and control specialised computer software in both a rehabilitation setting and a more commercial approach oriented to enhance the user's performance and/or experience in motor- and neurologically-intact individuals (Zhang, Wang and Fuhlbrigge, 2010; Huang, Yu, Wang, Zhao, Liu et al., 2014; Vuorvopoulos and Liarokapis, 2014). Most commonly, BCI systems make use of P300 waves (Mak, McFarland, Vaughan, McCane, Tsui et al., 2012; Sellers and Donchin, 2006), Steady-State Visual Evoked Potentials (Ortner, Allison, Korisek, Gaggl and Pfurtscheller, 2011), motor imagery (Pfurtscheller, Solis-Escalante, Ortner, Linortner and Muller-Putz, 2010) or combinations of these (Panicker, Puthusserypady and Sun, 2011; Pfurtscheller, Allison, Brunner, Bauernfeind, Solis-Escalante et al., 2010).

BMI systems, on the other hand, are commonly comprised of mechanic actuators such as motorised wheelchairs, prosthetic limbs or robotic devices and thus require a much more focal brain signal. This is usually acquired through microelectrode arrays implanted on the cortical surface (electrocorticography, ECoG) or deeper within the cortex and in direct proximity of a specific target area by acquiring local field potentials and even single cell recordings (Principe and McFarland, 2008; Hochberg and Donoghue, 2006). BMI are commonly employed in occupational therapy settings for

promoting motor rehabilitation after stroke (Ramos-Murguialday, Broetz, Rea, Laer, Yilmaz et al., 2013), amyotrophic lateral sclerosis (Chaudhary, Birbaumer and Curado, 2015), Parkinson's disease (Follett, 2000) and in sensory rehabilitation such as in auditory rehabilitation through cochlear prosthetics (Loeb, 1990; Merzenich, 1983). Restoring motor control after paralysis has also been achieved in laboratory settings and in a selected number of participants through controlling prosthetic arms (Schmidt, 1980; Hochberg, Serruya, Friehs, Mukand, Saleh et al., 2006; Wodlinger, Downey, Tyler-Kebara, Schwartz, Boninger and Collinger, 2014), and even a full ambulatory exoskeleton (Lopez-Lorraz, Trincado-Alonso, Rajasekaran, Perez-Nombela et al., 2016; Li, He, Yang, Qiu, Zhang et al., 2016).

Following this specific nomenclature, BCI refers to a system that records brain activity from the scalp, and therefore often implies a less invasive approach. However, this feature comes with a direct loss of specificity of the brain signal acquired, as also reflected by the small signal-to-noise ratios observed (Wolpaw, Birbaumer, Heetderks, McFarland, Peckham et al., 2000; Vaughan, Heetderks, Trejo, Rymer, Weinrich, et al., 2003). Signal-to-noise ratio (SNR) represents the amount of actual specific brain activity captured by the device over the accidental intrusion of external signals originating from the surrounding environment, but also internal signals originating from the user's brain but not related to the BCI task (Wolpaw et al., 2000). Low SNR also influences the choice of actuator that can be effectively linked to a BCI system, most commonly restricted to cursor control or target selection on a computer screen, resulting in a direct limitation on what the user can achieve in terms of environmental interaction and movement restoration (Principe and McFarland, 2008; McFarland and Wolpaw, 2008). Information Transfer Rate (ITR), defined as the amount of brain signal transferred per unit of time, is also generally lower in non-invasive compared to invasive applications (Wolpaw et

al., 2000; Baranauskas, 2014). In BCI techniques, brain signal has to travel through several layers of tissue including cerebrospinal fluid, skull and scalp before being captured by an externally located electrode (Hochberg and Donoghue, 2006). This not only results in a signal of relatively lower quality but it also renders the technique much slower than invasive applications, with delays between motor command initiation and actual action performance estimated to range between 2-4 seconds versus near-immediate responses in invasive approaches (Baranauskas, 2014; Waldert, 2016; Lebedev and Nicolesis, 2006; Milan and Carmena, 2010). As a result, although prosthetic control through BCI has been possible (Horki, Solis-Escalante, Neuper and Muller-Putz, 2011; McFarland and Wolpaw, 2008; Wolpaw and McFarland, 2004), the temporal resolution, accuracy, degrees of freedom, and reliability so far achieved are still much lower than that of similar applications with BMI (Schalk, McFarland, Hinterberger, Birbaumer and Wolpaw, 2004; Schwartz, Cui, Weber and Moran, 2006; Hochberg et al., 2006).

By recording directly from the proximity of the target area, brain signal acquired through BMI techniques usually benefits from much cleaner and richer signal that is suitable for controlling actuators that tend to offer higher degrees of freedom and are thus able to closely mimic real voluntary movement (Hochberg et al., 2006). Action-related sensory feedback, necessary for achieving fine movement control, is also currently only achievable through brain implants on the somatosensory cortex (Andersen, Musallam and Pesaran, 2004). Additionally, SNR is higher and an overall better performance in terms of spatial and temporal resolution is reported as compared to the non-invasive BCI approach (Principe and McFarland, 2008; Hochberg and Donoghue, 2006). Moreover, non-invasive BCIs usually require long set-up sessions prior to each use, sustained and undivided attention throughout, and user training that

can be longer than for BMI applications on occasion (e.g., Hochberg and Donoghue, 2006; Waldert, 2016; Thulasidas, Guan and Wu, 2006; Guger, Ramoser and Pfurtscheller, 2000). Training requirements may vary greatly based on the actuator being used with communication restorative systems, such as spellers, usually needing shorter training times as opposed to prosthetic limb control (Azom, Rana and Ahmad, 2013; Allison, Wolpaw and Wolpaw, 2014). Non-invasive, EEG-based BCI systems can reach high accuracy levels with as little as five minutes of training in a non-neurologic population with systems using P300 or SSVEP (Bell, Shenoy, Chalodhorn and Rao, 2008; Guger, Daban, Sellers, Holzner, Krausz et al., 2009; Perez-Marcos, Buitrago and Velasquez, 2011). Motor Imagery detection, most commonly used in prosthetic control, may take as long as several days (Guger et al., 2000).

The nature of the BMI approach, however, involves invasive brain surgery, often on multiple areas of the brain, that exposes the user to a risk of infection, several complications following surgery, and functional reorganisation of the brain that is virtually absent in BCI or non-invasive approaches (Hochberg and Donoghue, 2006). Follow-up surgeries might be needed as signal quality tends to deteriorate over time and the implant's longevity can vary in each individual (Lebedev and Nicolesis, 2006). The related risks are also a substantial limiting factor for the possible application of BMI in more commercially oriented applications as well as a determining factor in user acceptance within the patient population (Waldert, 2016; Blabe, Gilija, Chestek, Shenoy, Anderson and Henderson, 2015). Given the specific advantages and limitations of each technique with regards to temporal and spatial resolution, invasiveness, actuator options and degrees of motor control restoration the scale seems evenly balanced between proceeding with an invasive or a non-invasive course of action to this date: the final determining factor is the user's personal preference and approach to risk

(Hochberg and Donaghue, 2006; Baranauskas, 2014). Reports from individuals suffering from various forms of motor control deficits are quite heterogeneous, although practicality and non-invasiveness are a recurring and often determining factor in choosing an assistive technique, most participants respond favourably to surgical implants especially if those implants are able to significantly improve their ability to control voluntary limb movement (Collinger, Boninger, Bruns, Curley, Wang and Weber, 2013; Simpson, Eng, Hshieh, Wolfe et al., 2012).

In summary, despite the reported interest of potential end-users, BCI and BMI systems are a long way away from being introduced in standard commercial and rehabilitative practice for motor control. Limiting factors common to both approaches include the need for long training sessions, fatigue due to sustained and undivided attention during use, confinement to a laboratory setting, and accuracy and flexibility issues.

However, as previously discussed, these systems are often limited in the degree of movement or communication restoration they can offer as they rely on recognition or oddball detection procedures between a pre-selected array of items presented on a screen. Motor Imagery (MI), the act of mental rehearsal of motor actions, has been successfully used in both invasive and non-invasive BCI and BMI systems and often allows a higher degree of movement control over the selected actuator (Park, Looney, Rehman, Ahrabian and Mandic, 2013). However, training times for these systems are usually longer and vary significantly depending on the individual's MI proficiency from as little as few minutes to several hours or days (Paulraj, Yaacob, Adom and Nagarajan, 2007; Wang, Hong, Gao and Gao, 2007; Ferreira, Celeste, Cheein, Bastos-Filho, Sarcinelli-Filho and Carelli, 2008). Invasive BMI usually requires very little training in achieving initial control over the actuator but perfecting smooth action performance needs

consistent practice (Serruya, Hatsopoulos, Paninski, Fellows and Donoghue, 2002; Patil and Turner, 2008).

EEG-based techniques usually require the user to interact with the actuator through a screen or command console. The related eye and mental fatigue can alter the accuracy and efficacy of BCI and BMI systems, and such fatigue can occur after as little as 30 minutes of use (Roy, Bonnet, Charbonnier and Campagne, 2013; Punsawad and Wongasawat, 2013). Moreover, users have to maintain their attention on the command screen and this is often at the expense of other external activities such as talking, visual exploration of space, or even mental activities that might interfere with signal acquisition through EEG, such as counting (Myrden and Chau, 2015; Sharma, Baron and Rowe, 2009). This suggests that undivided attention should be sustained during the use of non-invasive BCI/BMI systems that might not be feasible in commercial but also long-term medical restorative applications where multitasking might be required.

The majority of both invasive and non-invasive BCI and BMI systems require the presence of trained technicians to supervise the correct set-up, use and function of the technique. The intervention of a carer might also be needed to assist users suffering from motor control deficits in employing the techniques (Anderson, 2004). This has severely restricted the use of BCI/BMI systems outside of the laboratory setting and in everyday use to this date. Moreover, whilst providing adequate training or requiring a third party's assistance might not be a definite limiting factor for BCI/BMI systems destined for commercial use, in the context of restorative practice the need for assistance might substantially impact the user's compliance and reception of the technique (Spataro, Chella, Allison, Giardina, Sorbello et al., 2017).

Accuracy levels appear to vary significantly within the literature and depend highly on the specific recording device, decoding algorithm, extraction technique and

actuator used (Guger, Edlinger, Harkam, Niedermayer and Pfurscheller, 2003). Additionally, a degree of individual variability in accuracy levels is often reported even when the same technique is used, often with little insight on the potential determining factors (Guger et al., 2009; Millan and Carmena, 2010). Typically, however, individuals with no neurologic or motor control deficits perform better and require, on average, less time to successfully employ the systems (Nijboer, Sellers, Mellinger, Jordan, Matuz et al., 2008).

Future research would benefit from investigating ways to maximise training sessions and reduce the overall training time needed in order to facilitate the implementation of BCI and BMI systems to regular commercial and medical practice. Exploration of novel processing algorithms that are able to account for the effects of fatigue and filter through confounding mental processes can counteract the loss of accuracy and efficacy of the system, however user comfort remains an open issue and alternative protective factors should be explored in order for these techniques to be feasibly introduced in day-to-day activities (Sykacek, Stokes, Curran, Gibbs and Pickup, 2003). Exploration of hybrid BCI/BMI systems allowing the user to perform a variety of actions might be preferable to those based solely on visual feedback as these might offer the possibility for more ecological applications (Gergondet, Kheddar, Hintermuller, Guger and Slater, 2012; Jeunet, Vi, Spelmezan, N'Kaoua, Lotte and Subramanian, 2015). Likewise, more simplistic approaches employing systems which require little preparation and set-up procedures, that can be operated by the user alone, regardless of their level of residual motor control, would potentially aid bringing the use of BCI/BMI techniques from a laboratory setting exclusively to home or office environments (Arico, Borghini, Flumeri, Sciaraffa and Babiloni, 2018; Toppi, Borghini, Petti, He, Giusti et al., 2016). Mobile EEG systems as opposed to standard wired ones and their

implementation of BCI techniques in smart-home systems offer one example of a successful trend in related research that can significantly boost the application of these systems in a more ecological and organic setting (De Vos, Kroesen, Emkes and Debener, 2014; Luo, Han and Duan, 2015; Edlinger, Holzner, Guger, Groenegress and Slater, 2009).

As well as improved decoding algorithms as discussed above, accuracy can also be dependent on the recording system and technique used. EEG-based BCI and BMI can achieve higher accuracy levels through EEG systems employing a higher number of active electrodes, however reducing the number of active electrodes can confer benefits in the potential reduction of accidental noise captured by channels irrelevant to the task and maximising user's comfort by employing lighter and more ergonomic systems (Arvaneh, Guan, Ang and Quek, 2011). For invasive applications, accuracy levels are usually higher when employing an array of multiple electrodes as opposed to single electrode-based implants (Baranauskas, 2014; Kennedy, Bakay, Moore, Adams and Goldwaithe, 2000). Most commonly, electrode arrays are implanted in brain areas directly related to movement control, such as the Primary Motor Cortex (M1), giving the user the ability to control prosthetic limbs to perform a desired action (Hochberg et al., 2006; Lebedev and Nicolelis, 2011; Chaudhary, Birbaumer and Curado, 2015). Although invasive approaches carry the highest level of accuracy achievable so far in decoding voluntary movement, the long-term stability of the implants is often under debate. Even when the electrode is successfully implanted and does not incur rejection, the long-term plasticity of the brain as well as the formation of scar tissue around the electrode can hinder their optimal functionality resulting in a decrease in the overall quality of the signal being extracted (Millan and Carmena, 2010; Lebedev and Nicolelis, 2006). Although implants have maintained their optimal efficacy for several years on some

occasions in both human and non-human primates, advancement in the field of biocompatible material, neuro-compatible coatings, and both surgical and post-operative techniques are key to ensure the implant's longevity and minimise the potential health risks associated with such procedures (Lee, Bellamkonda, Sun and Levenston, 2005; Rennaker, Miller, Tang and Wilson, 2007; Schwartz, Lebedev, Hanson, Dimitrov, Lehew et al., 2014). However, a lack of accuracy and functionality of brain implants might not be due to electrode displacement alone. Choosing the most suitable brain area to implant the recording electrode should also be taken into account and most commonly this has been the Primary Motor Cortex (M1) (Carmena, Lebedev, Crist, O'Doherty, Santucci et al., 2003; Nicolesis, Dimitrov, Carmena, Crist, Lehew, et al., 2003; Hochberg et al., 2006). Although certainly the brain area carrying the most detailed and accurate signal pertaining to voluntary movement control, M1 has been shown to display progressively decreasing functional activation in the case of long-term paralysis (Jurkiewicz, Mikulis, Fehlings and Verrier, 2010). Additionally, in the case of motor deficiency due to damage to the brain that includes M1, whether it be traumatic or following spontaneous haemorrhagic events, implants in this area will likely not be a feasible option.

The Posterior Parietal Cortex (PPC) has been successfully used in invasive BMI techniques in non-human primates (Hauschild, Mulliken, Fineman, Loeb and Andersen, 2012; Musallam, Corneil, Greger, Scherberger and Andersen, 2004) and, in only one instance so far, in humans (Aflalo, Kellis, Klaes, Lee, Shi, et al., 2015). Situated between the visual and sensorimotor cortex, the PPC holds the peculiar functional role of integrating both visual and sensorimotor inputs before transmitting information to the premotor and motor cortex (Culham, Cavina-Pratesi and Singhal, 2006). This means not

only that the signal extracted from the PPC carries rich visuomotor information suitable to control BMI actuators, but that it might also incur a lower degree of functional reorganisation following long-term paralysis.

Considering the PPC as an alternative site for the extraction of motor commands able to successfully control different actuators holds great implications for the feasibility of introducing BCI and BMI in standard rehabilitative practice. As previously mentioned, the PPC is not directly or exclusively involved in voluntary motor control, however it is part of a number of processes that take part in the planning of action performance (Cohen and Andersen, 2002).

Specifically, the PPC appears to be involved in the process of coordinate transformation. During the planning of a movement, such as reaching for a specific object, the location in space of reaching targets must be computed and internalised for the action to be effective (Soetching and Flanders, 1992). Moreover, when encoding the location of a target object, neurons must be able to do so with respect to a certain focal point and this could be located internally (within the body) or externally (in the surroundings of the observing individual). This also implies that spatial information gathered from the outside world is combined with proprioceptive information coming from several areas of one's body. In the visual cortex, the visual inputs originating from observing an object that individuals might want to interact with, is encoded with respect to the retina (Boussaoud and Bremmer, 1999).

In the Primary Motor Cortex (M1), space is encoded by using effectors as a reference, meaning the target's location in space is registered by relating it to the body or the reaching effector, such as the dominant hand (Gordon, Ghilardi and Ghez, 1994). For individuals to be able to successfully interact with the outside world, the retina-

centred maps compiled within the visual cortex need to be converted to the body-centred coordinates that are used by the motor cortex.

Although it is believed that the PPC might play a crucial role in this, the specifics of this conversion process remain unclear (Cohen and Andersen, 2002). One suggestion is that the spatial coordinates obtained through the visual cortex are sequentially modulated and shifted from retina-centred to head-centred first and finally shifted to be body- or effector-centred, and the locus of this transformation has been suggested to be the PPC (Jeannerod, 1991; Andersen, 1997). It has also been suggested that the PPC might present a similar spatial organization to that of the visual cortex. Adjacent locations in space are represented in adjacent neurons within the PPC in what is defined as a topographic representation of space (Schluppeck, Glimcher and Heeger, 2005; Konen and Kastner, 2008). Through observation of a visual stimulus, saccade endpoints are also topographically distributed within the resulting spatial maps of the PPC (Sereno et al., 2001).

The mechanism behind the encoding of space within the posterior parietal cortex itself is still under debate and different areas of the body, including retinae, eyes, head and limbs, have been shown to contribute to this spatial mapping to some extent (Andersen and Buneo, 2002; Batista, Buneo, Snyder and Andersen, 1999; Cohen and Andersen, 2002; Duhamel, Bremmer, Hamed and Graf, 1997). In the last three decades, researchers have been trying to identify the respective contributions of different areas of the body that could be used by neurons within the PPC to compute spatial coordinates of spatial locations. The assumption behind the processes of the encoding of space through reference frames is that if a change in the position of one of these areas is observed but the visual stimulus is kept fixed, the resulting spatial maps should also change accordingly (Snyder, Grieve, Brotchie and Andersen, 1998). In other words, if

the PPC was to use eye-centred coordinate frames when encoding for the spatial location of a fixed target object, moving the starting position of the eyes should result in an alteration of the maps obtained from observing the same fixed target whereas changes to another area of the body, such as the head or the dominant hand, should not affect the resulting spatial maps.

Evidence of eye-, gaze-, and head-reference frames has been established within the PPC of human and non-human primates by using the same concept. By modifying the eyes' starting position within the orbits, performance of memory-guided eye movements to the same target locations resulted in changes in the spatial maps obtained within the PPC that were consistent with the change in eye position of macaques (Andersen and Mountcastle, 1982; Andersen, Essik and Siegel, 1985; Bremmer, Thiele, Distler and Hoffmann, 1997). A similar effect has also been identified in humans (e.g., De Souza, Dukelow, Gati, Menon, Andersen and Vilis, 2000). By modifying the visual stimulus but not the position of the eye in the orbits, retina-centred coordinates can also be isolated in human and non-human primates (Batista, Buneo, Snyder and Andersen, 1999; Sereno, Pitzalis, Martinez, 2001; Konen and Kastner, 2008). However, a similar effect has also been observed when changing the position of the head but not the eyes in similar experiments with non-human primates, suggesting head-centred coordinate frames might also exist within the PPC (Brotchie, Andersen, Snyder and Goodman, 1995). Additionally, evidence of head coordinates within the human PPC has also been found (Sereno and Huang, 2006; Connolly, Vuong and Thiele, 2015). If altering the position of the head in relation to the body while fixing both the position of the eyes in the orbit and the retinal stimulation results in a change in the spatial maps obtained within the PPC, then, arguably, there is evidence of a higher-order reference frame not limited to the loci of eye and retina. Such higher-order coordinates

might play a substantial role in the context of reaching and grasping actions, and specifically in the process of hand-eye coordination and 'on-line' trajectory control of movement.

Evidence of the body- and world-reference frames has actually been identified in several areas of non-human PPC (Dunamel, Bremmer, Hamed and Graf, 1997). However, similar effects in humans have yet to be confirmed. Unpublished data from our research group shows how rotating the body under the neck but maintaining the position of the head and eyes and retinal stimulation as fixed results in a modulation of the spatial maps recorded within human PPC. In this experiment, a well-established saccadotopic task was used (Sereno et al., 2001) and participants performed the same task whilst the body was rotated 20 degrees to the left and right and compared to a non-rotated control condition. The response of the PPC was recorded using fMRI and a shift in the resulting phase maps was found when comparing the three conditions.

A control experiment using eye-tracking found no significant differences in saccade metrics suggesting that the accuracy and latency of end-points of memory-guided eye movements are not affected by the body rotations. Such results strongly suggest a body-dependent encoding of space within the human PPC.

Following these results, Chapter 2.1 investigates whether it is possible to isolate the contribution of a single limb to the saccadotopic maps of human PPC. By using the same saccadotopic task (Sereno et al., 2001) and altering the position of the dominant hand alone, finding a shift in the resulting phase maps of the PPC would further suggest the prevalence of body-centred and even hand-centred coordinate frames within this area. In other words, that the PPC takes into account the position of not only the body but also the reaching hand when encoding for eye-movements. This would have direct implications on the understanding of space encoding in the human posterior parietal

cortex and might also help to further clarify the role of this area in the intricate process of coordinate transformation from visual to motor cortices.

To ensure that no contribution was given by a change in saccades' endpoints (or accuracy) , a similar eye-tracking follow-up experiment was also performed and summarised in Chapter 2.2. Participants repeated the same saccadotopic task while the dominant hand was in two different positions and accuracy- and latency-related metrics were recorded. Finding a null effect would further strengthen the suggestion that any alteration found within the saccadotopic maps of the PPC are the result of hand-centred encoding of space rather than eye movement-related shifts.

A certain degree of variability has been reported across experiments investigating the topographic mapping of the human PPC (Konen and Kastner, 2008; Sereno et al., 2001; Connolly et al., 2015; Schluppeck, Glimcher and Heeger, 2005). These inconsistencies are reflected in both data quality and the distribution of such maps. Finding a direct link between hand and body positions and the saccadotopic maps of the PPC could also help to clarify the reason for such variability. This will not only have practical implications for future research on spatial encoding and coordinate transformation within the PPC but might also improve feasibility and accuracy and reduce individual variability in the use of PPC-based assistive BCI and BMI techniques. If the position of the body when computing eye movements to external targets affects the way space is encoded and therefore internally represented, the need of controlling for even subtle body position alterations for both research and rehabilitation applications becomes apparent.

In order to further the investigation on the possible beneficial role of the posterior parietal cortex in BCI/BMI assistive and rehabilitative practices, after

attempting to clarify the specific spatial encoding mechanisms of the PPC, Chapter 3 will examine the possible effects of long-term paralysis on this particular brain area. As briefly mentioned above, most standard invasive BMI approaches use the Primary Motor Cortex (M1) as the main extraction site on the assumption that, when functioning normally, this area serves as the focal point for voluntary motor control. However, evidence of a progressive and natural decrease of functional activation in M1 has been previously observed in a longitudinal study in a cohort of individuals suffering from paralysis following SCI (Jurkiewicz et al., 2010). Moreover, whilst the loss of activation has been reported to progressively increase during the first year after the onset of paralysis, the volume of grey and white matter of M1 appears to be no different from that of healthy controls (Crawley, Jurkiewicz, Yim, Heyn, Verrier, et al., 2004). This suggests that a functional reorganisation of the primary motor cortex at the expense of areas no longer under direct voluntary control of the individual with paralysis, rather than atrophy of these areas, might be the cause of the reported decreased functional activation. However, there is a paucity of evidence regarding the functional activity levels of individuals with long-term paralysis after SCI.

This project investigated the functional activity resulting from imagined movements to visual targets of individuals suffering from long-term paralysis (i.e., >2 years) using whole-brain fMRI images. The related activity of several focal brain areas was recorded and these included both frontally distributed areas, such as the Primary Motor Cortex (M1), Supplementary Motor Area (SMA) and Premotor Cortex (PM), and the posteriorly located PPC subdivided in Superior Parietal Lobule (SPL), and Anterior-, Medial- and Posterior- Intraparietal Sulci (aIPS, mIPS and pIPS). Participants taking part exhibited complete paralysis of the four limbs following a complete lesion of upper-cervical vertebrae (C4) but who were still able to communicate effectively and breathe

autonomously. Based on previous findings within the literature, a level of functional reorganisation during imagined movements of the dominant hand was anticipated and this would be at the expense of the Primary Motor Cortex that is no longer involved in the control of the same limb. Although examples of successful BMI-assistive techniques using M1 as extraction site do exist (Carmena, Lebedev, Crist, O'Doherty, Santucci et al., 2003; Nicolesis, Dimitrov, Carmena, Crist, Lehew, et al., 2003; Hochberg et al., 2006), a limitation on the efficacy and longevity of these implants has also been reported (Lebedev and Nicolesis, 2006). The functional reorganisation that M1 undergoes following paralysis might be the reason for such variability. Furthermore, the PPC has been shown to be successful in extracting a clear signal, sufficient to control a computer actuator in one instance (Aflalo, Kellis, Klaes, Lee, Shi, et al., 2015). Findings supporting a shift in motor imagery-related activation to more posteriorly located brain areas in long-term paralysis might further support the need for investigating the feasibility of PPC-based invasive BMI/BCI techniques. If individuals with long-term paralysis are exhibiting a natural decrease of functional activation of M1 over time whilst activation of subareas of the PPC remain comparable to controls, BMI-assistive techniques using this latter area might result in systems that are suitable to a wider number of the paralysed population following SCI even when the functional reorganisation of M1 has already taken place. Moreover, such findings might suggest the need of introducing motor imagery training in standard rehabilitation practice in order to maintain adequate activation levels of M1 comparable to that of controls.

While invasive applications of assistive BMI currently offer the highest level of natural and ecologically valid motor control, the risks associated with the specific invasive procedures might be a determining factor limiting the success of introducing

such techniques in standard rehabilitative practice. Although substantial progress has been made in recent decades in maximising the benefits of brain implants, some individuals suffering from various degrees of paralysis might prefer a less invasive approach. Surveys of a cohort of paralysed individuals appear to show extreme variability in the responses that is related especially to the degree of paralysis experienced in each case (Collinger et al., 2012). Non-invasive BCI approaches can be extremely beneficial especially to those who have lost communication as well as motor control. Moreover, non-invasive approaches appear in general to be more suitable to a non-clinical population, and for commercial use. Their possible integration in smart-home environments has been successfully achieved in both laboratory and home settings and allows for the restoration of some level of the lost independence (Blondet, Badarinath, Khanna and Jin, 2013; Lin, Lin, Chen, Lu, Chen and Ko, 2010; Holzner, Guger, Edlinger, Gronegress and Slater, 2009; Lee, Nisar, Malik and Yeap, 2013). However, the use of these devices in a non-controlled, home settings usually poses for the risk of introducing detrimental amounts of noise generated from both the surrounding environment and by the natural movements of the end-user (Minguillon, Lopez-Gordo and Pelayo, 2017).

As part of the present project, we had the chance to collaborate in an experiment introducing a novel algorithmic approach to allow for early detection of intended head movements through a standard, wet-based EEG and this is summarised in Chapter 4. If successful, following computations can be applied to account for the impending head movements in order to maximise the signal-to-noise ratio during real-time EEG-based assistive and commercial BCI techniques.

In conclusion, the following experiments will aim to offer novel information regarding the use and applications of BCI and BMI invasive and non-invasive approaches with a main focus on the role of the Posterior Parietal Cortex. Firstly, Chapter 3 will investigate the potential contribution of body and hand static changes to the spatial encoding of the PPC. This is crucial in the understanding of the process of coordinate transformation necessary for fine movement control. A control experiment (Chapter 2.2.) investigating the relationship between body position changes and saccade endpoint metrics will ensure that any alterations found within the saccadotopic phase maps of PPC are an actual reflection of the postural contribution to the way this area encodes for space. Positive results will hold implications for both future research paradigms in the context of spatial reference frames as well as practical applications of PPC-based assistive BMI techniques. Chapter 3 will then address the motor imagery-related residual functional activation of posteriorly located cortices after long-term and high-level cervical SCI in comparison to a group of matched controls. A level of activation comparable to that of controls might support the need for future investigation of PPC-based invasive BMI techniques that could be suitable and effective even for those individuals whose long-term SCI has resulted in a loss of motor imagery-related M1 functional activation. Finally, Chapter 4 will explore the possibility of early detection of voluntary head movements through an EEG-based BCI technique in both commercial and rehabilitative settings. Successful results will prove useful in the implementation of on-line correction of movement-related artefacts as well as maximising the accuracy of non-invasive BCI techniques.

2 Body and limb reference frames of the human Posterior Parietal Cortex (PPC)

The following chapter will cover our contribution on the topic of the reference frames existing within the posterior parietal cortex (PPC). As previously mentioned in the introduction, previous literature reports evidence for eye, retinae, head- and body-centered reference frames within the non-human PPC. In the following chapter, we hope to offer novel knowledge on the presence of whole-body and limb frames of reference within human PPC.

Chapter 2.1 will explore the possibility of torso rotations and hand position changes affecting the way human PPC encodes for space during the execution of memory-guided saccades. This work has been divided in three experiments that have been collated into one manuscript for publication purposes and it is hereby presented in its latest version.

Finally, a control experiment using eye tracking was completed to validate Experiment 3 and this is reported in **Chapter 2.2** of this manuscript. If a change in the phase maps of human PPC is shown when altering the position of the dominant hand, we need to ensure that such alterations are not due to a change in the endpoints and overall accuracy of the saccades executed when the hand is in different positions in space.

2.1 Subtle position alterations modulate the phase representations of functional MRI saccade topographic maps

Alessia Cacace[1], Joshua J. Podmore[1], Maria Olkkonen[1], Robert W. Kentridge[1] & Jason D. Connolly[1]

[1]Psychology Department, Durham University Science Site, Durham University Durham, United Kingdom, DH1 3LE

2.1.1 Abstract

Functional Magnetic Resonance Imaging-based parietal memory-guided saccade topographic maps provide vital insights into the topological organization of this key functional zone, owing to the parietal cortex being precisely situated between the visual (input) and motor (output) cortices involved in movement control. These maps have demonstrated that rapid saccadic eye movement vectors tile the parietal cortex. Nevertheless, a recent study reported that the saccade vector or phase maps are altered by 4° offsets in the static position of the eyes in the orbits. It is unknown to what extent changes in other body parts, for example, the torso or even a single hand may also modulate these topographic maps. This is important to know because it could improve the data quality of these maps. To investigate the dependence of parietal topographic maps on subtle alterations in body position, we collected memory-guided saccade topographic maps and rotated either the static torso by 20° (left or right) or changed the single static (right) hand position by 90° by bending the elbow. We report that these subtle static offsets of either the torso or the position of one hand disrupt the phase maps. These experiments emphasise the need for extremely body position-

consistent topographic mapping method protocols in future saccade topographic mapping experiments.

2.1.2 Main Introduction

Functional Magnetic Resonance Imaging (fMRI) represents a non-invasive neuroimaging approach based on changes in blood oxygenation levels to investigate the organization and function of different areas of the brain. Amongst other applications, it has been used successfully to discover the visual organization of the primary visual cortex (V1) in humans (Belliveau, Kennedy, McKinstry, Buchbinder, Weisskoff, Cohen, et al., 1991); to provide guidance in pre-surgical planning procedures (Pillai, 2010); to contribute to the physiological understanding of psychiatric conditions such as schizophrenia, depression, and bipolar disorder (Rosen and Savoy, 2012), and processes such as brain plasticity (Lomber and Eggermont, 2006).

FMRI has been further used extensively to explore the computation of saccades within the posterior parietal cortex (PPC) through a process called topography (Sereno, Pitzalis and Martinez, 2001; Silver and Kastner, 2009; Konen and Kastner, 2008; Schluppeck, Glimcher and Heeger, 2005). Topography plays a crucial role to further our understanding of the cortical distribution of information encoded within human PPC. By asking participants to perform delayed eye movements to sequential visual targets held in memory, it is possible to elicit an organised travelling wave of brain activity that will tile adjacent areas of the human PPC. These areas are referred to as being topographically organised and considerable progress has been made in defining them through the use of saccadic eye movement mapping (Sereno et al., 2001). A saccade is a rapid eye movement used to bring a peripheral visual stimulus onto the fovea and information regarding saccades has been shown to be stored in the lateral intraparietal area (LIP) of non-human primates (Andersen, 1997). A seminal study was able to locate a human homologue in the PPC (Sereno et al., 2001). According to these findings, human PPC seems to contain a representation of spatial coordinates gathered through saccadic

eye movements. In other words, the PPC stores the so-called saccade vectors which contain information regarding the direction and end-points of each performed saccade (Konen and Kastner, 2008).

Moreover, research indicates that saccades are organised in a topographic manner, where adjacent saccadic eye movements are represented by adjacent cortical tissue along the surface of the PPC (Konen and Kastner, 2008; Silver and Kastner, 2009; Sereno, Pitzalis and Matinez, 2001). This distribution has been identified by using a saccade topographic mapping approach where participants are asked to perform a series of eye movements to adjacent locations in space (Sereno et al., 2001). Such approach has been extensively used in related research and has led to the identification of further topographically organised regions within human PPC such as the intraparietal sulci IPS1 and IPS2 that may also constitute a potential equivalent of non-human primates area LIP (Andersen, 1997; Schluppeck et al., 2005). Previous literature has linked the topographic representation of delayed saccades in PPC to both the attention payed to visual stimuli and the planning of intended movements, which in this case includes saccades (Sereno et al., 2001; Mountcastle et al., 1975; Schluppeck et al., 2005). However, there is high variability in the quality of such saccade topographic maps (e.g., Eger, Sterzer, Russ, Giraud and Kleinschmidt, 2003; Konen and Kastner, 2008; Silver and Kastner, 2009; Sereno et al., 2001; Connolly, Vuong and Thiele, 2015; Schluppeck et al., 2005; Levy, Schluppeck, Heeger and Glimcher, 2007). While some research groups have reported a precise one-to-one mapping of adjacent contralateral saccade vectors that are represented on the adjacent surface points of the cortex (Sereno et al., 2001), others have only reported an overall contralateral bias (Connolly et al., 2015). A contralateral bias refers to the fact that leftward saccades are mapped onto the right hemisphere of the cerebral cortex and vice versa. Such maps are crucial to reproduce

because the topographic approach has been used to identify important functional areas such as the putative human homologue of the macaque lateral intraparietal area (LIP) that mediates saccade generation (Sereno et al., 2001).

In the present series of experiments, we explored one possible reason for such variability in the quality of these topographic maps across the different research groups. There may conceivably be subtle differences in the position of a specific body part in the scanner across runs, individuals, and studies. For instance, one shoulder may be raised more than the other due to uneven foam padding, the arms may be bent or straight, the hands placed on the stomach or along the torso, the legs bent or crossed at the ankles, or a combination of these. If such position alterations caused changes in the saccadotopic maps, saccades would no longer be reliably topographically mapped in the cortical tissue, leading to noise in averaging specific saccade vectors across fMRI scan runs. We investigated this potential issue by having participants make memory-guided saccadic eye movements to stimuli sequentially presented 'around the clock' as per previous saccade topographic mapping experiments (Sereno et al., 2001; Connolly et al., 2015; Schluppeck et al., 2005; Levy et al., 2007) but with the torso rotated by a relatively subtle offset of 20° to the left or to the right as compared to center. This was followed by a behavioural experiment using eye tracking to control for the possible contribution of torso rotations on the accuracy and latency of eye movements. Finally, in a second fMRI experiment, we changed the offset of only a single hand by bending the right elbow by 90°.

Based on the aforementioned variability reported within the existing literature, we expect that the saccadotopic maps hereby obtained will be affected by torso and hand position changes. We suggest that these changes are the result of body-centered reference frames existing within the posterior parietal cortex and supportive of similar

results reported in previous experiments (Connolly et al., 2015; Bosco, Breveglieri, Hadijdimitrakis, Galletti and Fattori, 2016; Boussaoud and Bremmer, 1999; Dunhamel, Bremmer, BenHamed and Graf, 1997; Pertzov, Avidan and Zohary, 2011; Mullette-Gillman, 2005; Mullette-Gillman, Cohen and Groh, 2009). In other words, according to these examples, when encoding for saccadic eye-movements, the PPC might be taking into account the position of the body in space. This means that different body positions will correspond to slightly different saccadotopic maps therefore resulting in different internal representations of the surrounding space.

Moreover, to ensure that the possible alterations of the resulting maps hereby investigated are not merely a reflection of a disturbance in the overall performance and accuracy of the eye-movements, the control experiment involving the use of eye-tracking technique will use the same methodological paradigm as the fMRI experiments. If changes in the saccadotopic maps of the PPC following body positional changes are the effect of body-centred reference frames, the metrics of accuracy and latency of the saccades should not be affected by the same positional alterations. We therefore anticipate that no significant differences will be found in the kinematic metrics of saccades even when these are performed with the body in different static positions (i.e., 20 degrees torso rotations to the left and right as compared to a neutral, center position).

Clarifying the process of saccadic encoding at different static body positions within human PPC will be crucial to continue to advance our understanding of the specific integrative role of this brain area during movement planning and execution. Findings supporting the hypothesis that body posture can affect the resulting saccadotopic maps in PPC, may suggest that proprioceptive feedback originating from the periphery of the body and visual feedback obtained during the execution of delayed

saccades, are integrated prior to the encoding process to produce saccadotopic maps that reflect the position of one's body in space. In the context of sensorimotor integration within PPC, this process could be explained as a way to aid the preparation of intentional movements toward visual targets.

2.1.3 Materials and Methods

The datasets for the three experiments in this manuscript are available via a Creative Commons Attribution 4.0 International (CC BY) license from the Durham Research Online Datasets Archive: http://dx.doi.org/10.15128/r3cv43nw803. The three experiments were approved by the Durham University Psychology Department Ethics Sub-Committee (approval number 14/01) and written consent was obtained from all participants. The 2 fMRI studies (Experiment 1 and Experiment 3) were also approved by the James Cook University Hospital MRI facility. A control for handedness was carried out using the Edinburgh Handedness Inventory (Oldfield, 1971) and only right-handed participants were tested.

2.1.3.1 Experiment 1

The purpose of the present experiment was to examine whether or not subtle 20° torso rotations modulate the phase representations (directional tuning) of posterior parietal saccade topographic maps.

Participants

Six participants with no neurologic or psychiatric disability and normal or corrected-to-normal vision agreed to take part in the first of two fMRI studies. Participant age ranged from 18 to 39 years of age (M=27.17; SD=8.08), with 3 females. Each participant was scanned twice for a total of 12 scanning sessions.

Stimuli and Task

The memory-guided saccade task as described in this section was developed by Sereno and colleagues (2001) and is presented in **Fig 1** (the same stimuli were also used for Experiments 2 and 3).

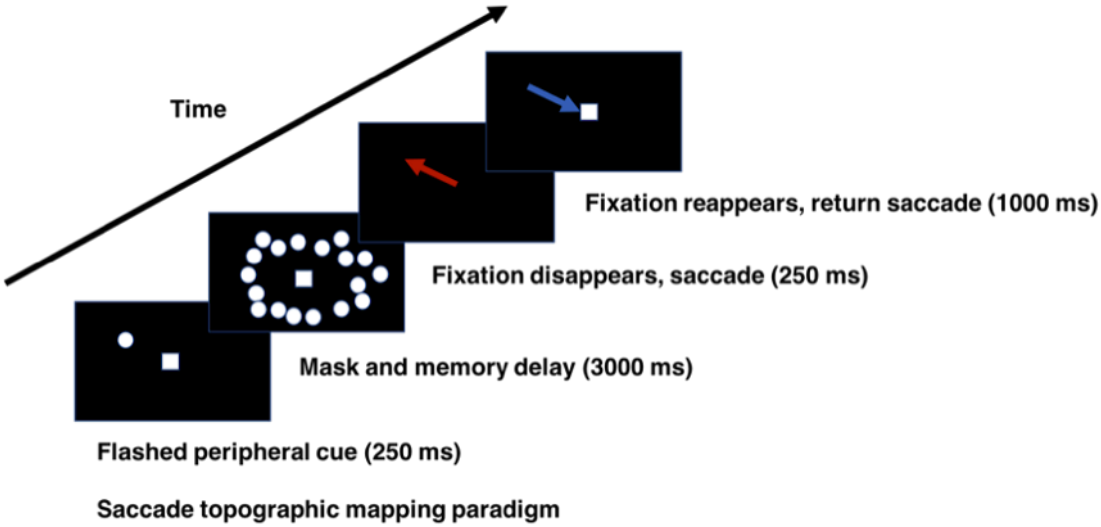

Figure 1. The delayed saccadic eye movement topographic mapping task. The experimental memory-guided saccade protocol used in all three experiments. A peripheral cue was flashed for 250ms, and represented the ultimate target for the memory guided saccadic eye movement. For the counter-clockwise (CCW) runs, this occurred at the 11 o'clock location (as shown here) and the 12 sequential targets were arranged around an invisible clock-face. For CCW runs, the order of presentation of targets appeared from 11 o'clock, 10 o'clock, 9 o'clock and so forth. For Clock-wise (CW) runs the targets appeared at 12 o'clock, 1 o'clock, 2 o'clock and so forth. For a single saccade trial within a functional run, a ring of 100 distractor dots were presented for a 3000ms memory delay interval and within an invisible annulus ring. The fixation square then disappeared, and the participant generated a rapid eye movement (saccade) toward the remembered location of the peripheral cue (red arrow). The participant's task was to immediately return their gaze to the fixation square once it reappeared.

The experiment was written in MATLAB R2009a (Mathworks, Natick, MA, USA), using the Psychophysics Toolbox (Brainard, 1997; Pelli, 1997). A saccade target (a 0.22° high contrast dot) appeared sequentially at 12 locations located on an invisible circle around

the starting gaze position (i.e. the fixation spot). The radius of this circle subtended 7.7° of visual angle.

On each trial, a fixation square appeared at the starting gaze position for 1000ms. A target appeared for 250ms, followed by a 3000ms mask of 100 distracter dots (0.22° high contrast dots). The distracter dots were randomly distributed within an annulus, which had an inner radius of 5.0° and an outer radius of 10.4° relative to the center gaze starting position. When the mask disappeared, participants then generated a saccade immediately toward the remembered target location and then immediately generated a saccade back to fixation (within 250ms). One complete cycle consisted of a saccade to each of the 12 target locations 'around the clock'. Participants performed 5 cycles or repetitions of the 'around the clock' task per experimental fMRI scanning run. Therefore, the stimulus periodicity was 5 cycles per run.

Procedure

A rotatable wooden platform was placed directly on the scanner bed, either flat (control condition or center) or tilted left 20° or right 20° relative to center. The participant was lying in the supine position on the scanner bed while they executed memory-guided saccadic eye movements (refer to **Stimuli and Task**). We ensured that the head of the participant remained fixed (or always facing vertical) in the head coil at all times via foam packing surrounding either side of the head. For a single experimental testing day and for each condition (Torso Center, Torso Left and Torso Right), fMRI data were obtained for four separate scan runs – and with a ~3 minute break in between each of these scan runs to adjust and tilt the platform. In each scan run, participants made delayed saccadic eye movements sequentially to 12 targets arranged around an

invisible clock-face. For two of these runs the targets proceeded clockwise (CW) and for the other two runs the targets proceeded in a counter-clockwise (CCW) fashion.

Every condition started with a CW run, followed by CCW, followed by CW, and finishing with CCW (24 runs in total per participant across the two sessions: 2 saccade directions x 3 postural conditions x 2 repetitions x 2 experimental sessions). The clockwise 'around the clock' delayed saccade targets started at 12 o'clock and the counter-clockwise targets at 11 o'clock. The 12 o'clock delayed saccade target location was followed by 1 o'clock then 2 o'clock and so forth. This procedure (starting at 12 o'clock for the CW runs and 11 o'clock for the CCW runs) allowed the CCW scans to be time-reversed and then averaged together with the CW scan runs. The CCW and CW averaging is possible because the CW runs that begin at the 12 o'clock location end at the 11 o'clock location, whereas the CCW runs start at the 11 o'clock location and end at the 12 o'clock location.

As the aim of this experiment was to examine possible effects of 20° torso rotations on the superior parietal cortical phase mapping of delayed saccades, a within-participants design was implemented. Although the conditions were pseudorandomized, the first condition always had to be center, owing to the fact that we had to safely place and secure (via substantial foam padding for stabilization) the participant on the MRI scanning bed. It is important to note that an MRI-compatible eye-tracker was not used in either fMRI experiments (Experiment 1 and Experiment 3).

MRI Compatible Equipment

The in-house custom-built non-ferrous MRI-compatible platform extended only to the participants' shoulders, ensuring that the head remained fixed (and was always facing vertical) in the head coil (**Fig 2**). Additional foam padding was packed inside the head

coil to ensure that the participant's head did not rotate with the 20° torso rotations. To further ensure participant stability and safety, four oblong MRI-compatible foam positioners (Newmatic Medical products, Michigan, USA) were placed alongside the sides of the participant's body to stabilize the torso across the three (center, left or right) torso position conditions. A 24-inch MRI-compatible BOLD screen monitor (60 Hz, 1920x1200 pixels) displayed the visual stimulus and was viewed via an angled mirror mounted onto the head coil. The angled mirror was situated at a ~8 cm distance from the participant's eyes.

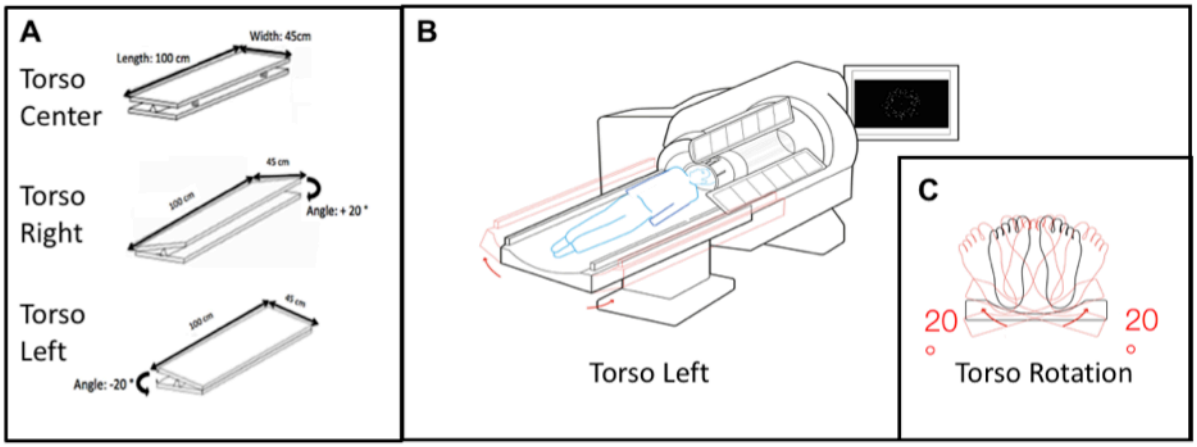

Figure 2. The experimental apparatus used to rotate the torso in Experiment 1. The custom-built MRI compatible platform that allowed for a torso rotation of 20° (Torso Center, Torso Left or Torso Right), with the participant's head remaining fixated in a vertical position within the head coil. Each participant's hands were placed straight and along the sides of their bodies.

Functional MRI Acquisition

Functional scans were obtained via a 3-Tesla MR scanner (Siemens Tim Trio) located at the James Cook University Hospital, Middlesbrough, UK. The participant's head was fixed in a vertical position and a 32-channel full head coil was used. The scanning and analysis protocol used was precisely adopted from a previous saccade topographic

mapping study demonstrating how different gaze directions can affect the representation of visual space in the posterior parietal cortex (Connolly et al., 2015).

The total duration of a single run was 270 s (4.5 s per trial × 12 clock positions × 5 cycles 'around the clock'). Each torso orientation (center, left or right) had 4 scan runs per experimental session (2 CW and 2 CCW). In total, 8640 saccades were generated overall and included in the present experimental dataset (Experiment 1) or 2880 saccades per torso orientation.

At the beginning of each scanning session, a T1-weighted high-resolution anatomical scan was collected with via standard 3T Siemens Tim Trio scanning parameters. We then acquired 180 (session 1 for each participant) and 180 (session 2 for each participant) functional volumes of T2*-weighted echo-planar functional scans for each of the delayed saccade topographic mapping runs and with the following parameters: TR=1.5; TE=30ms; field of view=192mm^2; voxel size=3 mm^3; flip angle=75°, matrix size=64x64x30; 30 coronal slices with 3 mm thickness. The functional volume was aligned with the back of the cerebral cortex (the inion, or visual cortex) and extended anteriorly (or forward toward the nose - to include all regions up until the posterior portion of the frontal lobe). For two of the twelve runs, 179 volumes were collected (one of the two scan days for S1 and S2) owing to radiographer error and from these we "clipped" the final four functional volumes (resulting in 175 volumes total) of each of these functional runs. This was carried out such that the analysis was then divisible by '5' (or at our stimulus periodicity - the number of 'around the clock' saccades repetitions in each functional scan run). An in-plane anatomical scan in the same slice orientation (coronal) as the functional scans was also collected for intra- and across-session functional scan alignment.

FMRI Data Analysis Procedure

All data were pre-processed and analyses were carried out using the MATLAB-based open source software suite 'mrTools' and the retinotopy rotating or flickering 'wedge' protocol that is imported or also used for the 'around the clock' saccade analyses procedure here. The Heeger (NYU, USA) and Gardner labs developed the software program used in both of the present fMRI experiments (Experiment 1 and Experiment 3) and are described in detail elsewhere (Merriam, Gardner, Movshon and Heeger, 2013; Gardner, Merriam, Movshon and Heeger, 2008).

Motion correction was carried out using the computational procedure of mrAlign in mrTools: (Interpolation method: cubic; number of iterations: 3; Robust: No; Crop: No) and the low frequency drift associated with fMRI data was removed by applying a high-pass filter with a cut-off of 0.01 Hz at each voxel in mrTools, identical to a previous experiment with the same functional run duration and also with same number of conditions (3) (Connolly et al., 2015).

The functional scans were aligned to the high-resolution MPRAGE via registration to an in-plane image. First, the T1-weighted 3D anatomical volume anatomy and the 2D in-plane anatomy were aligned via the mrTools-based mrAlign procedure, a combination of computer-based (Nestares and Heeger, 2000) and subsequent manual registration (the manual registration or "alpha slider" to make the 2 overlaid volumes partially transparent, was only used to confirm that the computational mrAlign registration was robust and accurate). Then, the functional data were aligned to the in-plane image, and finally to the MPRAGE via concatenating the two transforms.

The T1-weighted 3D anatomical surfaces were segmented using FREESURFER (Reuter, Schmansky, Rosas and Fischl, 2012) software via the 'recon-all' command

running in the Mac OSX Terminal Unix command shell. The surfaces were then converted to SurfRelax format via an mrTools MATLAB-based function and imported into mrTools (Connolly et al., 2015; Merriam et al., 2013; Gardner et al., 2008).

The functional activation maps presented below (**Figs 5 and 9**) are coherence-based maps. Coherence represents the fit between an identified reference waveform and the data (shown in **Figs 5 and 9**) and is derived via dividing the power at the frequency of interest from the power at all other temporal frequencies in the time series. The activation maps were computed via the mrTools mrLoadRet 4.5 'corAnal' procedure. The procedure enabled us to calculate the degree to which each voxel's time course correlates with a given sinusoidal modulation (in this case '5', corresponding to 5 saccade cycles 'around the clock'). Therefore, in our case, values approximating '1' represent near perfect signal modulation at the stimulus periodicity of '5' relative to noise whereas values approximating '0' represent almost no signal modulation at the stimulus periodicity relative to noise. To define the contrast-to-noise ratio (CNR), a Fourier spectrum was computed via mrTools software by interrogating the voxels in the particular functional data set via mouse-controlled "crosshairs" in the image GUI (**Figs 4 and 8**). This involves clicking the mouse on a voxel of interest in the mrTools mrLoadRet 4.5 Graphic User Interface (GUI) that displays the coherence maps. The CNR is a measure of signal quality within each voxel, quantifying the level of fMRI-BOLD activity at the Fourier peak relative to the noise that is represented by the extreme high frequency responses in the bottom right panel and coloured in green in **Fig. 4C**. A sinusoidal curve with 5 peaks corresponding to each of the five cycles of saccadic eye movements 'around the clock' was identified via fitting the data to a five-cycle reference waveform at each voxel. The coherence of the actual data time series and the best fitting sinusoid, as well as the phase (or timing of the fMRI-BOLD response relative to the

idealized sinusoid) were then computed. The Coherence threshold was set to c>0.25 using the mrLoadRet 4.5 software GUI of mrTools. Coherence-related activation was displayed on segmented and also on flattened maps of the grey matter surface.

We did not use any coherence threshold at all for the phase maps and polar plots that follow below (**Figs 4 – 6**) for the following two crucial reasons: 1. High coherence voxels are too likely located in different superior parietal cortex surface locations to be functionally compatible across conditions and are therefore likely to be carrying out very different types of underlying neural computations; and 2. So-called "tracking" of the voxels (or restricting the ROI and reusing the same ROI across the three different conditions (such that the "same" voxels are sampled across conditions) is unlikely to be reliable owing to participant intra-and inter-session head motion. This is likely due to differences in the actual cortical (brain) positioning on the scanner bed across the two scan sessions. As an alternative, we drew the ROIs manually on the segmented MR-surfaces using the well-known anatomical boundaries: the sulcal landmarks demarcating Brodmann's area 5 (i.e. superior parietal cortex). These ROIs include all of the possible voxels within superior parietal cortex and a reasonable comparison can be made. The sulcal boundaries were: those voxels posterior to the postcentral sulcus, anterior to the parieto-occipital sulcus and medial to the intraparietal sulcus. These were drawn on the segmented surfaces using the mrTools ROI drawing tool.

The mrLoadRet 4.5 software-computed phase measures were of key interest here, as these represent the actual saccade directions for each voxel on the segmented surfaces of the superior parietal cortex (Brodmann area 5) cortical tissue (**Figs 6 and 10**). The phase values represent the unique vector of a specific memory-guided saccadic eye movement toward one particular cue location on the segmented fMRI volumes. A time-shift of the reference 5 peak sinusoid of 4.5s (a single trial duration)

relative to the 12 o'clock starting location would be represented in a different colour than the 12 o'clock location. So, a 1 o'clock saccade would be shifted in the time domain by 4.5s (the duration of a single trial) relative to the 12 o'clock location for CW runs, the 2 o'clock would be shifted in the time domain by 9s (or 4.5s x 2), and the 3 o'clock position would be shifted by 13.5s (or 4.5s x 3), and so forth. Each of these positions would then be assigned a unique colour. Voxels were color-coded according to this phase shift and relative to the 12 o'clock (or 0°) phase shift 5-peak sinusoidal reference waveform. These were directly computed via the mrLoadRet 4.5 Software and displayed on the high-resolution anatomies and subsequent segmented anatomies.

To visualize the set of representations of saccade positions in a 360° circle, the phase data were exported from mrLoadRet 4.5 as variables and then imported into the MATLAB workspace. These values were then input into the polarhistogram function for the two respective Regions of Interest (or ROIs) (or for the left and right superior parietal cortices). [As drawn on the segmented surfaces using the mrLoadRet 4.5 ROI drawing tool.]

The ROI region approximated a square surface area (**Figs 6 and 10**). Saccade polar histograms were then calculated for each combination of participant, hemisphere, and condition and for both a single participant and on a cumulative basis (**Figs 7 and 11**). Differences between the circular pattern of the phases for each torso orientation (Torso Center, Torso Left and Torso Right) were quantified for each hemisphere via a non-parametric multi-sample test for equal median values (cm-test) via the MATLAB-based open source CircStat toolbox (Berens, 2009). The cm-test is a circular equivalent of the Kruskal-Wallis test, a non-parametric analysis of the median directions of two or more groups. The cm-test can be used to assess whether the median values of the compared groups are identical or not. In this occasion, this test was used due to data not

being normally distributed thus not allowing the use of a parametric circular tests. For interpretable visualization purposes for these polar rose histograms, we assigned each of the phase representations into 2 separate arrays corresponding to the two hemispheres via the MATLAB-based polarhistogram function (**Figs 7 and 11**).

2.1.3.2 Experiment 2

To determine whether or not saccade kinematics varied with the three different torso positions of Experiment 1, we measured saccadic eye movements outside of the scanner using the same delayed saccadic eye movement task in 10 neurologically healthy participants. While head position was fixed in a chin-rest, participants' whole body under neck was rotated left (20° Torso Left) or right (20° Torso Right) via an in-house custom-built rotatable chair. The body was facing straight in the third, Torso Center condition. The head was always facing sagittal vertical and therefore this involved the same protocol as was carried out in the functional MRI scanner, with the difference that the participant sat upright. Participants generated saccades to the 12 distinct locations around the clock per run (total time per run, 54 s) and thus served as an analogue to the functional MRI experiment. Five repetitions were collected per body orientation, thus totalling 15 runs per participant.

Possible kinematic effects of torso rotation on Reaction Time, Amplitude Error, Angular Error, and Cartesian Error were all measured via in-house custom MATLAB code. The right eye was tracked (combined pupil and corneal tracking) using an EyeLink II eye-tracking system (SR Research, Ltd, ON, Canada). The EyeLink II has a spatial resolution of <0.00001° and was used to record all of the Saccade Kinematics. The system utilizes video-based tracking technology to calculate the pupil's position in orbit

and it has a velocity threshold of 30° per second. The EyeLink II was set at a 250 Hz sampling rate, monitoring exclusively the right eye.

Reaction Time was calculated from when right eye velocity exceeded a predetermined threshold (22°/ second) relative to the initial saccade fixation start point, post disappearance of the fixation square. Amplitude Error defines the spatial disparity between desired and actual saccade landing point, measured in pixels, whilst excluding Angular Error scores. Angular Error describes the total distance in visual angle (discounting Amplitude Error) of saccade end-point from actual target location. Cartesian Error was calculated upon consolidation of both Amplitude and Angular error variables as visualized within a Cartesian co-ordinate frame to generate a global error score. The process of selecting saccades relevant to analysis involved placing a temporal cut-off point of 4500ms after trial initiation to exclude saccades executed in the subsequent trial.

2.1.3.3 Experiment 3

In Experiment 3, we ran a second fMRI study in order to investigate possible effects of a single hand position change on the superior parietal distribution of saccades (or possible modulations of their preferred vector or phase representations on the segmented surface maps by right hand position).

Participants

Seven participants with no prior history of neurologic or psychiatric disorders and normal or corrected-to-normal vision took part in the second of the two fMRI experiments. Each participant was scanned once for a total of 7 scan sessions. Participant age ranged from 20 to 31 years of age (M=27.43; SD=3.64), with 3 females. A

control for handedness was carried out using the Edinburgh Handedness Inventory (Oldfield, 1971) and only right-handed (M=+0.92; SD=0.09) participants were tested.

Experimental Procedure

The same well-established delayed saccade task (see above, **Fig 1**) was used to examine for possible effects in the directionality of the phase values upon changing static hand position to one of two possible locations (HR or HL). To investigate any modulation of changing the dominant right hand on the phase values in the superior parietal cortex, the hand position was altered by 90° during the task by bending the only right elbow and in a blocked run fashion. For position 1, participants had the right hand in the standard "neutral" position with the arm resting alongside the body (or hand right, HR), symmetric to the left hand, also resting alongside the other side of the body. Hand right therefore represents the baseline condition via which we can investigate replication of previous results and validation of the present experimental protocol. For hand left (HL), the dominant right hand was placed on the torso and with the elbow bent at a 90° angle and therefore a 90° difference between HL as compared HR. The experimental paradigm for Experiment 3 is depicted in **Fig 3.**

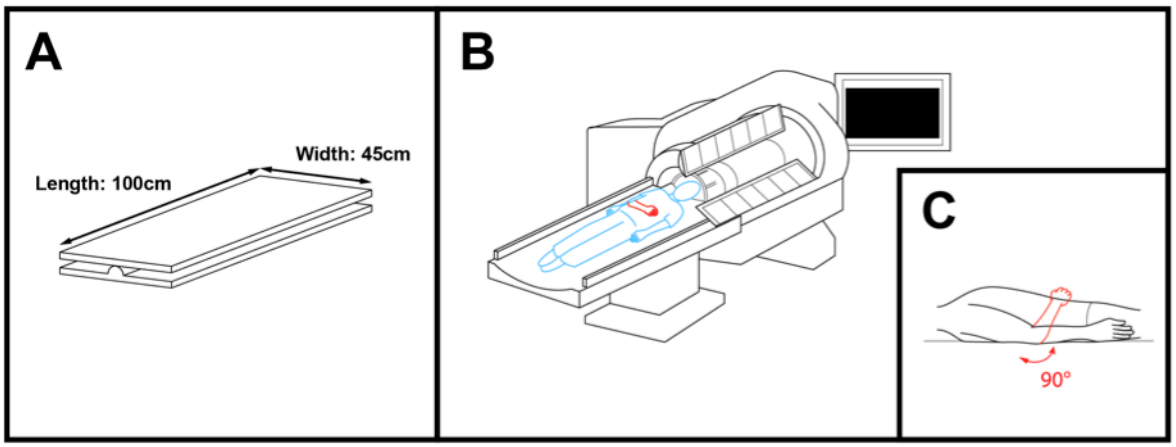

Figure 3. The experimental apparatus used to rotate the hand in Experiment 3. A: The MRI compatible platform was set at 0° (or flat, supine), with the participant's head remaining fixated in a vertical position within the head coil. B. The participant's right hand was placed straight and along the sides of their body or were instead rotated at the elbow by 90°. This paradigm enabled the examination of whether or not there is a shift in the preferred 'around the clock' saccade vectors in superior parietal cortex with the right hand rotated.

Participants performed 6 runs with the dominant hand in the HR position and 6 runs in the HL position and these two data conditions were collected in a pseudo-randomized order. Owing to the fact that the stepping direction (CW or CCW) of the saccade targets was alternated (as in Experiment 1), each experimental condition (the right arm in either HR or HL) had an equal number (n=3) of clockwise and counter-clockwise runs. The starting hand positions were randomly assigned to each participant to control for any possible order effects. The saccade paradigm was entirely unaltered here as compared to the control (gaze center) condition used in a previous experiment (Connolly et al., 2015) and also the Torso Control of Experiment 1 of the present study, therefore making the hand position the only experimental manipulation across conditions.

Magnetic Resonance Parameters

The scanning parameters used here are identical to Experiment 1. Pre-processing was the same as described above for Experiment 1. Again, the scanning, pre-processing and analyses protocol was reproduced and adapted from a previous study (Connolly et al., 2015) and performed using the MATLAB-based open source software package mrLoadRet version 4.5 of mrTools (Merriam et al., 2013; Gardner et al., 2008) and FREESURFER for T1-weighted anatomy segmentation (Reuter et al., 2013) prior to importing into the mrLoadRet 4.5 mrTools software for surface and flat-map analyses.

Region of Interests and Statistics

The superior parietal cortex Region of Interest (or Brodmann area 5), was defined in an identical fashion to Experiment 1. The circular statistical tests were carried out on the polar histogram plot values of our two regions of interest (the left and right hemisphere superior parietal cortex excluding the medial wall) using the CircStat MATLAB toolbox (Berens, 2009), and this approach is also identical to Experiment 1 (cm-test for equal median values). For this experiment, we compared the circular phase distributions of the left and right hemisphere superior parietal cortex when the hand was placed right (HR) as compared to left (HL).

2.1.4 Results

2.1.4.1 Experiment 1

Fourier Plots

Figure 3 illustrates the Contrast-to-Noise Ratio (CNR) for a representative participant for the Torso Center condition. In the averaged time series for the selected voxel there are 5 sinusoidal peaks that correspond to the 5 saccade repetitions 'around the clock' per functional run (i.e. at the stimulus periodicity, since there were 5 eye movement repetitions 'around the clock' in each single functional run). Looking at the bottom left panels (3B) for the left and right hemisphere accordingly, we can check the occurrence of the contralateral bias. Panel3B represent an average of the fMRI bold response in relation to the stimulus periodicity during one cycle around the clock in function of time for all 6 participants. A full cycle around the clock lasted 54s in total during which targets would appear sequentially starting from 12 o'clock. The 27s mark represents roughly the midline or the target arrangement and corresponding to 6 o'clock. Targets located between 12 and 6 o'clock represent the right side of space and targets located between 6 and 12 o'clock represent the left side of space. Bringing this back to the time domain, the time window between 0 and 27 seconds corresponds to targets presented in the right side of space; 27 to 54 seconds includes targets falling in the left side of space. According to the contralateral bias, a higher fMRI bold response for targets located to the contralateral side of space would be expected. This means that a higher fMRI response should be found for the time period corresponding to the presentation of targets located to the right side of space for the left hemisphere and to the left side of space for the right hemisphere. Referring back to panel 3B of **Figure 4**, the peak fMRI bold response for the left hemisphere appears to be around the 28 second mark,

whereas the right hemisphere shows a peak around the 20 second mark. It also is evident from the bottom left panel (3B) that the phases are inverted for these representative voxels for left (LH) as compared to the right (RH) hemisphere. The paradigm was therefore successful at inducing a minor contralateral bias for saccades known to exist in superior parietal cortex. As this is an average across participants, participant-specific plots (in **Figure 7**) help understand the reason for the low magnitude of the effect in this experiment as 2 of the 6 participants did not show the contralateral bias. Depicted in **Fig 4** are voxels representative of the high coherence pixels obtained on the flat-maps throughout the superior parietal cortex. The majority of these active voxels in **Fig 4** demonstrate this effect and across all of the participants we examined.

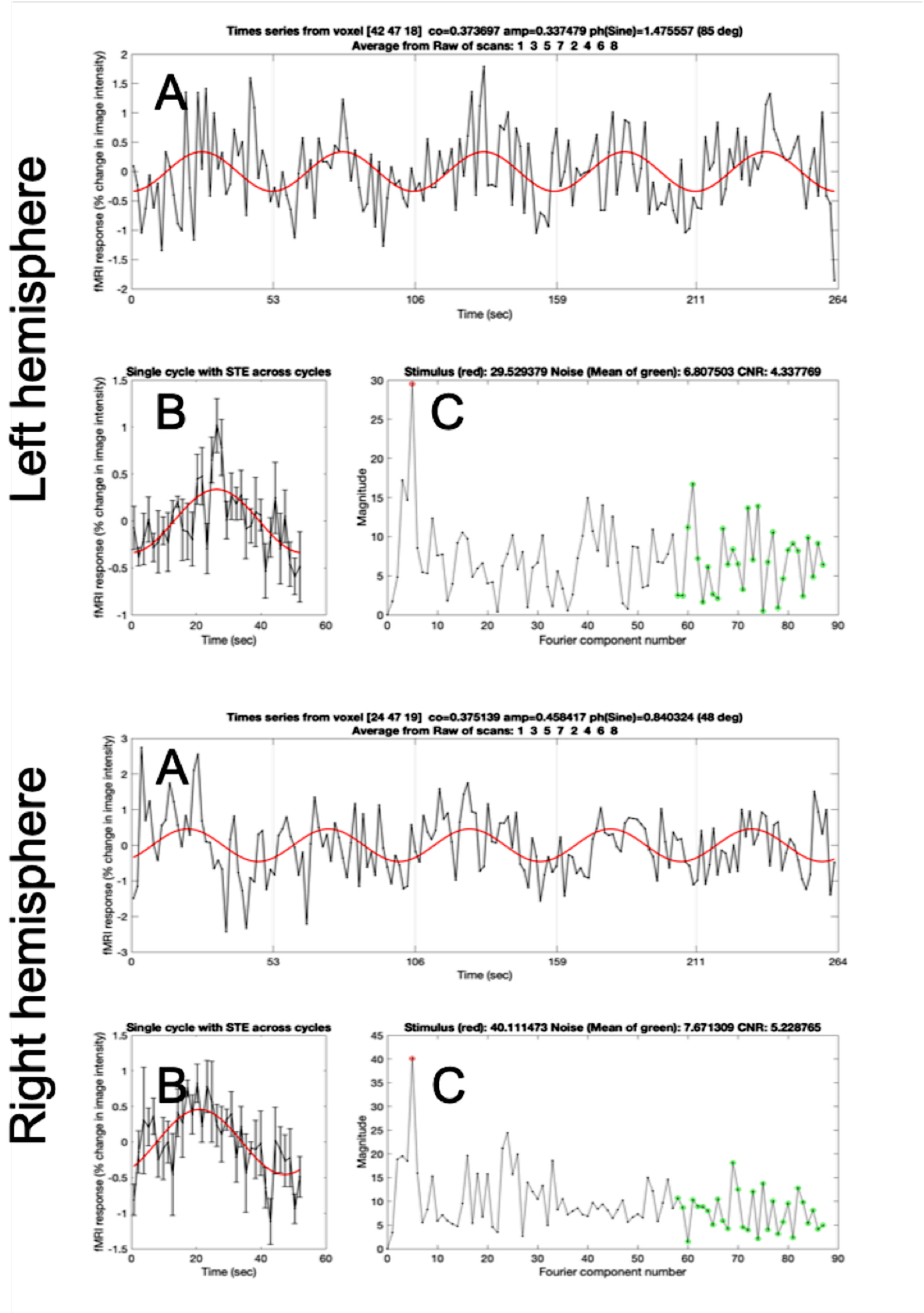

Figure 4. Averaged timeseries (A), mean BOLD responses (B) and Fourier spectra (C) for a representative participant for Experiment 1. The figure demonstrates the contralateral bias in the Torso Center position. These single participant plots represent

the Torso Center position (or control condition). The average time-series follows a sinusoidal pattern with 5 noticeable peaks. This dataset demonstrates a strong stimulus periodicity at 5 cycles per functional run, consistent with the stimulus periodicity (or 5 memory-guided saccade repetitions 'around the clock') per scan run. In the bottom right panel, the Fourier peak further shows a peak at '5'. LH: left hemisphere; RH: right hemisphere.

Coherence Maps

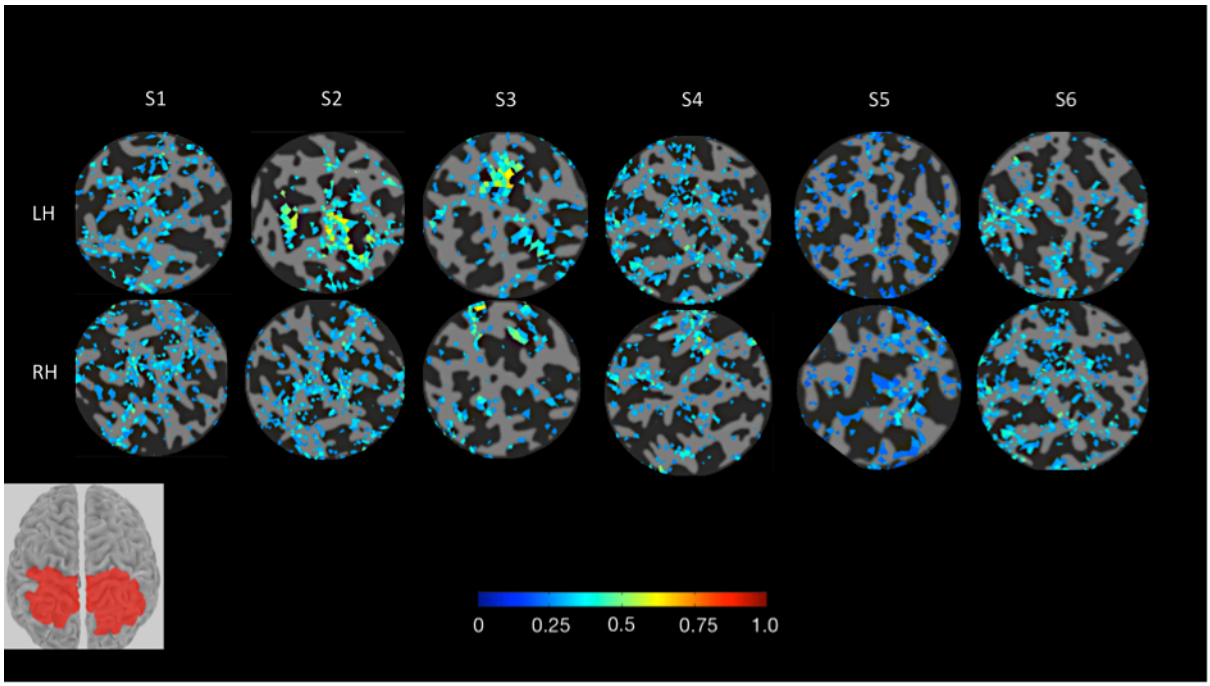

Figure 5. Computationally flattened representations of the superior parietal cortex in Experiment 1. The figure demonstrates high coherence (i.e. correlation with the 5-peak reference waveform) in every participant for the Torso Right condition that corresponds to the 5 saccades made to each target location. For this condition, all participants exhibited c>0.25 coherence voxels and all had clusters of voxels with =>0.7 coherence, or p<.000001. Insert: red colour indicates the area selected on the grey matter surfaces to be flat-mapped. LH: left hemisphere; RH: right hemisphere.

Regions of Interest

For 4 out of 6 of our participants, the superior parietal cortex voxels exhibited a contralateral bias in both the left and right hemispheres in the Torso Center condition. Memory-guided saccadic eye movements to the left side of the invisible clock-face are

over-represented in the right hemisphere and vice versa (**Fig 6**). In the left hemisphere, green (or right of fixation) voxels were overrepresented and red/violet voxels (or left of fixation) were overrepresented in the right hemisphere (S1 – S4). This indicates that certain regions of cortex within left superior parietal cortex represent rightward saccades and regions within the right superior parietal cortex overrepresent leftward saccades. This was not the case for Torso Left and Torso Right - only when the torso is centered (TC) on the scanner bed (or in the natural supine position) was the contralateral bias observed.

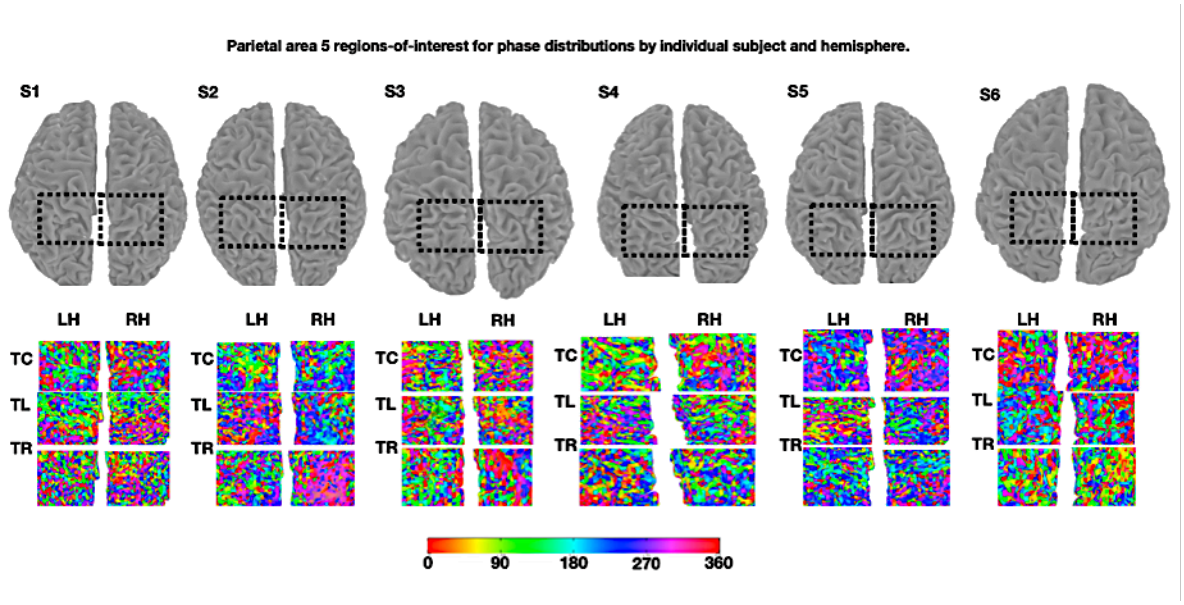

Figure 6. Regions-of-interest and phase maps by individual participant and hemisphere for Experiment 1. Top panel: superior parietal approximate ROI. Bottom panel: Phase maps across the entire superior parietal cortex for the control (or Torso Center), and also the Torso Left and Torso Right conditions for each the six participants tested. Green voxels that predominate in the left hemisphere of the superior parietal cortex for participants S1 – S4, exhibit a slight preference for delayed saccades toward the right hemifield relative to fixation, and violet/blue voxels that predominate in right superior parietal cortex indicated a preference for delayed saccades toward the left saccade hemifield relative to fixation. LH: left hemisphere; RH: right hemisphere.

Circular Statistics

The contralateral bias represented in the different phase values for each hemisphere was then confirmed statistically. There was a significant difference in the median phase values for the left as compared to the right superior parietal cortex for the Torso Center condition. Descriptive statistics for the phase representations for different torso orientations (median values and corresponding standard deviations) were as follows: Torso Left, Left Hemisphere: 297°(135), Right Hemisphere: 251° (71); Torso Center, Left Hemisphere: 147° (69), Right Hemisphere: 236° (62); Torso Right, Left hemisphere: 247° (71), Right hemisphere: 299° (60). These directions are visually displayed by the polar histograms in **Fig 7** in a cumulative plot (top row) and also for all of the individual participants (subsequent rows).

Via the cm-test, there was a significant contralateral bias for Torso Center (TC) across the two hemispheres, left hemisphere (LH) vs right hemisphere (RH), $p<.005$. There was also a significant effect and a marginally significant effect for Torso Left as compared to Torso Center for the left and right hemispheres $p<.0001$ and $p=.07$, respectively. There was a significant effect for both hemispheres for Torso Right as compared to Torso Center, $p<.0001$ and $p<.0001$. Polar histograms were then computed to visually display the saccade phase distributions across both the left and right superior parietal cortex for all three (left, center and right) torso orientation conditions. The cm-test does not provide degrees of freedom and this is why only the p-values are reported here.

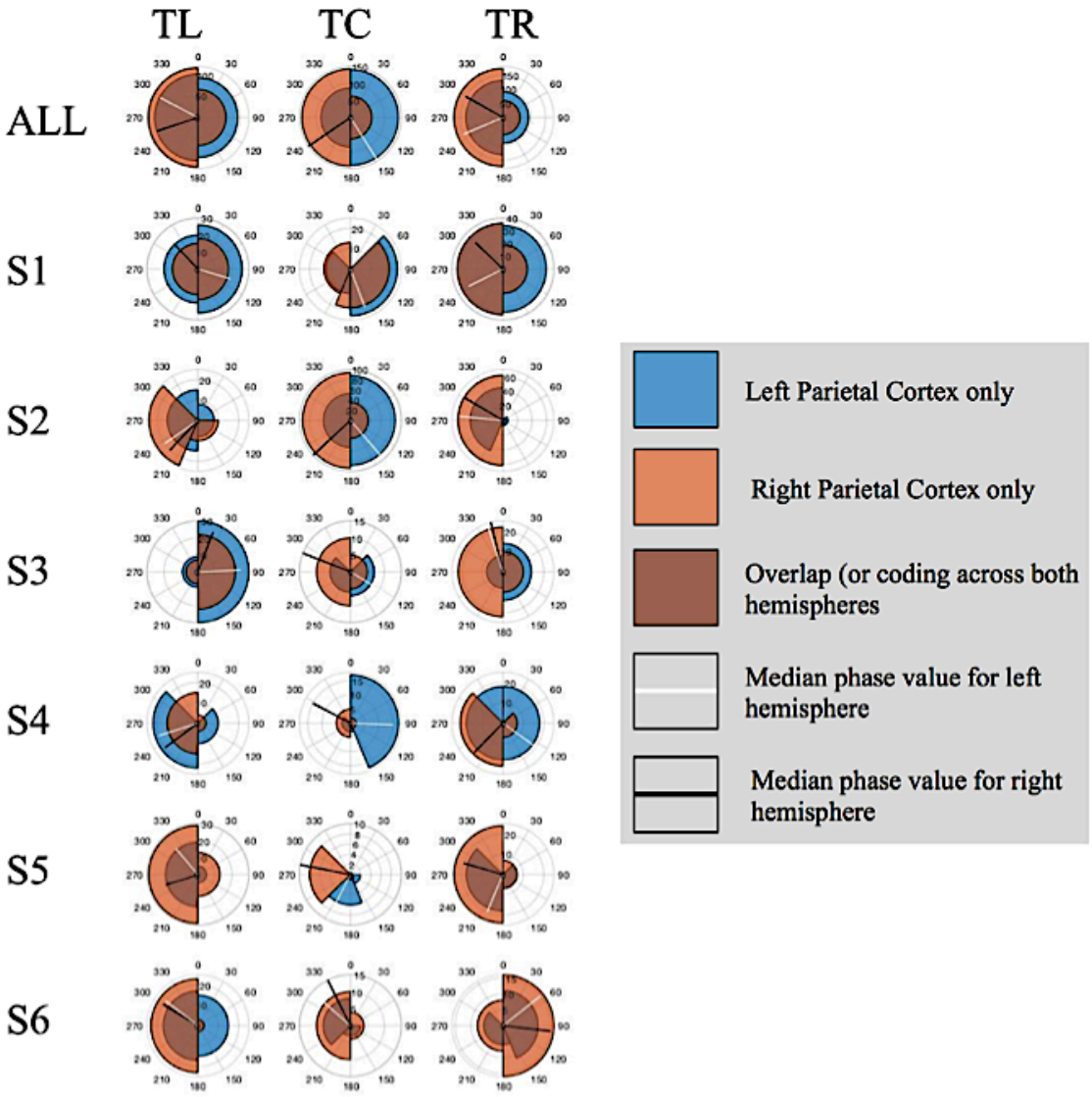

Figure 7. Participant-pooled (top row) and single participant polar histograms for the fMRI Experiment 1 (subsequent rows). The figure above shows group averaged activity in the top row and single participant activity in the subsequent rows (S1-6) during the Torso Left (TL), Torso Center (TC) or control condition and Torso Right (TR) condition. Activation for the left and right superior parietal cortex is represented in blue and orange colours, respectively, and the brown area represents activation of both the left and right superior parietal cortex. The white line represents the median for the left hemisphere and the black line the median for the right hemisphere. Eccentricity values reflect the average level of activation in the PPC at group and single-subject level during the delayed-saccade task with the centre of the plot representing no related activity. Note: full resolution figure is available in the Appendix (**Appendix A**).

Figure 7 shows how, with the torso rotated either to the left or right, the median phases shifted toward the left half of the polar histogram (or toward the left visual field). This is

highly prominent in the cumulative plots (ALL, top row). For Torso Left, this was the case, again, for 4/6 participants and also for Torso Right (4/6 participants showed the rotation effect). The median phases inverted their preferred direction for the left (LH) and right hemispheres (RH) for Torso Left as compared to Torso Right (or the black and white median lines inverted across the two hemifields). This was the case for all (6/6) participants tested. There is a level of hemispheric overlap (brown area) indicating the presence of voxels in both the right and left hemisphere showing activation for targets located in the left and right visual field and therefore not exhibiting hemispheric preference or contralateral bias. However this is a smaller portion of voxels in most of our participants. A significant degree of individual variability can also be noted. This is likely due to the amount of saccades performed as well as the limited control over the way saccades were performed by each participant and will be further explored in the discussion.

2.1.4.2 Experiment 2

Experiment 2 aimed to examine the effects of the same 20° torso rotations used in Experiment 1 on the accuracy and reaction time of saccades. The control experiment demonstrates that there was no effect of torso rotation on different saccade markers, **Table 1**. These data are for a separate, off-line experiment performed outside the scanner. The participants' torso was rotated by 20° via an in-house custom-built rotatable chair (refer to **Materials and methods**).

Reaction Time

The effect of torso rotation on saccadic reaction time was not statistically significant ($F(2,10)= 0.449$, $p= 0.082$, $\eta^2= 0.168$,) nor was the interaction significant between torso orientation and visual field (left versus right; $F(2,10)= 0.889$, $p= 0.151$, $\eta^2= 0.302$).

Amplitude Error

There was no significant main effect of torso orientation ($F(1.027, 5.137)= 0.460$, $p=0.532$, $\eta^2= 0.270$) or visual field ($F(1,5)= 2.913$, $p= 0.149$, $\eta^2= 1.076$) on saccade amplitude error. The interaction of torso orientation and visual field was also non-significant ($F(1.571, 7.855)= 0.280$, $p= 0.504$, $\eta^2= 0.280$).

Angular Error

Torso orientation did not show a significant effect on saccade angular error, ($F(1.723, 8.616)= 0.341$, $p= 0.690$, $\eta^2= 0.148$). No significant interaction was observed for torso orientation and visual field ($F(1.042, 5.212) = 0.567$, $p= 0.491$, $\eta^2=0.316$).

Cartesian Error

Neither the main effect of torso orientation nor visual field was significant ($F(2, 10)= 0.003$, $p= 0.997$, $\eta^2= 0.002$; $F(1,5)= 3.444$, $p=0.123$, $\eta^2= 1.206$). Finally, there was a non-significant interaction of torso orientation and visual field ($F(2,10)= 1.387$, $p= 0.294$, $\eta^2= 0.437$).

Summary

The results of the behavioural experiment demonstrate that saccade metrics are not dependent on torso orientation. The average delayed saccade Cartesian Error scores are

shown in **Table 1**. This circumvents potential claims that the shifting of superior parietal phase maps seen in **Experiment 1** are owing to differences in the landing error of saccades as a function of torso position.

Table 1

Average delayed saccade Cartesian Error scores

Visual Field	Torso Orientation	Mean (pixels) and Standard Error
Right	Right	124.39 (12.81)
	Left	144.50 (11.70)
	Center	140.10 (18.26)
Left	Right	163.40 (19.81)
	Left	141.60 (07.21)
	Center	145.76 (11.47)

The Mean and Standard Error values in pixels for the saccades across each of the different torso orientation conditions (Right, Left, Center) separated by visual field.

2.1.4.3 Experiment 3

Interpreting the leftward rotations for both Torso Left and Torso Right is complicated for the following reasons: both shoulders, both hands, both arms and both legs were rotated in the torso rotations of Experiment 1. The aim of Experiment 3 was to explore possible differences in the saccade topographic maps in the human posterior parietal cortex when the dominant right hand is placed in one of two possible static positions during the delayed saccadic eye movement phase mapping protocol.

Fourier Plots

A coherence analysis for the averaged time series of our data and a best-fitting sinusoid was computed (refer to **Materials and methods** for Experiment 1) and used the same coherence threshold of c>0.25 for this experiment as a threshold to filter out low CNR voxels as in **Experiment 1**. The number of remaining active voxels within our region of

interest was used to compute Fourier Spectra for each participant's hemisphere and condition. A representative averaged time series for HR (hand along the body and our control condition) and Fourier spectra are shown in **Fig 8**. Analogous to Experiment 1, these voxels are representative and were apparent in all participants. A representation of the coherence level for HR achieved by the 7 participants is presented in **Fig 9**.

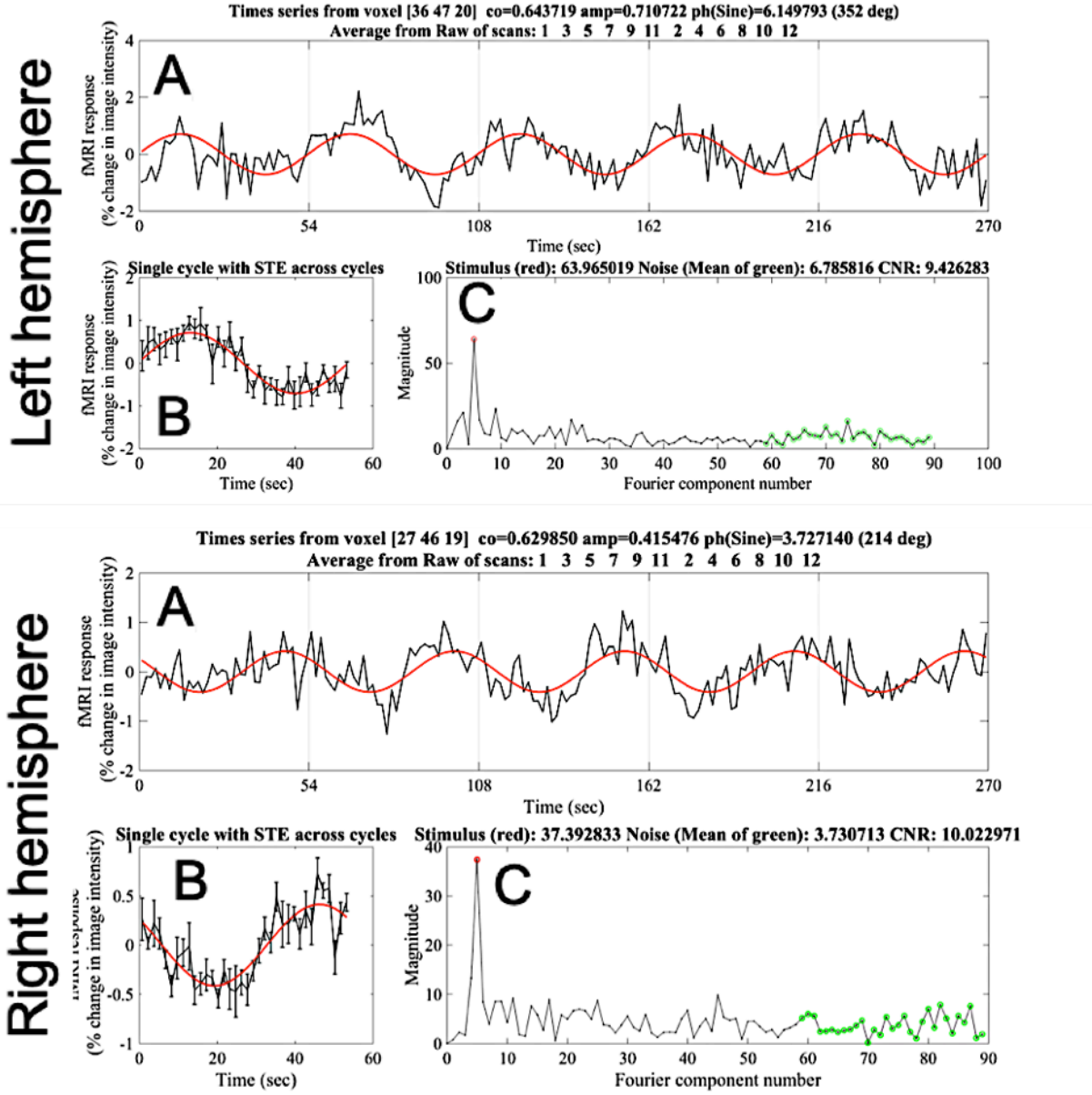

Figure 8. Averaged timeseries (A), mean BOLD responses (B) and Fourier spectra (C) for a representative participant in Experiment 3 demonstrating the contralateral bias in the HR (control condition) position. This participant's dataset

demonstrated a strong stimulus periodicity at 5 cycles per functional run, consistent with the stimulus periodicity (or 5 repetitions 'around the clock') per scan run. The single average time-series (bottom left panel) shows a peak for the green (or 90° phase orientations) in the left hemisphere and a phase trough corresponding to the opposing violet (or 270°) in the right hemisphere. In the bottom right panel, the Fourier peak further shows a clear peak at '5'

Coherence Maps

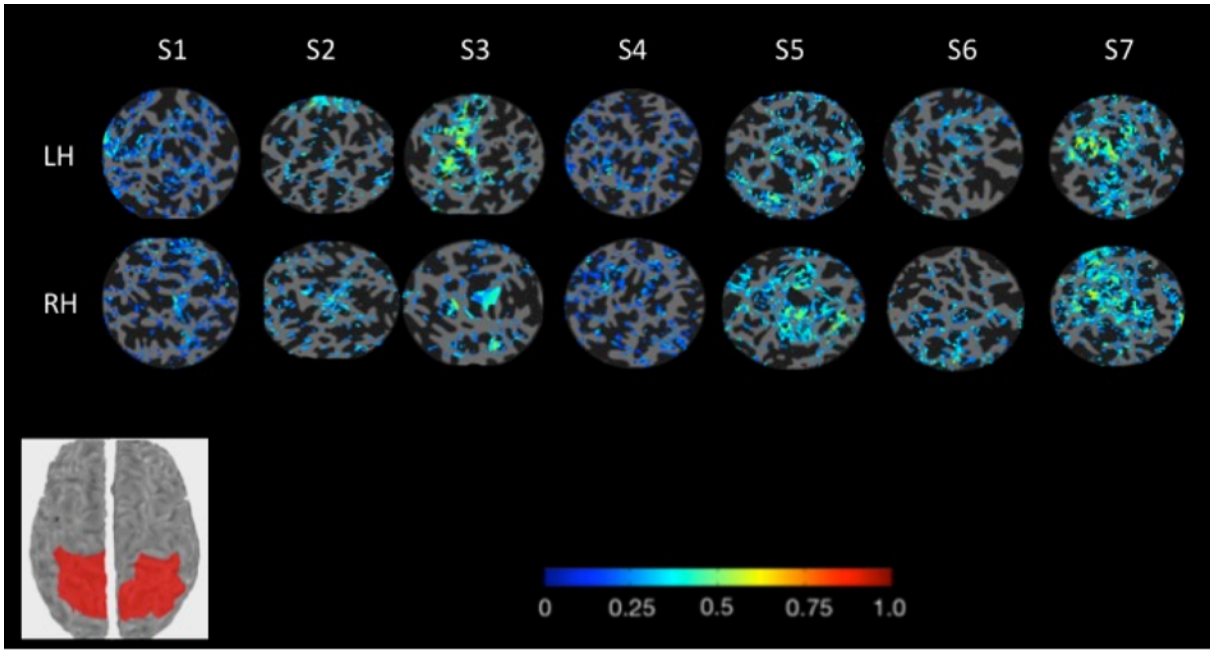

Figure 9. Computationally flattened representations of the superior parietal cortex that demonstrate high coherence (or correlation with the reference waveform) in every participant for the HR condition. For this condition, all participants exhibited c>0.25 coherence voxels and all even had clusters of voxels with c=> 0.7 coherence, or p<.000001 as in Experiment 1. Insert: the red colour on the segmented surface indicates the area selected on the grey matter surfaces to be flat-mapped and roughly approximates the superior parietal cortex whereas the ROI was determined via precise sulcus boundaries on the segmented surfaces (refer to Material and Methods). LH: left hemisphere; RH: right hemisphere.

Fig 10 presents the phase maps with coherence = 0 on segmented surface images for all 7 participants for both conditions of the static hand position experiment.

In the HR control condition, a higher relative proportion of the colour green is observed for the left hemisphere whereas the right hemisphere exhibits a relatively higher proportion of the colour violet/purple. This is quantified in Fig 11 and was also confirmed statistically. In the phase colour legend, green represents a phase value of 90° (right visual field) whereas purple/violet corresponds to a phase value of 270° (left visual field).

Regions of Interest

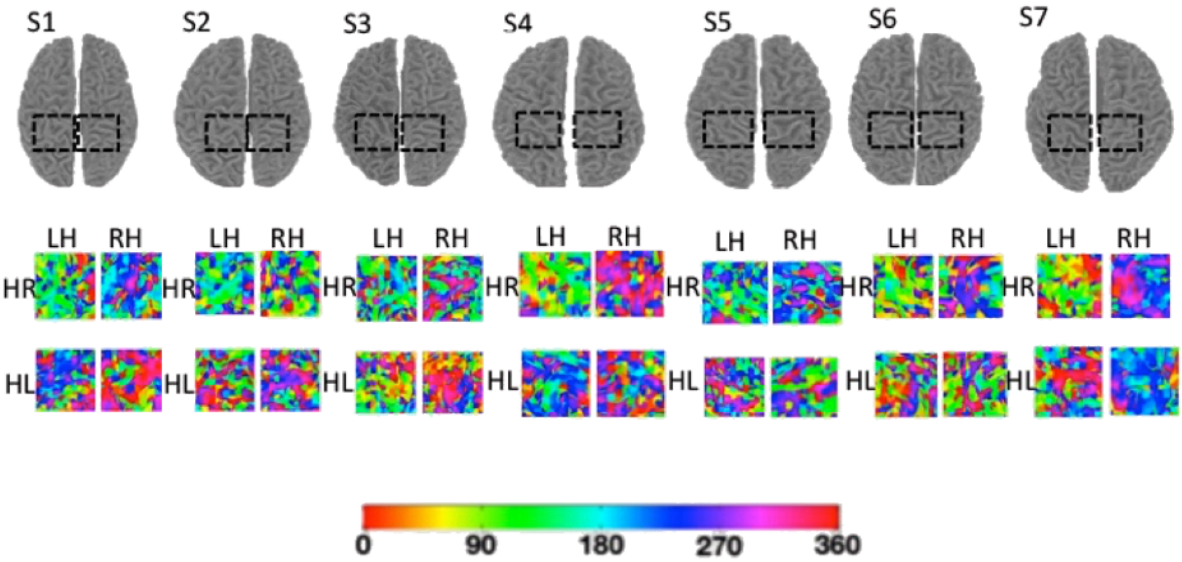

Figure 10. Regions-of-interest and phase maps by individual participant and hemisphere for the static hand position experiment. Top panel: approximate superior parietal ROI. Bottom panel: Phase maps across the entire superior parietal cortex for the control (or HR, and also the HL condition for each of the participants tested. Green voxels that predominate in the left hemisphere of the superior parietal cortex show a preference for saccades toward the right of fixation, and violet/blue voxels that predominate in right superior parietal cortex indicate a preference for saccades toward the left of fixation. LH: left hemisphere; RH: right hemisphere.

We defined our ROIs for each participant in an identical fashion to Experiment 1 (refer to Materials and methods) on the segmented brain images. We then imported these

ROIs onto the segmented brain image of the remaining condition and used the voxels contained in these boundaries to compute polar histogram plots in MATLAB. The polar histograms in **Fig 11** represent the phase maps for HR (Position 1 or the control condition) or HL (Position 2) in the superior parietal cortex for the left (LH) and right hemispheres (RH). **Fig 11** depicts the average median phases across participants for HR in the left and right hemispheres. Analogous to Experiment 1, we can then deduce whether or not the LH presents an over-representation of the right side of space and whether or not the opposite pattern holds true for the RH.

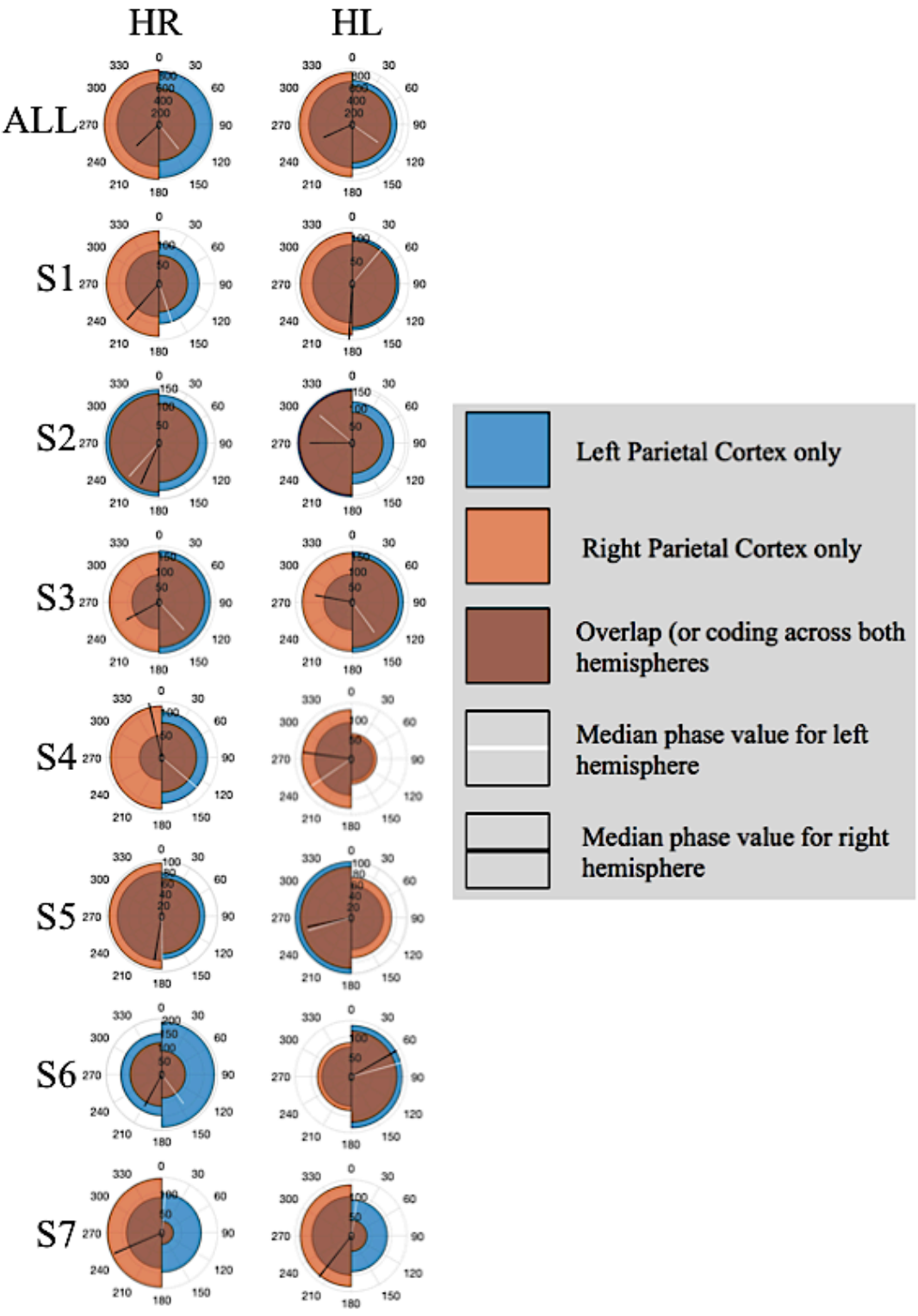

Figure 11. Participant-pooled (top row) and single participant polar histograms for the change in static hand position fMRI experiment (subsequent rows). The figure above shows group averaged activity in the top row and single participant activity in the subsequent rows (S1-7) during the Hand Right (HR) or control condition and Hand Left (HL) condition. Activation for the left and right superior parietal cortex is represented in blue and orange colour, respectively. The brown area represents activation of both the left and the right superior parietal cortex (overlap). The white line

represents the median phase direction for the left hemisphere and the black line the median phase direction for the right hemisphere. Eccentricity levels reflect the average level of activation recorded in the PPC at group and single-subject level during the performance of delayed saccades with the centre of the plot representing no delayed saccade-related response. Note: full resolution figure is available in the Appendix (**Appendix A**)

As visible in **Figure 11**, there is a contralateral bias for saccade location in superior parietal cortex in the HR (or control) condition for 6/7 of the participants tested (S1, S3-S7) and the cumulative plot (ALL, top row), shows a contralateral representation in the superior parietal cortex. For HL, this was not the case. In HL, the median phase preference shifted toward the left side of space, but this was only true for the left hemisphere (or the hemisphere contralateral to the dominant right hand). There is also a level of hemispheric overlap (brown area) indicating the presence of voxels in both the right and left hemisphere showing activation for targets located in the left and right visual field and therefore not exhibiting hemispheric preference or contralateral bias. However this is a smaller portion of voxels in most of our participants but S2, interestingly the only participant not exhibiting a median contralateral bias. Individual variability is visible in this occasion as well and will be explored further in the discussion. Note: critically, the hemispheric response asymmetry between the two hand positions argues against a simple change in the magnetic field in the brain due to the position of the limb.

Circular Statistics

Differences between the circular pattern of the phases for each hand position were quantified for each hemisphere via the same parametric multi-sample test for equal median values. For the right hemisphere superior parietal cortex for HR as compared to

HL revealed a non-significant difference with p=.1774. However, a highly significant effect for the left hemisphere superior parietal cortex for HR as compared to HL is reported, p=.001. Again, we cannot provide the Degrees of Freedom here owing to the nature of the statistic cm-test.

2.1.5 Discussion

The present experiments provide support for the idea that the phase maps (or saccade vectors) of the posterior parietal cortex for memory-guided topographic saccadic eye movements are altered by subtle static alterations of torso (**Experiment 1**) or even a single hand position (**Experiment 3**). Existing related literature reports topographic maps in the PPC but these are often not identical between studies despite the methodological paradigms being the same (Sereno et al., 2001; Schluppeck et al., 2005; Kastner et al., 2007). If static changes in the position of the body can alter the phase maps of saccades, this may be a crucial contributing factor to the variability reported in the literature. This is important to establish in order to allow future studies of memory-guided saccade topographic mapping to enhance their Contrast-to-Noise Ratio (CNR). The more consistent these phase maps are across participants and conditions, the more feasible it is to average the maps to reveal the signal. This can have a significant impact on the general understanding of the role of the PPC in multisensory integration. PPC has been associated with a number of processes including, amongst others, attention, movement intention and actuation (Andersen and Zipser, 1988; Snyder, Batista and Andersen, 2000; Buneo and Andersen, 2006). However, a clear distribution of anatomical locations within PPC for the computation of these processes has yet to be defined (Schluppeck et al., 2005; Connolly et al., 2015; Mullette-Gillman, 2005; Colby and Goldberg, 1999; Snyder, 2000). Topography has already helped significantly in mapping areas of the PPC (Sereno et al., 2001; Schluppeck et al., 2005; Connolly et al., 2002; Connolly et al., 2015), however, the variability evident within the existing literature could hinder further progress.

Although only the superior parietal cortex was investigated in the present study, the results from the current series of experiments may contribute toward explaining differences in signal quality across earlier delayed saccadic eye movement topographic mapping studies and thus provide novel knowledge on the functional organisation of this brain area as well as method-based constraints for those carrying out similar future experiments. Specifically, the participants' fixation mid-line, hand position, shoulder position, waist position, or leg position (crossed or uncrossed) could cause alterations in the underlying cortical phase maps and overall data signal quality. It is therefore important that cognitive neuroscientists that engage in future parietal and frontal topographic studies of delayed saccades rigidly control for the participant's entire body configuration and fixation location relative to the sagittal midline of the face.

Comparison with earlier delayed saccade topography studies

Previous studies have successfully confirmed the occurrence of memory-guided saccade topographic mapping in the human Posterior Parietal Cortex (i.e., Sereno et al., 2001; Schluppeck et al., 2005;Kastner et al., 2007). Within the existing literature, however, there seems to be little mention of the exact position of the participants' body during the scanning procedures. Although all of these earlier studies mentioned above report saccade topographic maps and show very low levels of noise recorded, there is high variability in the maps found even when the stimuli used are kept the same. If the topographic mapping represents the way the posterior parietal cortex encodes for space during visual exploration, and the visual stimuli is kept consistent across experiments, the resulting maps should be closely replicated and less variability should be found. One argument I am proposing with this study is that it could be the case that the body position of the participants was not actively controlled for and keeping this

equal across sessions, and across experiments, would have minimised the variability and also improved their already high signal quality.

The implications of the findings hereby reported can be also relevant to future studies that employ either parietal or frontal memory-guided saccade-related topographic mapping protocols.

However, there are also other methodological differences between these studies and the present experiments that should be considered in order to properly assess the possible contribution of static hand and torso. These might also help to explain the nature of the significantly lower CNR hereby obtained as compared to the aforementioned examples (Sereno et al., 2001; Schluppeck et al., 2005;Kastner et al., 2007). Notably, these authors used dental impression-based bite bars that were individualised for each participant and a Siemens Small Flex coil that were not used in the present experiments and both of these differences would have enhanced their signal-to-noise ratio (Sereno et al., 2001; Schluppeck et al., 2005). Kastner and colleagues (2007) used a 3Tesla scanner and a standard birdcage coil similar to those used in the present study. However, they also applied a higher resolution of 2 x 2 x 2 mm voxels that may have contributed to the higher quality of topographic maps found.

The overall amount of scanning in the previous studies mentioned was also far superior to that of the present set of experiments with often two to three scanning sessions each lasting ~1.5 hours and with a number of performed saccades falling between 720 and 1,440 (Sereno et al., 2001; Schluppeck et al., 2005). For comparison, in the present experiment 1, participants executed only 480 saccades per Torso Orientation Condition and this is across our two experimental sessions. Additionally, in one occasion (Kastner et al., 2007), authors presented their targets at ~10° eccentricity (whereas we presented at 7.7° eccentricity) and therefore the saccades were of a

relatively greater amplitude as compared to the present study which could also have contributed to a higher CNR. As previously stated, the CNR is a representation of the level of fMRI-BOLD activity recorded during the presentation of the stimuli compared to the level of brain activity not directly elicited by the task, or noise. Therefore, the CNR represents a direct measure of the quality of the signal recorded within each voxel and a summary of the level of coherence and phase averaging –definitions for which can be found in "Materials and Methods – fMRI data analysis and procedure"- held by the data. So, our coherence and phase averaging was likely reduced owing to the fact that we had fewer saccades of smaller amplitude in the Torso Center condition (and also identically in the Torso Left and Torso Right conditions) because of additional experimental conditions (3) per session. This will have diluted the number of saccades per condition in our experiment. The low number of saccades per condition may have contributed to the high individual variability reported in our results (**Figure 7** and **11**). Being able to collect more data through additional testing sessions may have allowed us to replicate findings present in the previous literature with regards to the overall data quality. The same arguments can be made with regard to the relatively lower CNR for the 3 static eye position experimental conditions of a previous delayed saccade parietal topographic experiment by Connolly and colleagues (Connolly et al., 2015). To further corroborate this view, Experiment 3 of the present study had 2 rather than the 3 conditions of Experiment 1 and exhibited relatively 'cleaner' maps in the human superior parietal cortex. This difference can be quantified in the lower amount of noise registered in the phase maps of Experiment 3 as compared to Experiment 1 and can be also noted by comparing panels C of **Figure 4** and **Figure 8.** In these graphs, the average amount of noise registered (green dotted line), the hemodynamic response to the stimuli (red dotted peak) and the ratio between these, the CRN, are reported on the top of the panel.

A higher CRN reflects higher quality of data collected and therefore higher quality fMRI images and resulting phase maps. This provides evidence that sufficient data averaging is vital. Acquiring 6 fMRI runs per subject might have aided us in meeting the same amount of data averaging reported in previous literature.

Furthermore, a different coherence threshold was also applied. Where previous studies set a coherence threshold of $c > 0.2$, we instead used anatomical boundaries to carry out further analyses on all voxels in only the superior parietal cortex with a coherence of 0.

The performance of saccades in the scanner was not controlled for. A head-mounted, fMRI compatible eye tracker may have helped filtering adequate saccadic eye-movements to the displayed targets similarly to the way data was handled for the control experiment (Experiment 2). This may have had a positive effect in the signal quality hereby reported and/or function as a support for the individual variability recorded in the related phase-maps.

The sample size to condition number ratio also functioned as a limit to the analytical and statistical options that could be adopted. In the future, adequate number of participants and scanning runs should help in containing this issue and allow for more conventional statistical methods to be used. This would allow comparing the results with those available in the existing literature in a more direct way as well as aid strengthening findings.

Because of the other methodological differences detailed above, we cannot conclude that our experimental static position changes account for any contrast-to-noise ratio differences between the present study and previous examples in the existing literature. Nevertheless, based on our results, body configuration is a key methodological constraint that all parietal and frontal topographic mapping scientists

should be made aware of. To the best of our knowledge, the specific postural position is not stated in these early manuscripts, but presumably could have affected – or weakened their CNR – relative to their already outstanding maps, should foam padding have unevenly raised one of the two shoulders (Experiment 1) or even if one of the participants' hands have been resting on the stomach (Experiment 3).

Implications for spatial coordinate representations

The present results also have a non-methodological bearing on the functional nature of spatial reference frames in superior parietal cortex. When the torso was rotated, preferred saccade directions in the right hemisphere shifted toward the left side of visual space and somewhat surprisingly the same was also true for the left hemisphere. Moreover, the median phase directions actually inverted for Torso Left as compared to Torso Right and this was true for all of the participants examined in Experiment 1. It was then established that the differences in the phase maps in the superior parietal cortex shown in Experiment 1 were not due to changes in the quality of saccades as executed in the three torso rotation conditions (Experiment 2). This was achieved by performing behavioural eye-tracking assessments using the same memory-guided saccade paradigm alongside analogous torso rotation manipulations using a rotatable chair. In all four saccade kinematic measures tested (Reaction Time, Amplitude Error, Angular Error & Cartesian Error) torso orientation had no significant effect. These findings are in line with previous literature employing eye-tracking-based paradigms with comparable manipulations of torso position (Scherberger, Goodale and Andersen, 2006; Grubb and Reed, 2002). Interpreting the leftward rotations for both torso left and torso right in Experiment 1 is complicated, however, for the following reason: both shoulders, both hands, both arms and both legs were rotated. This led us to carry out

the single hand static rotation condition of Experiment 3. Nevertheless, the observation that these median phases rotate in such a significant fashion demonstrates that body-centric coding may be highly prevalent throughout human superior parietal cortex. The subtle change in the static hand position of Experiment 3 is also clearly registered within the human superior parietal cortex when performing saccades to a certain location in space and this is reflected in a shift in the encoded saccade-end points. In other words, since it is the right hand's position that was changed across the two conditions, the contralateral (or left) superior parietal cortex must contain a dominant-hand based frame of reference. Such a finding supports results in the existing literature arguing in favor of a hybrid or exclusive body-centered coding in both the non-human primate and human parietal cortex (Connolly et al., 2015; Bosco et al., 2016; Boussaoud and Bremmer, 1999; Duhamel et al., 1997; Pertzov et al., 2011; Mullette-Gillman, 2005; Mullette-Gillman et al., 2009). Owing to the fact that the behavioral paradigm (the memory-guided saccade task) that was used in HR and HL was held constant, the eye movements, retinal stimulation and the head position were all the same across the two conditions. Assuming the eyes, the two retinae or the head represent the only frame of reference when coding for saccades, this would result in an exact replication of the phase maps recorded in HR. However, this was not the case. This conclusion is further supported by the fact that the results of HR (in Experiment 3) and Torso Centre (in Experiment 1), taken alone, replicate findings of previous studies with regard to the contralateral bias (Konen and Kastner, 2008; Sereno et al., 2001; Connolly et al., 2015; Schluppeck et al., 2005; Kastner et al., 2007). According to this well-established effect, memory-guided saccades aimed at targets located to the right side of space of the observer, will elicit a stronger fMRI-bold response in neurons located in the left hemispheric PPC and vice-versa for targets located to the left of the observer. In both

Experiment 1 and 3, our control conditions (Torso Centre for experiment 1; Hand Right for Experiment 3), we clearly show a contralateral preference in human PPC (**Figure 4** and **8**). The observation of a change in the phase maps for the contralateral superior parietal region of interest relative to the dominant (right) hand (or only in the left hemisphere), suggests that an additional factor has come into play when coding for space. As the only manipulation in the current study was the location of the dominant hand in HL with respect to HR (control condition), we can conclude that the dominant hand is the only recognizable cause for the observed change in the recorded phase maps. This has significant impact on a methodological level, suggesting that in order to achieve reliable and valid topographic maps of the PPC during delayed-saccades, the position of the body in space should be controlled for during the experimental sessions. Furthermore, it supports our basic understanding of the encoding processes existing within PPC used to transform visual coordinates, and to integrate these with proprioceptive feedback originating within the body in preparation for action.

These results therefore further enhance our knowledge with regard to the underlying nature of spatial reference frames in this essential sensorimotor area of the human cerebral cortex.

2.1.6 Conclusions

The present results provide important methodological insights to enhance the data quality for parietal and frontal delayed saccade topographic fMRI studies. In the parietal cortex, there exists a disparity in the data quality and conclusions across these fundamental experiments. Although efforts are made by cognitive neuroscientists to make sure eye position remains constant across experimental conditions, we demonstrate that subtle alterations in the posture of the torso or a single hand can

induce alterations in the phase representations on the cortical surface. Although it is unknown whether or not earlier studies controlled for shoulder or hand position etc. per se, it is possible that such controls could have enhanced their already high CNR. Future experiments using parietal or frontal topographic fMRI procedures must constrain torso, arm/hand, midline eye and leg positions over different experiments and experimental conditions. To acquire optimal maps, the participant must be largely physically restricted and all body parts must be positional-consistent across studies to enhance both CNR and comparability.

2.1.7 Acknowledgements

The authors wish to thank Konstantin Volkman (Cambridge University, UK) and Simon Thurlbeck (Durham University, UK) for the diagram of the torso rotation experiment and the hand position experiment, respectively and Dr Colin Lever for comments on the manuscript.

2.1.8 Funding

Alessia Cacace is part of the Innovative Training Network 'Perception and Action in Complex Environments' (PACE). The PACE project has received funding from the European Union's Horizon 2020 research and innovation programme under the Marie Sklodowska-Curie grant agreement No 642961.

2.2 The effect of subtle static hand position changes and imagined eye movements on saccadic eye-movement kinematics in neurologically intact individuals

2.2.1 Abstract

The effect of proprioceptive feedback originating from the body on eye-movement performance and proficiency is still being investigated. Whilst some evidence exists on how manipulation of proprioceptive feedback can help decrease symptoms of neglect, results on neurologically intact individuals are mixed. If postural changes and body position can alter the performance of eye movements, reliability of eye-movement based diagnostic and rehabilitation techniques is under debate. Additionally, extensive practice of saccades is linked to increased accuracy and lower reaction times in healthy population. However, scarce evidence is found on the effects of practice through imagined eye movements. In this study, we investigate the effect of static hand positions as well as the imagined eye-movement practice on the accuracy and reaction times of memory guided saccades. Seven participants with no prior history of neurological conditions were asked to perform a series of saccades to memory held locations whilst their hand was in two different positions. Additionally, participants performed a series of imagined eye movements prior to the execution of real eye saccades to the same locations. Overall, we found no significant differences in the accuracy and reaction times of memory guided saccades when manipulating the dominant hand position. No significant differences were found in saccade metrics if preceded by practice through imagined eye movements. These results suggest that body position alterations that do not include the head or the neck do not affect performance of saccades. Moreover, practicing eye-movements through performance of imagined saccades does not seem to

facilitate following real performance of saccades. Implications for assistive techniques for motor impaired individuals are discussed.

2.2.2 Introduction

The ability to move and interact within the world requires a number of intricate processes that include visual exploration of space. By observing, individuals are able to map their surroundings and construct a detailed representation of objects or obstacles present in their immediate environment. An open debate exists on how exactly humans compute environmental information and in particular to what part of the body external space is related during that computation. Sensory afferent information originating from various parts of the body is aggregated and interpreted to create an internal sense of the position of the body in space and the body in relation to visual cues, which is necessary to execution of motor behaviour (Karnath, 1994). The posterior parietal cortex has been suggested as the key area of the brain where this integration process takes place (Andersen, Essick and Siegel, 1985; Andersen, Snyder, Li and Stricanne, 1993; Ilg, Schumann and Thier, 2002).

In the previous chapter, we reported how static alteration of torso and hand positions affects the way the posterior parietal cortex codes for saccadic eye movements. We discussed how these findings suggest that proprioceptive feedback originating from the torso, neck and hand seem to also be taken into account when encoding for space. We also reported that similar torso rotations do not affect the overall spatial accuracy and latency of saccadic eye movements, suggesting that proprioceptive integration might not have an effect on the way individuals perform

saccades; however, existing literature appears divided on the matter (Harris, 1994; Campbell and Robson, 1968; Schulmann, Godfrey and Fisher, 1987).

Proprioceptive feedback originating from the extra-ocular muscles has been linked to one's ability to orient oneself and interact with the physical world. Stretch receptors present on these muscles can provide information about the distance and location of objects in relation to the viewer's eyes (Cohen, 1960). Stretching of these muscles may occur during voluntary eye movements, when the eyes are exploring the external space but the head is relatively fixed, as well as by head movements where one's gaze is fixed but the head is moving (Harris, 1994). The effect of this feedback system on eye movements has been investigated mainly in relation to postural balance, and integration between proprioceptive feedback originating from the motor and visual systems appears to be necessary to diminishing body sway (Cambell and Robson, 1968). Being able to freely observe a scene has a positive impact on postural stability of participants asked to stand on one foot that significantly decreases when the eyes are closed (Edward, 1964; Gingsburg, Cannon and Nelson, 1980; Day, Steiger, Thompson and Mardsen, 1993). This suggests that visual input and proprioceptive feedback from the body are integrated to maintain balance. Similarly, integration between these cues is crucial in informing individuals on the nature of visual perception and body motion. A modification of the retinal image produces a change in the visual perception of a scene and this might be the result of eye movements alone, a movement in the scene being viewed, or movement of the head and body as well as whether this is voluntary or the result of external, uncontrollable factors. Being able to integrate visual and motor feedback can be crucial, therefore, in detecting self-motion and the nature of that motion (Harris, 1994).

However, the integration is not always infallible. A moving scene can induce illusory visual-vestibular interaction resulting in individuals perceiving self-motion when actually being stationary (Dichgans and Brandt, 1978). Sudden manipulation of only the visual input of individuals standing still induces body counter sways congruent with the resulting retinal manipulation (Gingsburg, Cannon and Nelson, 1980; Paulus, Straube, Krafczyk and Brandt, 1989). In other words, individuals adjust their posture according to the change of visual cue even when the proprioceptive feedback from the body standing on stable ground should counteract this. Similarly, performing saccadic eye movements to fixed targets as well as pursuit eye movements on moving targets appears to negatively affect stationary balance (Schulmann, Godfrey and Fisher, 1987).

Although this might suggest to some extent that visual cues can alter and overwrite proprioceptive feedback in the process of coding visual inputs, evidence is scarce on whether the opposite effect exists, where proprioceptive feedback originating within the body affects the performance of eye movements.

Externally applied vibration of the extra-ocular muscle induces illusory target shifts in healthy individuals and the effect appeared to summate when concurrent stimulation was applied to muscles located on the neck and ankle (Roll, Vedel and Roll, 1989). The vestibulo-ocular reflex (VOR), defined as a compensatory eye-movement initiated when a movement of the head is detected and aims to stabilize retinal images, is negatively affected by active, voluntary movements as opposed to static alteration of the position of the trunk in both non-human primates (Paige and Tomko, 1987) and healthy human primates (Morrow and Sharpe, 1993). Interestingly, reduced accuracy of saccadic eye movements is reported if the head, eye and torso are not aligned (Rossetti, Tadary and Problanc, 1994; Wexler, 2003; Harrar and Harris, 2009). A shift in saccades to the remembered locations of previously presented visual targets is also reported

when altering the position of the head relative to the body and the direction of the shift is opposite to the direction of the head displacement (Kopinska and Harris, 2003; Harris and Smith, 2008).

A further example of proprioceptive feedback influencing visual perception is reported in hemi-spatial neglect, a condition in which the affected individuals are unable to attend to the contralesional side of space, typically as a result of damage to the brain's parietal lobe (Vallar and Perani, 1986), frontal lobe (Husain and Kenard, 1997) and temporal lobe (Karnath, Ferber and Himmelbach, 2001).

Scanning therapy, a technique based on asking individuals to direct their gaze to the otherwise unattended side of space, has been commonly used to ameliorate signs of neglect (Diller and Weinberg, 1977; Weinberg, Diller, Gordon, Gerstman, Lieberman et al., 1977; Pizzamiglio, Antonucci, Judica, Montenero, Razzano and Zoccolotti, 1992). However, hemi-spatial neglect often comes with a level of unawareness that renders self-administered techniques quite limited in everyday use outside the laboratory environment and the effects are therefore transient (Paltron, Malhotra and Husain, 2004).

In a search for more universally applicable and effective rehabilitation techniques, related research has investigated the possible contribution of vestibular and proprioceptive alteration on the manifestation of neglect. Transcutaneous electrical stimulation applied to the contralesional side of the neck has been shown to temporarily improve neglect bias (Vallar, Rusconi, Barozzi, Bernardini, Ovadia, Papagno and Cesarani, 1995). Bilateral administration of a 100Hz vibration on the neck, as well as vestibular stimulation and torso rotations, induced a reduction in the signs of neglect in the patient population (Karnath, Christ and Hartje, 1993; Karnath, 1994; Karnath, 1995; Wiart, Come, Debelleix, Petit, Joseph, Masaux and Barat, 1997) and was later

reported to be long-lasting and significantly improve patients' quality of life (Schindler, Kerkhoff, Karnath, Keller and Goldenberg, 2002).

Related research on neurologically intact individuals reported the induction of neglect-like symptoms to the contralateral side of space following neck muscle stimulation and vestibular stimulation (Karnath, Fetter and Dichgans, 1996). A follow-up showed that proprioceptive and vestibular stimulation does not affect covert attention-related exploratory visual perception of space in healthy controls (Rorden, Karnath and Driver, 2001).

As a whole, these findings suggest that proprioceptive and vestibular feedback are a key factor in the presentation of hemi-spatial neglect. Furthermore, these factors support the hypothesis that sensory integration of peripheral cues based on whole body-centred rather than exclusively retinal-centred coordinate frames exist when planning and computing visuo-motor behaviour (Karnath, 1994). In other words, proprioceptive, vestibular afferent information is centrally integrated with visual feedback and can therefore affect visual perception in the representation of egocentric space (Karnath, Fetter and Dichgans, 1996).

Unpublished work by our research group investigating the effect of torso rotation and hand displacement on saccadic eye movements reported significant differences in the accuracy of eye movements to remembered visual target locations (Crane, Podmore and Connolly, 2016 -unpublished). Subtle, involuntary head placement alterations occurring, but not controlled for, during the extreme torso rotations make the decoupling of the contribution of each individual manipulation of head, hand and torso quite hard to achieve. Later work on the effect of torso rotation alone on saccadic eye movements' accuracy reported no significant shifts in the localization of visual targets (Cacace, Podmore, Olkkonen, Kentridge and Connolly, 2019 – submitted).

When investigating the accuracy of eye movements, however, we must take into account the effects of practice. Fewer localisation errors as well as shorter reaction times might also be the result of repeated eye movements to the same locations, thus reflecting the effect of learning rather than proprioceptive facilitation. However, research on saccades' improvement has reported that accuracy and reaction times were only positively affected after days and sometimes months of continuous practice with a large number of saccades (~>200) performed in each session and the practice effect was not found to be long lasting in following re-tests (Fischer and Breitmeyer, 1987; Green, King and Trimble, 2000; Ettinger, Veena, Crawford, Davis, Sharma and Corr, 2003). Additionally, randomisation of the target locations further diminishes the effects of practice (Fischer and Ramsperger, 1986).

There is a general lack of evidence that a similar effect might be visible when imagining rather than executing saccades. However improvement through practice is recorded when executing limb or full body imagined movements on the subsequent execution of real movements in healthy and neurologically- impaired individuals (Gould, Damarjian, and Greenleaf, 2002; Dijkerman, Ietswaart, Johnston and MacWalter, 2004; Stevens and Phillips Stoykov, 2003).

As a final note, it is widely documented that a general level of inaccuracy exists when performing saccades. Individuals tend to perform larger saccades that go beyond the displayed target when moving towards it (centrifugal saccades) and perform shorter saccades in the return movement towards the centre (centripetal saccades). In other words, saccades tend to be hypermetric for far targets and hypometric for near targets (Becker, 1972; Robinson, 1973; Findlay, 1982; Kapoula, 1985; Kapoula and Robinson, 1986). It is also reported that saccadic eye movements to peripheral targets are usually the result of an initial pre-planned saccade that accounts for ~90% of the

distance from fixation to the target and a ~10% corrective saccade (Frost and Poppel, 1976; Kapoula and Robinson, 1986). A rightward bias has also been documented in the healthy population with significantly shorter latencies to saccades executed to the right visual field than those to the left visual field (Van Allen, 1973; Pirozzolo and Rayner, 1980). This is something of importance and that will need to be taken into account, especially in the context of data analysis and correct saccades selection.

The study of the possible implications of postural alterations and practice effect on eye movements' accuracy and reliability has particular relevance not only in the context of experimental research but also in the clinical and rehabilitative setting (Ramat, Leigh, Zee and Optican, 2007). Eye movements as well as saccades have been successfully employed as a diagnostic aid in schizophrenia (Fukushima, Fukushima, Chiba, Tanaka, Yamashita and Kato, 1988; Ross, Heinlein, Zerbe and Radant, 2005), multiple sclerosis (Mastaglia, Black, Cala and Collins, 1977; Meienberg, Muri and Rabinau, 1986), learning disorders (Pavlidis, 1985), attention deficit hyperactivity disorder (Munoz, Armstrong, Hampton and Moore, 2003), Huntington's disease (Folstein, Leigh, Parhad and Folstein, 1986; Beenen, Buttner and Lagne, 1986), Parkinson's disease (Leigh and Riley, 2000), dementia with Lewy bodies (Mosimann, Muri, Burn, Felblinger, O'Brien and McKeith, 2005) and hemi-spatial neglect (Meienberg, Harrer and Wehren, 1986). Failure to obtain accurate, reliable and replicable metrics can lead to misdiagnosis and result in ineffective or missing treatment that has considerable implications on the patient's wellbeing.

In the context of rehabilitation, eye movements and saccades are also often a key part in a number of brain computer interface (BCI) techniques. Most commonly, non-invasive and assistive BCI techniques make use of electroencephalography (EEG) to detect and transform brain signals, establishing a direct connection between the user

and the effector of choice (Walpaw, Birbaumer, McFarland, Pfurtscheller and Vaughan, 2002). The use of eye movement-related potentials is justified not only because of their high reliability and replicability but also because these are often the least- or last-affected in the event of motor disability (Leveille, Kiernan, Goodwin and Antel, 1982; Kotchoubey, Lang, Winter and Birbaumer, 2003). P300 (Krusienski, Sellers, McFarland, Vaughan and Wolpaw, 2008), steady state evoked potentials (Yi, Qiu, Wang, Qi, Zhao, He, Zhou, Jiang and Ming, 2017) and hybrid (Yin, Zhou, Jiang, Chen, Liu and Hu, 2013) BCI all rely on correct and accurate detection of eye movements and saccades.

Even more interestingly, in the event of loss of voluntary eye movement control as a result of locked-in syndrome, EEG-based BCI might be tailored to assist the population by detecting and utilising imagined or intended eye-movements (Pineda, Allison and Vankow, 2000; Babiloni, Cincotti, Lazzarini, Milan, Mourino et al., 2000).

In the present experiment, to further investigate the contribution of static, proprioceptive feedback on saccadic eye movements' accuracy we manipulated the position of the dominant hand on eye movements performed to remembered locations of visual targets. The hand was placed straight along the torso, in a control position we are going to refer to as Hand Right (HR), or bent with the arm at a 90-degree angle and with the hand resting on a desk in a Hand Left (HL) position. Based on previously reported findings on the effect of static and non-voluntary head and body displacement (Paige and Tomko, 1987; Morrow and Sharpe, 1993) and static torso rotations (Cacace, Podmore, Olkkonen, Kentridge and Connolly, 2019) we expect no significant differences in the accuracy and latency of eye movements in the two hand positions.

Finally, to investigate whether imagining saccadic eye movements facilitates subsequent performance of real eye movements to the same targets, we instructed

participants to imagine saccades to one visual field and compare the recorded latency and accuracy results to those of real saccades to targets displayed on the same visual field. Existing literature reports significant practice-dependant improvement on saccades' metrics. However, as stated above, this is usually reported over multiple testing sessions, spread over several weeks or months and therefore a large number of executed saccades often exceeding 200 per participant overall (Fischer and Breitmeyer, 1986; Green, King and Trimble, 2000; Ettinger, Veena, Crawford, Davis, Sharma and Corr, 2003). Additionally, these examples do not use delayed-saccades but anti-saccades and visually guided saccades and this is something to take into account when shaping our predictions. A connection between practice through imaginary movements and real movements is also documented (Gould, Damarjian, and Greenleaf, 2002; Dijkerman, Ietswaart, Johnston and MacWalter, 2004) but evidence on a similar effect when executing saccades is scarce. Based on these findings, this experiment aims to investigate whether practice of imagined delayed-saccades can influence the accuracy and latency of subsequently performed real delayed-saccades. Because of the link across imagined and real movements and the overall positive effect of practice on saccadic eye-movements, we anticipate a certain degree of facilitation of real saccades when preceded by imagined execution of eye movements to the same targets. This could be an indication that imagined saccades aid the proficiency of accurate saccadic performance. However, the use of delayed-saccades as opposed to visually guided- or anti-saccades, and the overall fewer trials as compared to that of previously used methods, means that we may not find comparable results to that of the existing literature.

2.2.3 Methods

Participants

Fourteen undergraduate and postgraduate students (males= 2), aged 20-29 (M= 21.92; SD= 3.09) were recruited from the Department of Psychology at Durham University (UK). Participants responded to an advert posted on the university's internal participant pool and were rewarded with academic credit where applicable.

In designing the experiment and identifying suitable participants, we had to consider hand and eye dominance as factors. The relationship between hand and eye dominance is unclear to this date, with cases of incongruence reported in 35% of right-handers showing left-eye dominance (Bourassa, 2010; McManus, 2010). It has been suggested that eye dominance influences accuracy in eye movements; higher accuracy was reported when tracking nine participants' self-reported dominant eye (Marmitt and Duchowski, 2002). Nevertheless, a later study reported no significant difference in accuracy between the dominant and non-dominant eyes of six participants (Cui and Hondzinski, 2006), although smaller offsets as well as more reliable calibration were identified when tracking the dominant eye in a comprehensive study on eye tracking data quality in 149 participants (Nystrom et al., 2013).

We therefore controlled for eye dominance using both the Edinburgh Handedness Inventory (EHI) (also known as the Oldfield Test) and a performance-based test (an alteration of the 'hole-in-card' test as described in Cui and Hondzinski, 2006).

All participants were also right-handed as confirmed by administration of the EHI (Oldfield, 1970). Only those participants demonstrating right side dominance for both hand and eye were included in the study (M= 91.63; SD= 8.33).

To control for individual differences in motor imagery proficiency and preference, we administered the Movement Imagery Questionnaire-revised second

edition (MIQ-RS II, by Gregg, Hall and Butler, 2010). The MIQ-RS II is a self-report questionnaire investigating the individuals' ability to perform a series of mental movements starting from a sitting position. It consists of seven kinaesthetic and seven visual items participants' are asked to rate on a seven-point Likert scale with 1 being the lowest rate on the scale for movements that are "very hard to see" or "feel" and 7 being the highest for movements rated "very easy to see" or "feel".

Previous literature employing the MIQ-RS II and its predecessor, the Movement Imagery Questionnaire (MIQ), determined that a score lower than 25 in each subscale (visual or kinaesthetic) indicated an overall difficulty to imagine (Page, Levine, Sisto and Johnston, 2001; Page, Levine, Sisto and Johnston, 2001 b; Gregg et al., 2007). For this reason, only participants scoring above 25 in at least one of the two subscales were included in the present study.

All participants had normal or corrected to normal vision and no prior history of neurological or psychological illness assessed as self-report. Based on the findings of a previous study on the use of contact lenses on calibration efficiency (Nystrom et al., 2013), we instructed participants to wear glasses where visual aid was required.

The study received ethical approval by the Durham University Ethics Sub-Committee and all participants gave informed consent prior to testing.

Participant 10 withdrew from the experiment at the start of the third run and was therefore excluded from the final analysis resulting in a total sample size of 13. A summary of participants' details can be found in **Table 2**.

Table 2

Participants' Information

	Age	Sex	EHI Score	Eye	MIQ-RS II (Kin) 1	MIQ-RS II (Vis) 1	MIQ- RS II (Kin) 2	MIQ-RS II (Vis) 2
1	23	M	+100	Right	42	40	42	42
2	20	F	+75	Right	31	38	38	40
3	28	F	+91.6	Right	34	39	40	44
4	20	F	+83.3	Right	35	29	40	32
5	22	F	+91.6	Right	39	33	43	35
6	29	F	+83.3	Right	32	49	38	49
7	20	F	+100	Right	39	38	42	38
8	20	F	+83.3	Right	42	36	44	36
9	20	F	+100	Right	32	27	38	25
10	20	M	+91.3	Right	33	35	38	42
11	22	F	+100	Right	40	32	42	32
12	21	F	+91.6	Right	32	34	32	34
13	20	F	+100	Right	39	26	42	30

Participants' age, sex, handedness (EHI), eye dominance (Eye), and motor imagery proficiency for kinaesthetic (Kin) and visual (Vis) imagery on sessions 1 and 2

Materials

A desktop-mounted and angled EyeLink 1000 (SR Research, Ottawa, Canada) eye tracker was used in the present study. The EyeLink 1000 was placed below a computer screen at a distance of 52 centimetres from the participants' eyes. The stimuli were presented on a computer screen with a 1024x768 resolution sitting also 52cm away from the participants. The sampling rate 1000Hz and the illuminator power was 100%.

We used a nine-point calibration system with a 1000 millisecond pacing interval between targets. Additionally, calibration targets were displayed in random order and the first point was repeated to increase accuracy as per the instructions of the SR Research's User Manual. To avoid confounds, we used an operator-controlled approach to select fixation points in both calibration and validation procedures. Calibration was repeated until adequate levels of accuracy were achieved for each run (defined as "GOOD" result on the EyeLink 1000 interface). Saccade sensitivity was set to "HIGH" as the purpose of the study was to investigate small and fast-occurring saccades. The Auto-Threshold function was used prior to each run to accurately threshold the pupil. Pupil tracking was set to "centroid" rather than "ellipse" as this method is the most accurate in determining the actual pupil position (Goldberg and Wichansky, 2002). Participants sat on a height-adjustable chair with their head fixed on a chin- and forehead-rest mounted at the end of the desktop. The height of the chin-rest was kept constant, and the chair's height was adjusted to suit the participant as required.

A custom-built horizontal screen was placed on the desktop and used to obscure the participant's view of their hands (see *Procedure* for further information).

Stimuli

Participants completed a slight variation of the classic memory-guided saccadic eye movement task initially developed to investigate retinotopy in the parietal lobe (Sereno, Pitzalis and Martinez, 2001) and subsequently employed in a number of related research usually employing functional Magnetic Resonance Imaging (fMRI) (Schluppeck, Glimcher and Heeger, 2005; Kastner et al., 2007; Connolly, Vuong and Thiele, 2013). Briefly, a 0.22° high contrast, white dot would appear at one of 12 possible locations on a black background. The 12 locations were fixed around a 7.7°

radius invisible circle surrounding the centre of the screen. Each target was separated by 30° and would appear sequentially starting from the top of the circle (0°) and continuing clockwise or counter-clockwise until a full 360° rotation was completed (**Figure 12**).

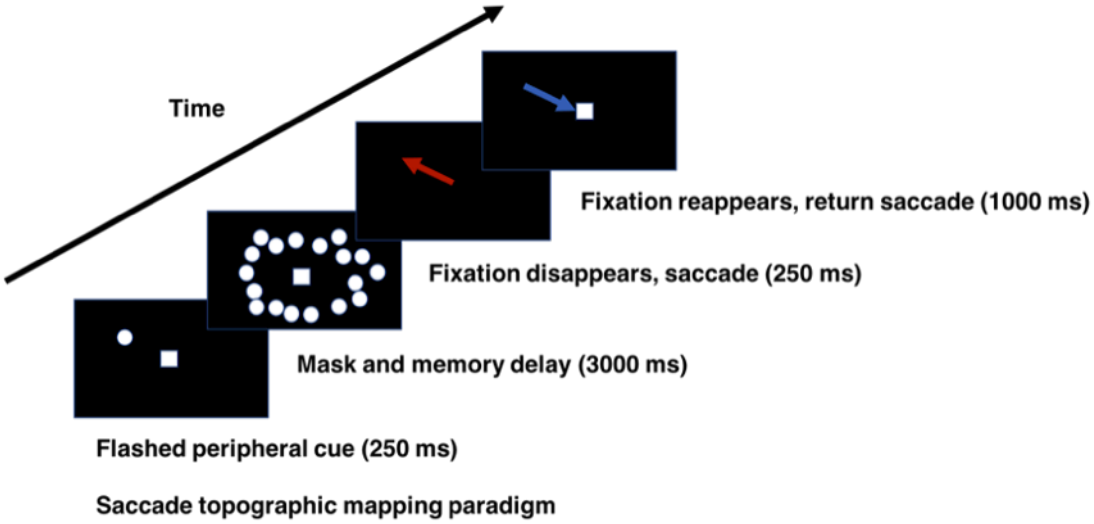

Figure 12. The classic memory-guided saccadic eye movements task. The above diagram is a representation of the stimuli used in the present experiment. Starting from the bottom panel, as indicated by the black arrow, a fixation point appears on screen followed by a peripheral, high-contrast cue. A confounding mask of 100 cues is then presented inducing a 3-second delay from the presentation of original cue to the moment the participants are required to initiate the saccade. This is signalled by the disappearance of the fixation point (third panel). Participants were instructed to perform the eye movement to the remembered location (red arrow) and return to the fixation point (blue arrow) as quickly as possible. The fixation point would finally reappear signalling the start of a new trial. Peripheral cues were presented in either a clockwise or a counter-clockwise direction.

In the present study, participants were informed of the kind of movement to perform at the beginning of each cycle by text appearing on screen. The instruction would read: "Imagined Right" if participants were to perform imagined eye movements to targets appearing in the right visual field and real eye movements to targets appearing in the left visual field; "Imagine Left" if participants were to perform

imagined eye movements to the left visual field and real eye movements to the right visual field; "Real Only" if real movements were to be performed on both visual fields. For each run, the sequence of conditions was pseudo-randomised but fixed so that a "Real Only" condition always followed one of the two imagined conditions (**Figure 13**). This was based on evidence within the existing literature showing a general facilitation of the performance of real movements of the body and limbs following motor imagery of the same movement. Although different in the actuator (body and limb as opposed to eyes), the same principle was applied in the present experiment so that we could investigate whether or not memory-guided saccade overall accuracy improves by prior execution of imagined and/or real saccades to the same targets. In other words, whether performing real and imagined memory-guided saccades to the same targets would facilitate subsequent iterations of the same task.

Example of condition sequence for two sample runs

Run 1: Imagined Right First		Run 2: Imagined Left First	
1. Imagined Right	2. Real Only	1. Imagined Left	2. Real Only
3. Imagined Left	4. Real Only	3. Imagined Right	4. Real Only

Figure 13. Example of the condition sequence for two sample runs. The numbers 1-4 identify the specific cycle around the clock. A cycle where imagined movements were performed to targets displayed on either visual field was always followed by a cycle where real saccadic eye movements were performed to both visual fields.

After disappearance of the instructions, a white fixation dot would appear at the centre of the screen for 1000ms and participants were instructed to hold their gaze at this location. A peripheral target would then be presented for 250ms at the first

location, 0° or 12 o'clock. A mask annulus of 100 randomly generated high contract dots was then presented for 3000ms forcing a delayed memory interval. The annulus had a 5° minimum inner and 10° maximum outer radius. The fixation dot then disappeared for 1000ms before the appearance of the next target. Targets would progress in either a clockwise or a counter-clockwise manner and participants were informed on this, verbally by the experimenter, at the beginning of each run.

It is important to note that participants were asked to hold fixation and to only perform the eye movement when the fixation dot was no longer visible. Participants were instructed to attend to the location the peripheral cue was presented, hold this in memory, and finally perform the saccade to the location as accurately as possible and to then return to the original fixation location as quickly as possible before the start of the next trial.

A full trial, from the first presentation to final disappearance of the fixation dot took a total of 4.5 seconds. A full cycle was completed when all targets going from 0° to 360° were presented resulting in a total time of 54 seconds. One run consisted of 4 consecutive cycles for a total time of 3.6 minutes. 16 runs were performed by each participant in two separate sessions resulting in a total of 57.6 minutes of raw data excluding breaks and 384 real eye movements performed by each participant for a grand total of 4992 real saccades used in the present dataset.

When performing imagined eye movements, participants were instructed to hold fixation and only mentally perform the saccade.

Procedure

Participants completed the EHI and the variation of the hole-in-card test first. They then proceeded to complete the MIQ-RS II. One practice run (or more, if needed) was then

offered to let participants familiarise with the stimuli and task. Participants were then instructed to adjust the height of the chair to allow their head to be placed correctly on the chin- and forehead- rest but so that no strain was placed on their neck. Participants were also instructed to limit movement as much as possible once recording started.

At the start of each run, the participant's hand was moved by the experimenter in one of two possible positions: straight along the torso (Hand Right) or bent at the elbow and at a 90° angle with the upper arm and placed under the occluding screen on the desktop (Hand Left). A black square on the bottom panel of the occluding screen defined where the participant's hand should be in the Hand Left condition. Prior to each run for Hand Left, the experimenter would make sure the hand was placed within the black square. **Figure 14** shows the experimental setting.

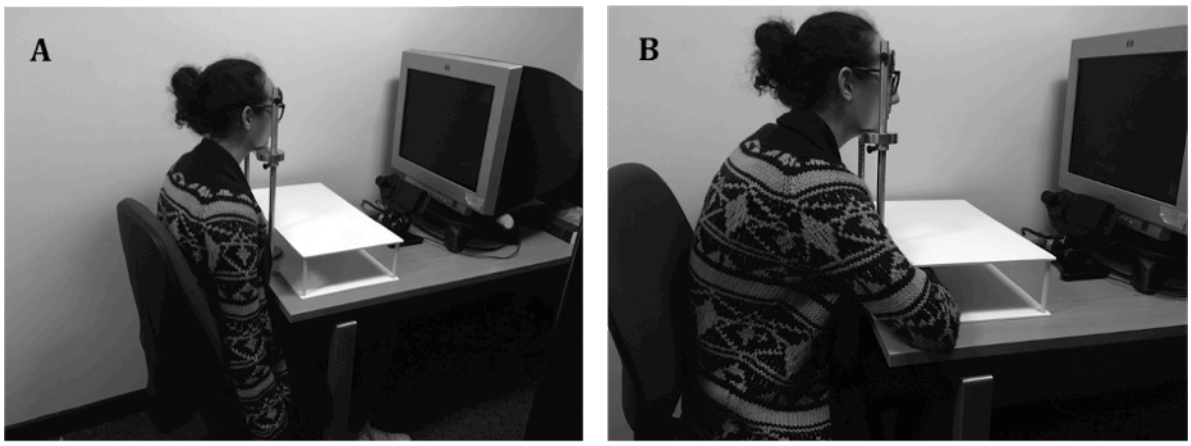

Figure 14. The experimental setup. The participant sits on a height-adjusted chair and with their head placed on a chin- and forehead-rest. The participant's hand is placed along the torso (A) in the condition "Hand Right" and placed under the white screen (B) in the condition "Hand Left".

Participants were then informed on which direction the targets will move, whether clockwise or counter-clockwise. Text instructions at the beginning of each cycle would instead inform them on the priming condition i.e. performing the imagined

eye movements for targets on the left side of screen, right side of screen or whether both sides required real movements to be performed.

After each run, participants were given the chance to rest and stretch for as long as needed. This also allowed to alter the position of their hand before the start of the new run. Because of this, calibration and validation were performed before the start of each run.

Participants completed a total of 16 runs in two separate sessions with at least a one-day break in between to avoid excessive fatigue.

The order of hand position (Right or Left), target direction (clockwise or counter-clockwise) and priming condition (Imagined Right, Imagined Left or Real) was pseudo-randomised across the two sessions to avoid order effects.

The MIQ-RS II was then administered once again at the end of the second session.

Data analysis

The questionnaires used were scored following their specific guidelines.

The EHI was scored by assigning a +2 to items where a strong preference to the right hand was indicated and -2 if strong preference to the left was reported instead. 0 would indicate no specific preference. A final handedness result was then calculated by using the following formula: 100*((Right - Left) / (Right + Left)) (Oldfield, 1970). As a result, a score of +100 indicates a strong right-handedness, -100 indicates strong left handedness and 0 indicates complete ambidexterity.

The MIQ-RS II was scored by adding the values reported for the individual subscales (Kinaesthetic and Visual imagery). The minimum value of 7 indicates severe

difficulties imagining movements whereas a maximum value of 42 indicates a highly confident imager.

Raw data (.edf) was firstly converted using the EDF2ASC translator program (SR Research, Ottawa, Canada). The resulting ASC files were then further transformed by an purpose-written C (Kernighan and Ritchie, 1978) program extracting a total of eight metrics. Target Location showing the target displayed out of the 12 possible clock positions; Trial Number, showing the trial associated with the Target Location displayed, from 1 to 48; Saccade End Location X and Saccade End Location Y, in pixels, determined the precise location of each eye movement's end point registered by the eye tracker; Saccade Duration, in milliseconds and Saccade Amplitude, in degrees of visual angle, showing the total duration and amplitude of each eye movement performed; Reaction Times, in milliseconds, showing the time difference between the disappearance of the confounding annulus (cue for the participant to initiate the eye movement) and the start of an eye movement; and Tracked Eye defining which to which eye the specific metric belonged to, right (1) or left (2). All of the above metrics were imported on an .xls file.

We then imported the .xls file in a purpose-written Matlab (Mathworks, Mastrik, USA) program.

It is important to note that the metrics obtained from the raw data included all eye movements performed by the participants for both eyes and in the time window occurring from the disappearance of the confounding annulus to the appearance of the fixation dot, signalling the start of the next trial. In order to isolate correct memory guided saccades to the cued target from involuntary saccades or wrong eye movements we applied a number of inclusion criteria and filters to the raw data based on both stimuli-specific and literature based parameters (Baloh, Sills, Kumley and Honrubia,

1975; Wilson, Glue, Ball and Nutt, 1993; Salvucci and Goldberg, 2000) as follows. We firstly extracted the metrics for the right eye only, given that all of our participants showed right-eye dominance. We then proceeded to apply a Saccade Amplitude threshold selecting all those eye movements falling within 8 to 15 degrees of visual angle. Eye movements outside of this window would likely be too small or too large possibly as the result of involuntary retinal oscillation or generally incorrect eye movements (Abel, Troost and Dell'Osso, 1983).

A threshold was also applied for Saccade Duration, discarding eye movements with abnormally low (<20ms) or high (>200ms) durations that would likely be too short or too long to classify as a correctly executed saccade (Abel et al., 1983). Finally, a spatial threshold was applied on the x-axis based on the screen resolution and target location effectively discarding those eye movements with end points not corresponding to a near-target area. For the specific resolution of the screen hereby used we selected as external boundaries pixels from 1-44 and 980-1024 as these would most likely be eye movements directed too far from any of the actual targets. Additionally, we applied a mid-line boundary rectangle for pixels falling between 420 and 604, as these would correspond to eye movements directed at the centre of the screen and to targets 12 and 6, as these are not specifically aligned to either left or right visual fields.

In the case of multiple eye movements satisfying these initial filters, only the one falling closer to the actual displayed target, and therefore more accurate, was selected and the others discarded. However, it is important to notice that, because of the high strictness of these filters, on some occasions not all targets will produce data, often due to saccades not satisfying the amplitude, temporal and spatial criteria at the same time. This resulted in a total of 455 saccades being excluded, 9.2% of the overall data collected, resulting in a total of 4537 real saccades used for the statistical analysis.

To allow for comparison of visual fields, we then separated the eye movements in left and right visual field based on the target location: targets and the associated eye movements falling before Target Position "6" constituted the right visual field (rVF) and targets falling after position "6" made the left visual field (lVF).

To allow for investigation of the priming effect of real or imagined eye movements on execution of subsequent real eye movements, we separated eye movements based on the specific and unique cycle they were executed in. To reiterate, participants performed four cycles around the clock in each run. Each cycle had a unique occurrence of either real or imagined eye movements to each visual field. Participants were informed at the beginning of each cycle on what kind of movement they had to perform. We therefore separated all cycles in which participants performed real eye movements when primed by the execution of real eye movements and all cycles where participants were instead primed by execution of imagined eye movements.

Finally, to investigate the effect of hand position, we also separated data based on the location of the hand as assigned at the beginning of each run.

The next part of our script calculated the kinematic errors for each of the targets that produced a valid saccade. The amplitude error was defined as the difference between the distance of the fixation dot (the centre of the screen) and the actual target displayed, in pixels (220), and the distance between the fixation dot and the saccade end point on the x-axis (Saccade End Location X) as recorded by the eye tracker. Positive values for this variable would mean the saccade was farther away from the centre than the actual displayed target, whereas negative values would identify saccades closer to the centre. The angular error was defined by the difference between the distance, in angles, from the fixation dot and the displayed target and the distance between the fixation dot and the recorded saccade end point. Positive values for this variable would

identify saccades farther clockwise than the actual target whereas if farther counter-clockwise it would result in a negative value. Finally, the Cartesian error was calculated by comparing the saccade end points for each target to the actual target location for both the x and y axes.

The final portion of the script was intended to compute averages for all of the above-defined variables for the different priming conditions and hand positions in the left and right visual field. This resulted in three 13 x 8 matrices, where 13 is the number of participants included in the analysis and 8 is the total number of resulting conditions by visual field (2 levels), hand position (2 levels) and priming condition (2 levels). Averages were then imported in SPSS (IBM, New York, USA) to allow for statistical comparisons. We performed a 3-way Repeated Measures Analysis of Variance (ANOVA) in a 2x2x2 model with visual field, hand position and priming condition as fixed variables.

2.2.4 Results

This section is going to report the mean results for each of the four metrics of Angular Error, Amplitude Error, Cartesian Error and Reaction Times. Additionally we will also report the results of the MIQ-RS II administered during the experiment.

Amplitude Error

The mean results for amplitude error are reported in a bar graph in **Figure 15**. Upon general inspection of the average data, a main difference for visual field is shown. Interestingly, saccades performed toward the left visual field result in positive values for amplitude error whereas the opposite result is shown for the right visual field. This means that saccades performed to targets appearing on the left side of the screen, or left

visual field, were hypermetric or farther from the centre of the screen. In contrast, participants tended to perform shorter, hypometric saccades, closer to the centre of the screen for targets appearing in the right visual field. This seems to be the case regardless of condition and hand position.

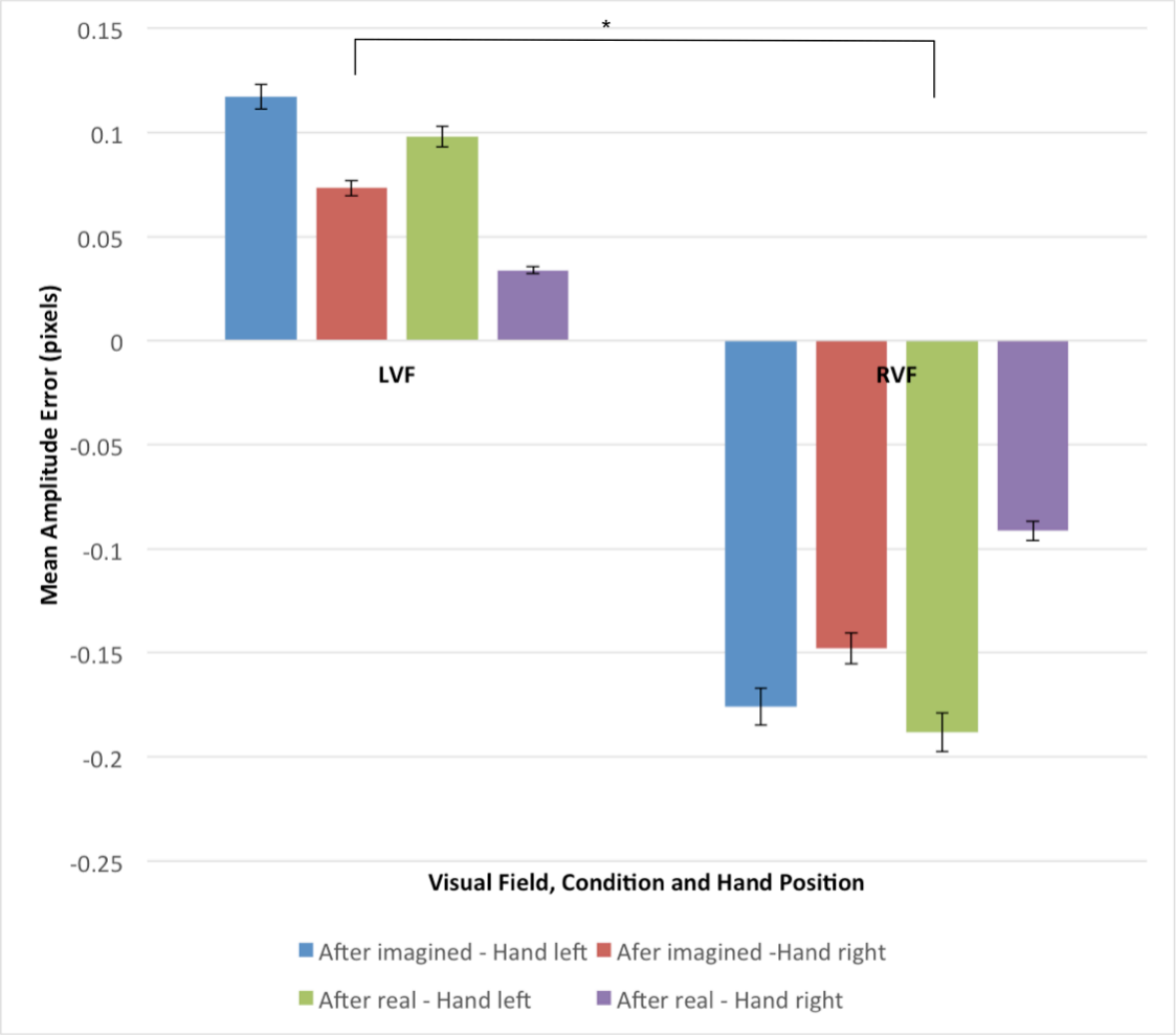

Figure 15. Mean Amplitude Error for the effect of condition and hand position in each visual field. Saccades performed to the left visual field (LVF) were farther from the centre than the actual target position or hypermetric. These were significantly different from saccades performed to targets displayed in the right visual field (RVF). These were generally shorter or hypometric, and therefore closer to the centre. The different conditions, after real eye movements (Ar) and after imagined eye movements (Ai), and the different hand position for "Hand Right" (hR) and "Hand Left" (hL) do not seem to contribute with this effect. Error bars represent the Standard Error.

A Repeated Measures ANOVA with visual field, hand position and priming condition as factors showed a significant main effect of visual field on the amplitude error of memory guided saccades, $F(1,12) = 15.36$, $p = 0.002$, $\eta p^2 = 0.562$. Mauchly's test of sphericity indicated that the assumption of sphericity has been met for all variables ($p < 0.001$). Inspecting the mean values for the main effect of visual field we can again notice that saccades were generally hypermetric (M= 0.08; SD= 0.16) for the left visual field and hypometric (M= -0.15; SD= 0.22) in the right visual field. No significant interactions were found. However, a near-significant effect was reported for the interaction of visual field and hand position ($F(1,12)=0.423$, $p = 0.055$). Follow-up paired sample t-tests between Hand Left and Hand Right for each visual field separately, however, found no significant differences.

Angular Error

The mean results for Angular Error are reported in a bar graph in **Figure 16**. As visible from the graph, there is be no visible separation across the eight conditions. Moreover, all of the values are in the positive domain suggesting participants tended to overshoot their saccades overall. A positive angular error means saccades' end points were located farther clockwise than the actual target location.

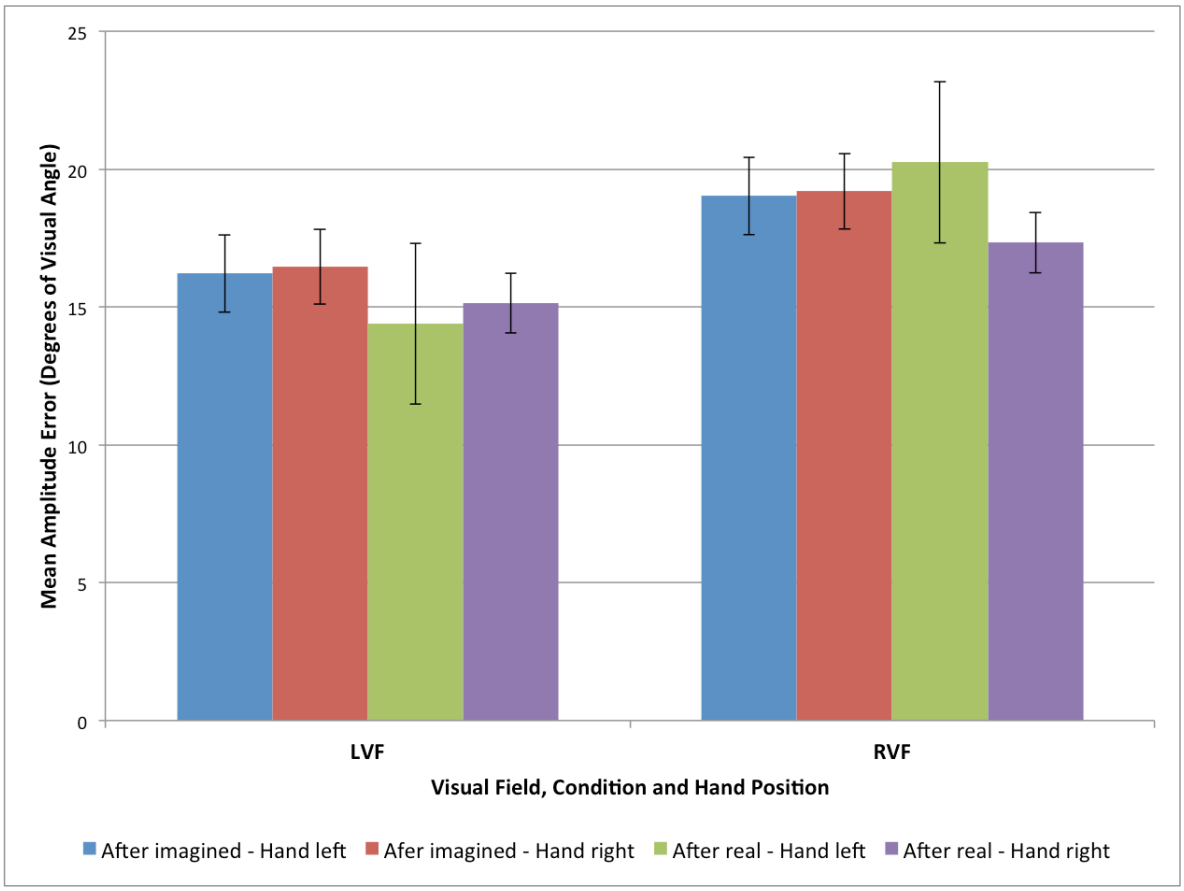

Figure 16. Mean Angular Error for the effect of condition, hand position in each visual field. Saccades' angularity is overall similar for each group. Relatively higher angularity is visible for the right visual field (RVF) as opposed to the left visual field (LVF). This might suggest that participants performed saccades falling slightly farther clockwise in the RVF and slightly farther counter-clockwise saccades to the LVF. This seems to be the case regardless of the prior condition, after real (Ar) or imagined (Ai), and hand position, right (hR) or left (hL). Statistical investigation, however, shows these differences to be not significant. Error bars represent the Standard Error.

A Repeated Measures ANOVA on the angular error of memory guided saccades showed no main effects or significant interactions found for visual field, condition and hand position, $F(1,12) = 0.144$, $p = 0.181$, $\eta p^2 = 0.144$. In other words, saccades' angularity was not different for targets in the right and left visual field. Prior execution of either real or imagined saccades to the same locations did not affect the angularity nor did the alteration of the dominant hand position.

Cartesian Error

The mean results for Cartesian Error are reported in a bar graph in **Figure 17**.

No particular differences are visible from the graph alone. It is important to notice however, that given how the Cartesian Error is calculated, only positive values are to be expected.

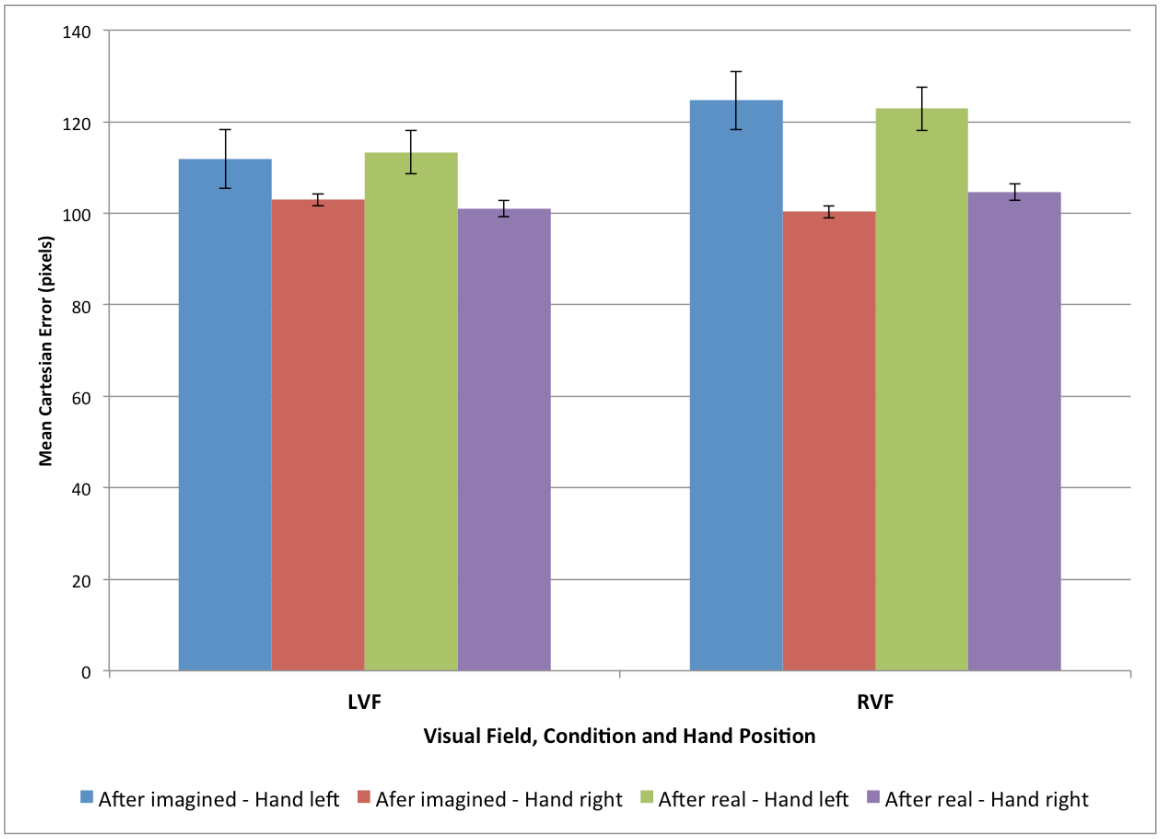

Figure 17. Mean Cartesian Error for the effect of condition and hand position on each visual field. The average Cartesian error is smaller in the hand right (hR) position as opposed to the hand left (hL) position in both the left (LVF) and right visual field (RVF). Prior performance of real or imagined eye movements to the same target locations does not seem to affect the average Cartesian errors. Statistical investigation, however, shows no significant differences for this metric. Error bars represent the Standard Error.

A Repeated Measures ANOVA on the values for Cartesian error showed no main effects or significant interaction for our variables, $F(1,12) = 0.664$, $p = 0.431$, $\eta p^2 = 0.52$.

Figure 18 shows saccades performed during one complete real trial by a randomly selected participant. The target location is indicated by an "x" whereas the observed saccade endpoints are indicated by an "o". These have been colour-coded to reflect the intended direction of saccades. If participants were supposed to perform a saccade to the right visual field, the endpoint was coded "green"; if they were supposed to perform a saccade to the left visual field, it was coded "red". In this case, the participant performed saccades to the intended location in all occasions as all green endpoints are to the right and all pink endpoints are to the left. The diagram also offers the opportunity to visualise some common characteristics of saccades hereby recorded. The saccades recorded for targets 1 and 5 represent what were defined as hypometric saccades. These fall closer to the centre than the actual target and also correspond to shorter saccade amplitude. Vice-versa, saccades directed at targets 7, 8 and 9 are hypermetric or farther from the centre as compared to the actual target location and therefore correspond to higher saccade amplitude. Additionally, targets 1 and 11 report saccades that clearly reflect amplitude errors as these fall farther clockwise and counter-clockwise respectively as compared to the actual target location.

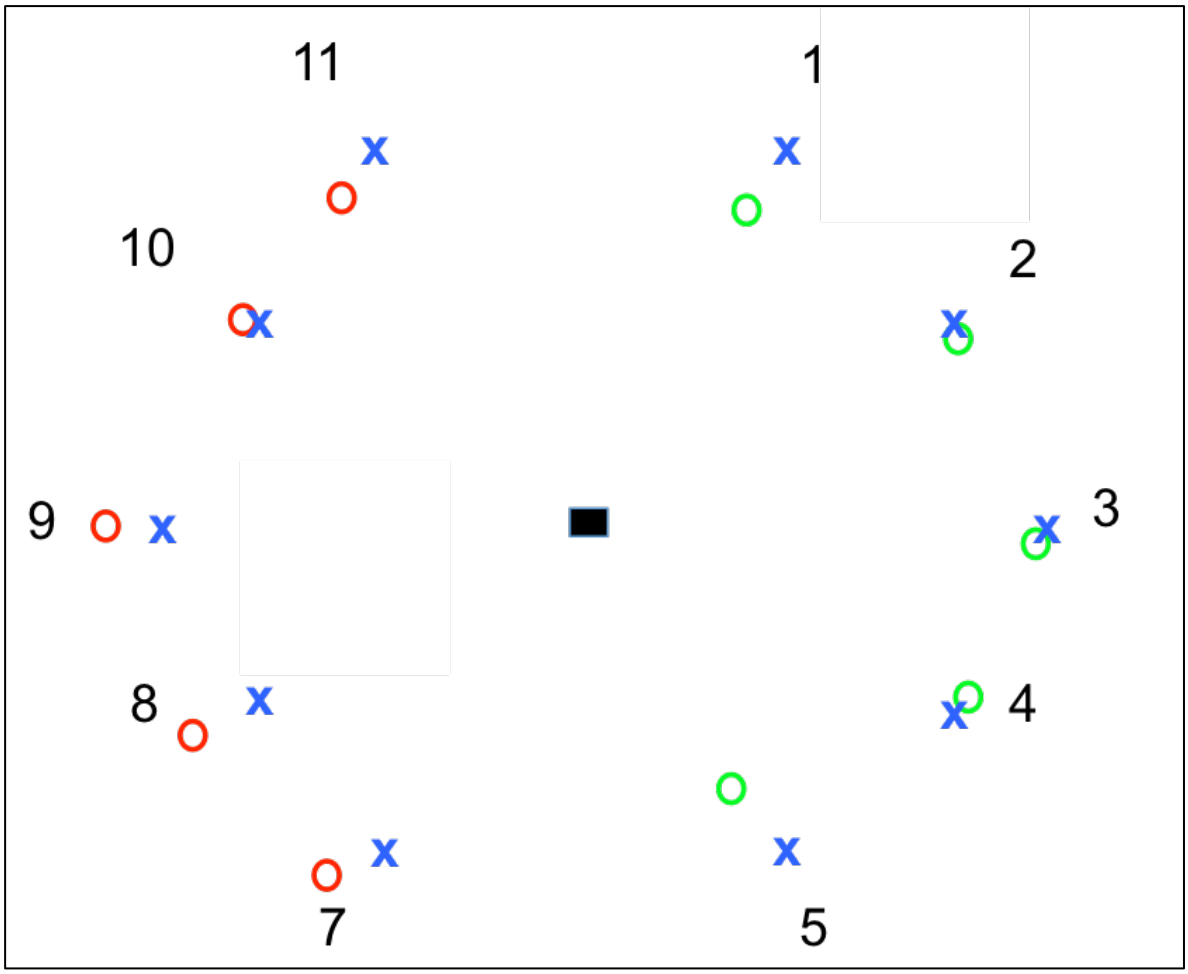

Figure 18. A diagram showing saccades endpoints of one randomly selected participant. Highly accurate saccades are performed for targets 2, 3, 4 and 10. Hypermetric saccades are recorded for targets 7, 8, and 9. Hypometric saccades are visible for targets 1 and 5. Angular errors are recorded for saccades to targets 1 and 11.

Reaction Times

The mean results for reaction times are reported in **Figure 19**. Participants appear the slowest at initiating saccades to targets in the left visual field, after imagining the eye movements to the same locations and when their hand is in the "right" position. Scores are lowest for saccades initiated to the left visual field, after real eye movements to the same targets and when the hand is in the "left" position.

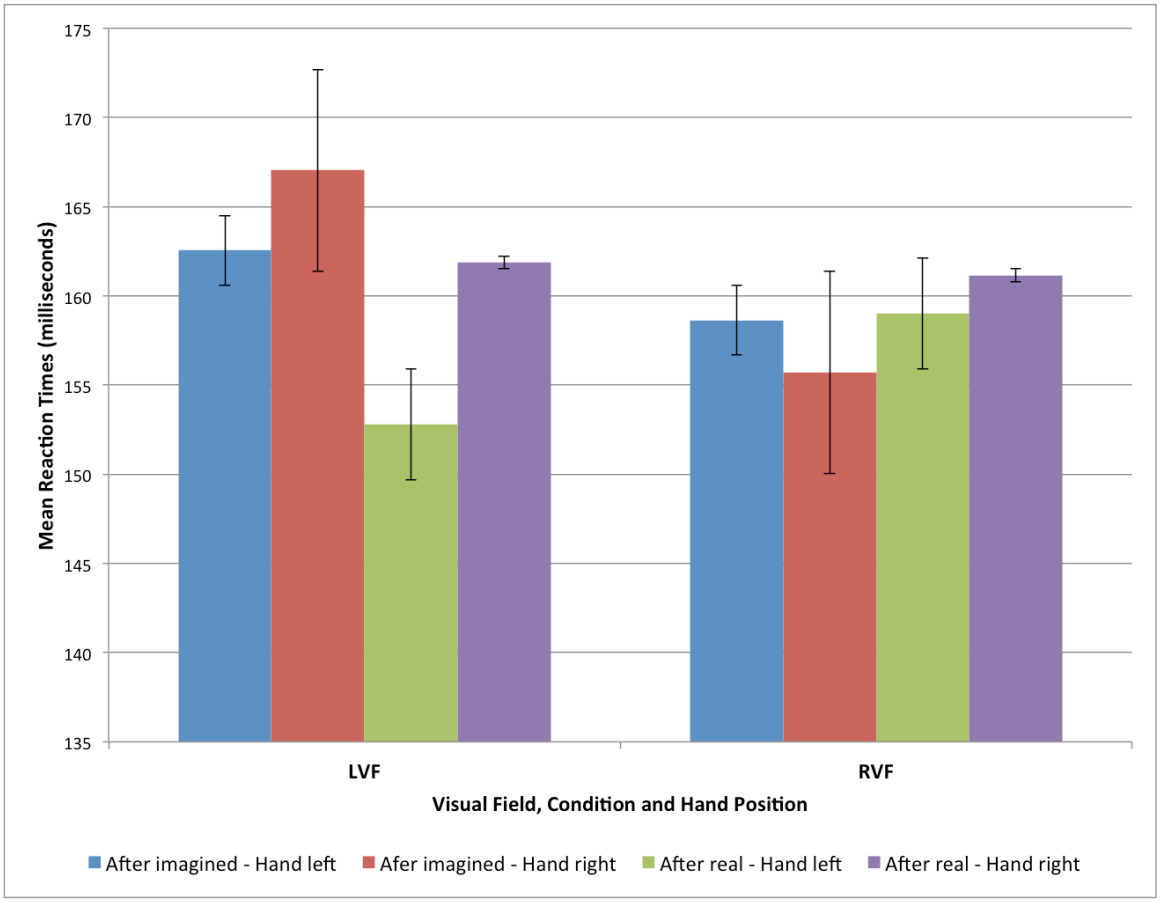

Figure 19. Mean Reaction times on the effect of condition and hand position in each visual field. Participants initiated saccades faster to targets on the left visual field (LVF), after performance of real eye movements to the same locations (Ar) and when their hand was in the left position (hL). Participants were slower, on average, in performing saccades in the Left visual field (LVF), after imagined saccades to the same locations (Ai) and with the hand in the right position (hR). Statistical comparisons, however, show these differences were not significant. Error bars represent the Standard Error.

A Repeated Measures ANOVA on the results for reaction times showed overall no main effects or significant interactions, $F(1,12) = 0.175$, $p = 0.136$, $\eta p^2 = 0.175$.

In summary, the position of the dominant hand in space did not interfere with the accuracy of delayed saccades. Similarly, prior performance of either real or

imagined saccades did not affect the overall accuracy of subsequently executed delayed eye-movements.

Movement Imagery Questionnaire – Revised Second Edition (MIQ-RS II)

A paired sample t-test was conducted to investigate potential differences in the ability to perform imagined movements before and therefore at a naïve-stage and after completion of the two sessions of the present experiment.

A significant difference for the Kinaesthetic subscale on session one (M= 36.15; SD= 4.09) and session two (M= 39.92; SD= 3.17) was found, $t(12)=-5.85$, p=0<001. Participants were more confident in performing kinaesthetic imagined movements at the end of the two sessions, after having performed a number of imagined saccades. Looking at the mean values for each subscale, a +3.77 point increase is reported between the two sessions.

A significant difference for the Visual subscale on session one (M= 35.07; SD= 6.13) and session two (M= 36.84; SD= 6.51) was also found, $t(12)= -2.56$, p=0.025. Similarly as above, participants report slightly higher confidence (+1.77) in performing visual imagined saccades at the end of the experiment.

No significant differences were found when comparing the Kinaesthetic and Visual subscale within the same session suggesting neurologically intact participants show no specific preference between the two subscales

2.2.5 Discussion

In the present experiment we investigated the effects of two static hand positions and practice of motor imagery of eye-movements on accuracy metrics and reaction times of memory-guided saccades. Our data provide support for the idea that changing the static

position of the dominant hand when performing saccades does not seem to alter accuracy metrics such as angular, amplitude and Cartesian error. However, we report an interaction of visual field in the amplitude error of saccades thus inferring that, on average, participants performed shorter or hypometric saccades to targets located in the right visual field and wider, or hypermetric saccades to the left visual field. These results are consistent with previous findings identifying a rightward bias in right-handed individuals whereby, when performing saccades to fixed targets, individuals tend to perform shorter movements for targets located to the right visual field than for those located to the left (Pirozzolo and Rayner, 1980).

This effect is not influenced by either the position of the hand in space or the performance of imagined or real eye movements prior to the execution of the task, as these interactions were non-significant. However, we cannot conclude that eye movements to either visual field will result in a change in the overall accuracy of memory-guided saccades as no significant interactions were found when investigating the other two metrics of Cartesian and angular error.

Interestingly, our results do not support previous findings identifying a rightward bias in the latency of saccades to stationary targets in right-handed individuals (Van Allen, 1973; Pirozzolo and Rayner, 1980). It has been suggested that this bias could be the result of handedness- or eye dominance-related hemispheric asymmetry in sensori-motor organisation (Pirozzolo and Rayner, 1980, Kolesnikova, Tereshchenko, Latanov and Shulgovijskii, 2010). However, reaction times in the present study did not differ for targets displayed in either visual field despite participants showing right preference for both hand and eye. Such results might confirm previous studies finding little to no correlation between handedness and eye dominance during saccades performance to fixed targets (Constantinidis, Smyrnis, Evdokimidis, Stefanis,

Avramopoulos, et al., 2003; Vergilino-Perez, Fayel, Lemoine, Senot, Vergne, Dore-Mazars, 2012; Bargary, Bosten, Goodbourn, Lawrence-Owen, Hogg et al., 2017). This could suggest that the latency of memory-guided saccades is similarly not affected by handedness and/or eye-dominance; however, future studies including left-handers might be needed to compare results with those existing in the literature.

When investigating the contribution of the hand position we report no main effects or significant interactions in both the accuracy and latency of saccades in our sample. This suggests that proprioceptive feedback originating from altering the position of the dominant hand is not interfering with the individual's ability to perform eye movements. Existing studies have established a link between visual and proprioceptive feedback in a top-down fashion whereby visual information is taken into account in modifying body posture to maintain balance (Edward, 1964; Gingsburg, Cannon and Nelson, 1980; Day, Steiger, Thompson and Mardsen, 1993).

Evidence of bottom-up integration usually includes body postural changes that affect the position of the head relative to the body and induce a substantial stretch of the neck muscles (Kopinska and Harris, 2003; Harris and Smith, 2008). The lack of interaction of hand position and saccades in the present study, could be explained by the fact that both the head and neck of participants were stabilised and so only a minimal change in the body position occurred.

Additionally, in the previous chapter, we demonstrated that small torso rotations, in which the head is fixed, do not affect the accuracy and latency of saccades. Taken together, these results support the suggestion that proprioceptive feedback coming from the body, when the head is kept stable in reference to the body, does not have a substantial effect in the performance of memory-guided saccades; in other words, the hand position in space does not interfere with the way individuals perform

memory-guided eye movements. We therefore conclude that small positional changes of the hand in space, when this is not altering the alignment of the head or stretching the muscles of the neck, will not affect saccade metrics of accuracy and latency.

Contrary to our initial predictions, we report no main effect or interactions in the latency and accuracy of participants performing real saccades after imagining eye-movements to the same locations. Such results might suggest that, although imagined movements of the body have been shown to improve the performance of actual movement in relatively short training sessions (Gould, Damarjian, and Greenleaf, 2002; Dijkerman, Ietswaart, Johnston and MacWalter, 2004; Stevens and Phillips Stoykov, 2003), the same might not be true for memory-guided saccades. One reason could be that, much like with the execution of real eye-movements benefitting from practice only when this is extensive and repeated in time (Fischer and Breitmeyer, 1987; Green, King and Trimble, 2000; Ettinger, Veena, Crawford, Davis, Sharma and Corr, 2003), a much higher number of imagined saccades is needed to positively impact subsequent performance of real saccades.

However, future studies involving a substantially higher number of recording sessions and therefore imagined saccades performed are needed to investigate whether the motor imagery of eye movements behaves similarly to body motor imagery in facilitating the performance of real movements (Gould, Damarjian, and Greenleaf, 2002; Dijkerman, Ietswaart, Johnston and MacWalter, 2004).

Successfully linking motor imagery to improved accuracy or reaction times in the execution of eye-movements could be beneficial to partially increase the feasibility of BCI-based assistive techniques. Eye fatigue has been identified as one of the factors limiting the application of BCI techniques in standard rehabilitation practice (Punsawad and Wongsawat, 2013; Volosyak, Valbuena, Luth, Malechka and Graser, 2011; Myrden

and Chau, 2015). Most eye movement-based BCI approaches require high accuracy performance levels to successfully operate, usually achieved through extensive training (McFarland, Sanacki, Vaughan and Wolpaw, 2004). Being able to pair imagined movements to the actual performance of eye-movements during training sessions might help to limit the early onset of fatigue. The addition of imagined eye-movement practice to standard training sessions could also increase and strengthen related EEG activity commonly used in non-invasive BCI (Guger, Daban, Sellers, Holzner, Krausz, et al., 2009; Tan, Jansari, Keng, Goh, 2009).

Finally, we report an increase in the self-reported confidence level in performing motor imagery after the two recording sessions. The effect was visible for both kinaesthetic and visual motor imagery. Additionally, no significant difference was reported between the two subscales suggesting that healthy individuals can perform similarly in both kinaesthetic and visual tasks and show no particular preference. Kinaesthetic and visual motor imagery have been linked to the recruitment of different brain areas (Guillot, Collet, Nguyen, Malouin, Richards, et al., 2008; Neuper, Scherer, Reiner and Pfurtscheller, 2005). BCI assistive techniques involving the performance of motor imagery within the healthy population could therefore prioritise choosing the motor imagery subtype that best complements their technique in order to increase accuracy and overall performance, as well as maximising signal acquisition for the chosen extraction site over the individual's preference. Similarly, if a neurologically- or motor-impaired cohort is involved, prioritising their specific preference over that of healthy controls could then be feasible and more beneficial.

In conclusion, the current study offers new insight on the relationship between body position changes and motor imagery facilitation in the context of BCI assistive

techniques. The practice of saccades through motor imagery did not seem to facilitate the actual performance of eye movements to the same targets, however future studies involving a higher number of sessions and number of executed imagined saccades might be needed to confirm this. Most notably, in the case of BCI utilising eye-movement detection alone, subtle alterations of the position of the body, when these do not include the head and neck, will not significantly alter the end points and latency of eye-movements to fixed locations in space. However, in the previous experiment, we report how hand-centred coordinate frames affect saccadotopic maps of the Posterior Parietal Cortex of individuals performing the same saccadotopic task hereby used. BCI techniques relying on invasive extraction methods (i.e. micro-electrode implants) might benefit from controlling the individual's position during recording sessions; this will be addressed further in the main discussion.

3 Functional Magnetic Resonance (fMRI) reveals reduced motor imagery activation in long-term, C4 complete Spinal Cord Injuries.

3.1 Abstract

Injury to the spinal cord often results in lifelong paralysis and the lack of effective treatment means permanent loss of independence for those affected. Brain-Computer Interface (BCI) techniques could offer an alternative option to restore some of the lost mobility, however these techniques are still far from being included in the standard rehabilitative practice. Debate on the most suitable extraction sites is one of the identified limiting factors. Successful BCI applications extract brain signal from the primary motor cortex (M1), however longitudinal studies on individuals with Spinal Cord Injury (SCI) highlight a consistent decrease of activation and volume in this area within the first year following paralysis (Jurkiewicz, Mikulis, Fehlings and Verrier, 2010). As an alternative, the posterior parietal cortex also produces reliable and consistent signals suitable for BCI control (Aflalo, Kellis, Klaes, Lee, Shi, et al., 2015) but information regarding the development in long-term paralysis is lacking. In the present study we aim to investigate functional activity in the brain during hand-motor imagery in individuals living with long-term paralysis following SCI. Four participants with high-level (C4) spinal injury sustained on average four years prior to recruitment and matched controls performed motor imagery of their preferred hand to 2D flashing targets in a 3T MRI scanner. We collected information on the residual activation and the total number of active voxels during motor imagery in seven regions of interest including primary motor cortex, supplementary motor area and posterior parietal cortex. Results show on average less activation registered in the primary motor cortex and similar or higher activation in the superior parietal lobule in patients compared to

matched controls. Similarly, the total number of active voxels is smaller in motor areas as compared to posterior areas. Although with a limited sample size, these results support the suggestion that in naïve individuals, where no motor imagery rehabilitation has been performed, long-term paralysis affects the functional connectivity of the motor cortex and associated areas more so than in posteriorly located areas. This also suggests that BCI assistive techniques focusing on extracting brain signals from regions located within the posterior parietal cortex could be suitable to a larger portion of the target population. Finally, implementation of early motor imagery training in the rehabilitative setting could help to maintain levels of activity within the motor cortex comparable to that of controls.

3.2 Introduction

Spinal Cord Injuries (SCI) are a relatively common problem that creates significant suffering, both physical and psychological, to thousands of people. There are approximately fifty thousand cases in the UK alone (www.spinal-research.org), and an international incidence rate estimated at 50 per million population per year (Sekhon and Fehlings, 2001). Due to the high risk of comorbidity, the mortality rate is estimated between 48.3% and 79% of the affected population - dependent upon prompt admission to hospital. Respiratory and circulatory complications are the leading causes of death (De Vivo, Krause and Lammertse, 1999; Garshick, Kelley, Cohen, Garrison, Tun, Gagnon and Brown, 2005; Sekhon and Fehlings, 2001). Trauma to the spinal cord can often result in severe loss of motor control, impacting on the overall quality of life of the affected individual (Kwon, Tetzlaff, Grauer, Beiner and Vaccaro, 2004). Although there are no restorative treatments currently available, traditional physical and medical

rehabilitation can help, especially when intervention is delivered promptly. Rehabilitative therapy administered as early as 8 weeks after onset of paralysis has been shown to increase the chance of first-year survival by 88% (McDonald and Sadowsky, 2002; De Vivo, Richards, Stover and Bette, 1991; Dobkin, Barbeau and Deforge, 2007). Once the SCI is established, stabilised, and the residual motor control is evaluated, individuals should continue to be monitored by a specialised team, with annual follow-ups (Thuret and Lawrence, 2006).

For those individuals whose SCI resulted in paraplegia or quadriplegia, there is a lack of approved treatment options. Consequently, managing the condition often requires major life adjustments, confinement to a wheelchair, and a severe loss of independence (McDonald and Sadowsky, 2002). Increased life expectancy in the target population (contributed in part to the more common implementation of early therapy) alongside the permanence of the condition poses crucial questions on patient quality of life and the factors actively limiting this, as perceived by the individuals living with SCI. Recent research surveying individuals with SCI identified that participants most wished to restore lost motor function, followed by control of excretory and sexual functions (Simpson, Eng and Hsieh, 2012; Anderson, 2004).

Paralysis in SCI is the result of injury to the tissue composing the spinal cord. The injury itself acts as a barrier preventing the natural flow of the sensory-motor efferent and afferent neural signals that are necessary to control one's own body. However, both the neural pathways located above and below the injury remain intact (Ho et al., 2014). Rehabilitation for this cohort therefore aims to limit the impact of paralysis on the daily life of the injured individuals by utilising these existing intact neural pathways and maximising any residual function control. Surgical tendon transfer from areas still under the individual's control has been successfully used to restore fine hand

movement where it has been lost in paraplegia (Johnstone, Jordan and Buntine, 1988). Transcutaneous and direct electrical stimulation make use of intact motor-neuronal connections and have been used as a means of passive physical exercise, as a support for bodily function control and even to restore some degree of upper and lower motor control by inducing muscle contraction (Keith, 1996; Ho, Triolo, Elias, Kilgore, Di Marco et al., 2015). Most of these techniques, however, are only available and perform best in a laboratory setting, require specialised teams to run and, most importantly, do not offer the possibility to restore voluntary control over movement (McDonald and Sadowski, 2002).

Brain-Computer Interface (BCI) approaches, a relatively nascent technology able to detect and use brain signals to control a variety of external devices (i.e. prosthetics, robots, tablets), have been explored as a rehabilitation option in SCI and paralysis (Collinger, Boninger, Bruns, Curley, Wang and Weber, 2013; Rohm, Schneiders, Muller, Kreilinger, Kaiser et al., 2013; Birbaumer, Murguialday and Cohen, 2008). Whether through a non-invasive approach, such as using electroencephalograms (EEG) (i.e. Sellers and Donchin, 2006), or by surgically implanted microelectrode arrays (i.e. Hochberg, Serruya, Friehs, Mukand, Saleh, et al., 2006), these techniques work based on the assumption that the brain of individuals with SCI is intact and not affected by the injury. If the functional connectivity of the brain is intact, BCI-based assistive techniques have the potential to positively impact the perceived quality of life of the individuals living with SCI by restoring some of their lost independence. When asked, people with several degrees of paralysis following SCI generally reported a strong interest in the possible implementation of BCI restorative techniques even when this would require invasive or surgical procedures (Collinger et al., 2013). In recent years, researchers have successfully extracted motor imagery information when recording

from arrays implanted in the primary motor cortex (i.e. Hochberg, Serruya, Friehs, Mukand, Saleh et al., 2006) as well as neural populations located within the posterior parietal cortex (i.e. Aflalo, Kellis, Klaes, Lee, Shi, et al., 2015). In spite of the positive reception for the procedures from paralysed individuals and successful implementation under research conditions, BCIs have yet to be adopted as an option in standard rehabilitative practice. Technical inconsistencies regarding extraction sites, as well as confinement to the laboratory setting, long training times, high associated costs and potential health risks, have all been identified as plausible limiting factors (Rupp, 2014).

More importantly, research on functional connectivity following the onset of paralysis owing to SCI has variability in the results and this is also dependent on the level and type of injury (complete or incomplete) and elapsed time after the injury. In the context of BCI assistive techniques, this is particularly important to identify the extraction sites most suitable to ensure detection of strong and reliable brain signals. Generally, a high degree of functional re-organisation is reported following SCI but high variability in the results is reported. When compared to healthy individuals with fully preserved motor functions, individuals with novel, low-level SCIs show in some cases an initial increased activation in motor and premotor areas (i.e., Sabbath et al., 2002; Curt et al., 2002a). Individuals with paraplegia also show increased activity within the sensorimotor cortex, contralateral thalamus, superior parietal lobule and bilateral cerebellum during hand movements of the unaffected limb (Curt, Bruehlmeier, Leenders, Roelcke and Dietz, 2002). This is particularly interesting as it would suggest that re-organisation is not directly linked to the loss of voluntary control of the limbs but a direct consequence of the injury itself. Additional sensorimotor and posterior activation not visible in controls has also been highlighted (Jurkieicz, Mikulis, Fehlings and Verrier, 2010). Because of the nature of SCIs, both afferent and efferent connections

are severed as a direct result of the damage to the spinal cord. This means that both motor commands as well as sensory information and proprioceptive feedback coming to and from the body are altered to a degree that is commensurate to the level and type of injury. For example, a complete injury of the lumbar area means the loss of motor control and sensory feedback to areas below the injury whilst those locate above preserve the original connectivity and functions. This has a direct impact on the sensorimotor representation of the body whereby intact areas take over the sensory representation once corresponding to now deefferented areas (Dietz and Curt, 2006). This has been shown in both animal models (Wall and Egger, 1971; Nardone et al., 2013) and human participants (Dahlberg et al., 2018; Nardone et al., 2013). Attempted and imagined foot-movement related functional activity has been shown to be unaffected in long-term paraplegia (Hotz-Boedenmaker, Funk, Summers, Brugger, Hepp-Reymond et al., 2008). However, later longitudinal studies highlighted a consistent and progressive decrease in the activation of the contralateral primary motor cortex (M1) in individuals suffering from paralysis after SCI during attempted movements over a 12 months period of time (Sabre et al., 2013; Jurkiewicz, Mikulis, Fehlings and Verrier, 2010). Both of these studies relied on quantifying the volume activation within the patient cohort at different time points and did not directly compare results to matched controls with preserved motor functions (Dahlberg et al., 2018). Residual activation in higher-level SCI resulting in quadriplegia is less documented but similar effects of decreased activity within the motor cortex have been suggested (Athanasiou, Klados, Pandria, Foroglou, Kazavidi, et al., 2017; Corbetta, Burton, Sinclair, Conturo, Akbudak and McDonald, 2002) together with a higher level of grey and white matter volume loss over time (Ziegler, Grabher, Thompson, Altmann, Hupp et al., 2018; Turner, Lee, Martinez, Medlin, Schandler et al., 2001). Substantial

brain activity during attempted and imagined body movements has been reported within the posterior parietal lobe, although evidence on the long-term effects of paralysis on this area is scarce (Turner, Lee, Martinez, Medlin, Schandler et al., 2001).

In the current study, we aim to investigate the functional brain activation during hand motor imagery of individuals suffering from quadriplegia following SCI. Where previous literature has focused on early onset paralysis alone (Curt et al., 2002; Sabre et al., 2013; Jurkiewicz et al., 2010), we wish to further explore the effect of paralysis on motor imagery related brain activation in the case of long-term, complete and high-level SCI resulting in quadriplegia. We anticipate lower activation of motor areas when compared to matched controls, and similar or higher levels of activity in supplementary motor areas and posterior parietal cortex areas consistent with previous findings in a similar cohort (Turner et al., 2001). Findings will contribute to the general understanding of the effects of long-term paralysis on the performance of motor imagery in naïve participants, as well as providing further insight on the application of Brain-Computer Interfaces in the rehabilitation of lost motor control.

3.3 Methods

Participants

Six individuals with spinal cord injury and six age, sex and handedness matched controls were recruited for the purpose of this experiment. One individual from the spinal cord injury group withdrew prior to testing due to a health complication linked to their condition. Another individual from the same group withdrew after a training session for similar reasons. Consequently, the two matched controls were also excluded from the present study.

The remaining participants were right-handed as measured by the Edinburgh Handedness Inventory (EHI; Oldfield, 1971) with a mean score of 91.39(SD: 9.30). For the spinal cord injury group, the age range was 29-51 (M: 42.5; SD: 10.27). When age matching our control group, ±3 years was allowed resulting in a slightly younger sample with a range of 29-49 (M: 41.25; SD: 9.03).

Participants in the Spinal Cord Injury group were selected based on having sustained a complete injury to the spinal cord of the cervical area no less than 2 years prior to the recruitment date (April 2018). Injury location of all participants in this group was C4 and the average time since the injury occurred was 4.75 years (SD: 2.75).

Additionally, participants in this group reported no current or past neurological impairments as further confirmed by their general practitioner and Consultant Neurosurgeon. However, due to the nature of their condition all individuals from the SCI group retained no proprioceptive or sensory feedback in the affected areas of the body located below the injury. Controls were defined as to have no spinal cord injury and no current or past movement or neurological impairments.

Participants in both groups had normal or corrected to normal vision.

All participants provided written informed consent. For participants in the spinal cord injury group, consent forms were signed by their carer in the presence of the consenting participant, carer, experimenter and research nurse.

The study received ethical approval by the ethics committee of Durham University as well as the National Health Service (NHS).

Table 3 and **4** summarise details of the recruited sample, including individual scores of the EHI.

Table 3

Participants' Information: Spinal Cord Injury Group

	Age	Sex	EHI Score	Injury Location	Injury Year
S1	40	M	+ 91.30	C4	2015
S2	29	M	+ 100	C4	2010
S3	50	F	+ 73.91	C4	2002
S4	51	F	+ 100	C4	2016

Table 4

Participants' Information: Control Group

	Age	Sex	EHI Score
S1	40	M	+ 91.30
S2	29	M	+ 100
S3	47	F	+ 91.30
S4	49	F	+ 83.33

Apparatus and Stimuli

A reaching board was built to allow participants to perform the reaching and imagined reaching movements. The board measured 50 x 30 cm, was built out of MR-compatible

polymer and provided for an adjustable angle such that it could be safely and comfortably placed on each participant's torso. Four fibre optic cables were mounted on the board and served as reaching targets. Cables were placed on the board so that two would fall on the left and two on the right side of the midline of the board (**Figure 20**). This was to maximise the distance between targets in the limited amount of space allowed by the scanner bore.

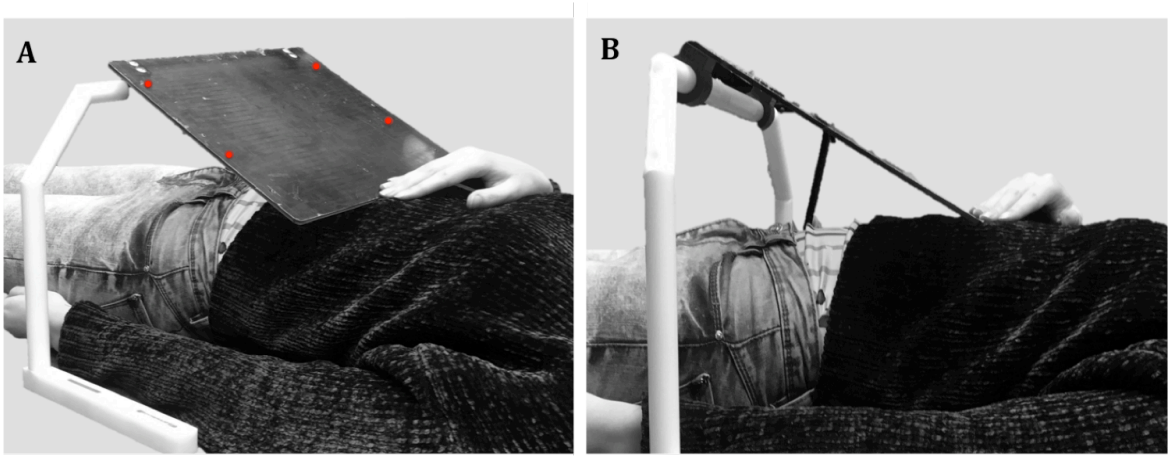

Figure 20. The reaching board. The figure above shows the board used to display the 2D LED targets here represented by the red dots (A). The holding structure has a pentagonal shape to maximise the width and height use of the scanner bore and accommodate for different body size and shape.

To ensure direct view of the reaching targets, a wooden wedge measuring 10 cm at the highest point was placed underneath the bottom MRI head coil as previously used in similar setups (Cavina-Pratesi, Monaco, Fattori, Galletti, McAdam et al., 2010). Additionally, to maximise the head tilt, foam padding was added on the bottom head coil and resting underneath the participants' head and the MRI padded bed was removed. As a result of the head tilt, only the bottom of a 12-channel head coil could be used to collect brain images and this was additionally paired with a 4-channel flex coil. A custom built, foam leg rest was placed under the participants' legs to ensure comfort

and reduce risk of back strain due to laying on the scanner bed for the duration of the experiment.

The stimuli consisted of one of the four optic cables flashing light for 250ms. Stimuli always started with the top left target to which the other three targets followed sequentially in a clockwise or counter-clockwise manner selected at random. The clockwise and counterclockwise motion was introduced to simplify the task but maintain enough variability and avoid an order effect.

To protect our participants from potential hearing damage due to noise produced by the scanner, earplugs and foam paddings were used to isolate the participants' ear canals.

To block the view of the reaching hand, participants wore a black glove.

Procedure

Recruiting and questionnaire data collection was carried out at the Spinal Cord Injury Unit at the James Cook University Hospital in Middlesbrough (UK).

Participants were offered a short training session (~20 minutes, including preparation) during which they could acclimatise with the scanner bore and practice the reaching task. This additional session was usually carried out at the moment of recruitment and several weeks before the data recording sessions.

On the day of scanning, participants were asked to complete the Edinburgh Handedness Inventory as well as a modified version of the Motor Imagery Questionnaire Revised II (MIQ-Res-II; Gregg, Hall and Butler, 2010). The MIQ-Res-II was modified to accommodate for the specific motor limitations of the Spinal Cord Injury group. Specifically, items that requested to actuate the movements were deleted and only their imagery version was kept (see **Appendix B**).

When in the scanner, participants had their preferred hand placed in a starting position, with their arm bent and the hand resting on their thorax and corresponding to the bottom of the reaching board. The other hand was placed along the body. The participants were also instructed to always maintain fixation and wait until the target was no longer visible before initiating the reaching movement.

Once the fMRI recording session began, participants were required to perform one of three tasks:

1- Perform an imagined reach movement to the location where the target appeared. Participants were instructed to wait until the target was no longer visible and immediately imagine moving their preferred hand to reach for the location to then move their hand back to the start position. Additionally, they were instructed to keep the imagined movement as natural as possible in speed and form.

2- Keep fixation for the entirety of the trial whilst targets are displayed.

3- Perform real reaching hand movements to the target locations and back to the starting position (controls only).

The MIQ-RS II questionnaire was administered once again at the end of the imaging session to confirm their preferred kind of imagery (visual or kinaesthetic).

Functional MRI parameters

Brain images were collected at the Neuroscience Unit of the James Cook University Hospital in Middlesbrough (UK) using a Siemens Trim Trio 3T functional magnetic resonance imaging scanner.

At the start of every session, a standard localiser was run and repeated any time participants requested a break. T1-weighted anatomical images were then collected.

These had a resolution of 192x256x256, echo time (TE) of 30ms, repetition time (TR) of 2sec, a 512mm2 field of view (VF) and flip angle (FA) of 75 degrees. High-resolution in-plane anatomical images were also acquired with parameters with similar values except a resolution of 320x320x30.

For the functional data we acquired T2∗-weighted gradient-echo-planar images (EPI) with a TR of 2 seconds, TE of 30ms, VF of 96 mm2 and FA of 75 degrees. Each functional run comprised of 180 volumes of 3mm voxels in a 96x96x28 matrix and a 3 mm slice thickness encompassing the whole brain.

The study design chosen was a slow event-related design. A total of 12 runs was collected. Of these, 6 were of the "imagined" condition and 6 were of the "fixation" condition. Additionally, participants in the control group completed 6 more runs of the "real" condition. For each condition, half had the targets moving in clockwise sequential progression and the remaining half, in a counter-clockwise progression. Each trial consisted of one of the four targets flashing light on the board for 250 ms. However, trials lasted 14 seconds in total and this was to allow for the fMRI-BOLD signal to fully return to baseline levels and to control for and minimise motion related artefacts in the "real" condition performed by the control participants. Additionally, one cycle was completed when all four targets had appeared. Runs were counterbalanced. Each run consisted of 5 cycles and lasted 4.66 minutes which equates to ~1.5 hours per session including breaks and preparation for the spinal cord injury group and ~2 hours for the control group.

fMRI Preprocessing and Analysis

Functional data was analysed using the Matlab-based software mrTools (Roth, Heeger and Merriam, 2018; Birman and Gardner, 2018). Preprocessing started by computing a

two-step alignment to compensate for drifting, repositioning after breaks and slight movements during testing. We first aligned the functional scans to the first collected functional. The T2*-weighted functional scans were then aligned to the in-plane high-resolution anatomical images taken at the very start of the session. We then applied a high-pass filter with a cut-off of 0.01 Hz. A 5-iteration, robust motion correction with cubic interpolation was also performed.

To proceed with the event-related analysis, I compiled stimfiles of both timing- and volume-based information regarding our stimulus time. Stimfiles are simple text-based files containing a coded description of the events occurring during trials for the full duration of a run. For the purpose of this experiment, I indicated when the lights on the board were activated (stimuli on) as well as the times in between (stimuli off). I indicated this in a combination of timing and functional volumes and assigned each of these to individual variables. In other words, the stimfiles included all the volumes and the seconds in a specific run when a stimulus was on and all the volumes and seconds corresponding to no stimulus presented. For example, each one of the trials lasted 14 seconds. Of these 14, the lights were activated at 1750 milliseconds and deactivated after 250 milliseconds. In the stimfiles, I indicated that the stimuli were presented in this specific time window as well as every seven functional volumes collected starting from the second one. For illustration purposes, **Figure 21** depicts the experimental trials.

Trial	Time (sec)	Target	Volume	Event
1	1	1	1	WAIT
1	2	1	1	WAIT for 750ms then TARGET ON for 250ms
1	3	1	2	ACTION (participant performs task)
1	4	1	2	ACTION (participant performs task)
1	5	1	3	WAIT
1	6	1	3	WAIT
1	7	1	4	WAIT
1	8-14	1	4-7	WAIT
2	15	2	8	WAIT
2	16	2	8	WAIT for 750ms then TARGET ON for 250ms
2	17	2	9	ACTION
2	18	2	9	ACTION
2	19	2	10	WAIT
2	20	2	10	WAIT
2	21	2	11	WAIT
2	22-28	2	11-14	WAIT

Figure 21. An illustration of the first 2 trials of the experimental paradigm. The Time and Volume factors were used to compile the stimfiles. The red lines indicate the repetition time (TR = 2) applied. The same time sequence is used for trial 3 and 4. Here the predictors used were "Target On" and "Target Off" lasting for 250ms.

We then proceeded to link the stimfiles to each individual raw scan and to concatenate our motion corrected functional scans into one cumulative scan. We collected a total of 180 volumes for each run; therefore, our concatenated scans contained a total of 1080 volumes for each condition (Imagined, Fixation and Real).

An event-related analysis was then computed on the same software with standard parameters. This is used to produce a map of the residual (r2) originating from the difference between the variance of the estimated hemodynamic response and that of the original time courses (for further information see Gardner, Sun, Waggoner, Ueno, Tanaka and Cheng, 2005). The timecourse is calculated by using the "target on" and "target off" as main predictors as the latter corresponds to the cue for participants to

perform either a real or imagined movement. As visible in **Figure 21**, the duration of the target display is 250ms. This is then compared to the activity recorded during times where no action is performed between the "target off" predictor and the "target on" following the start of a new trial. As stated above, this is computed by also taking into account the estimated hemodynamic response. I then produced 3D anatomical segmentations by using the recon-all function in Freesurfer (Fischl, 2012). These were then imported into mrTools using the 'mri_convert' function and the segmented images were subsequently used to draw our Regions of Interest (ROIs).

Regions of Interest

To define our regions of interest (ROI) we used a mixture of Atlas-based (Damasio, 1995) and literature-based coordinates (Puce, Constable, Luby, McCarthy, Nobre, Spencer et al., 1995; Picard and Strick, 1996; Chu and Black, 2012; Hoshi and Tanji, 2004; Connolly, Vuong and Thiele, 2015) and drew each region on the segmented surfaces by using the mrTools drawing tool. We utilised this approach rather than a functional-based localisation to maintain consistency across the two groups. Although the motor cortex could be identified by eliciting motor responses from the control group, the same could not be achieved for our SCI group.

In total, we defined seven ROIs for each hemisphere: Primary Motor Cortex (M1), Premotor Cortex (PM), Supplementary Motor Area (SMA), Superior Parietal Lobule (SPL) and anterior, medial and posterior Intraparietal Sulcus (aIPS, mIPS and pIPS). The seven regions of interest drawn on the brain surface of one participant is visible in **Figure 22**.

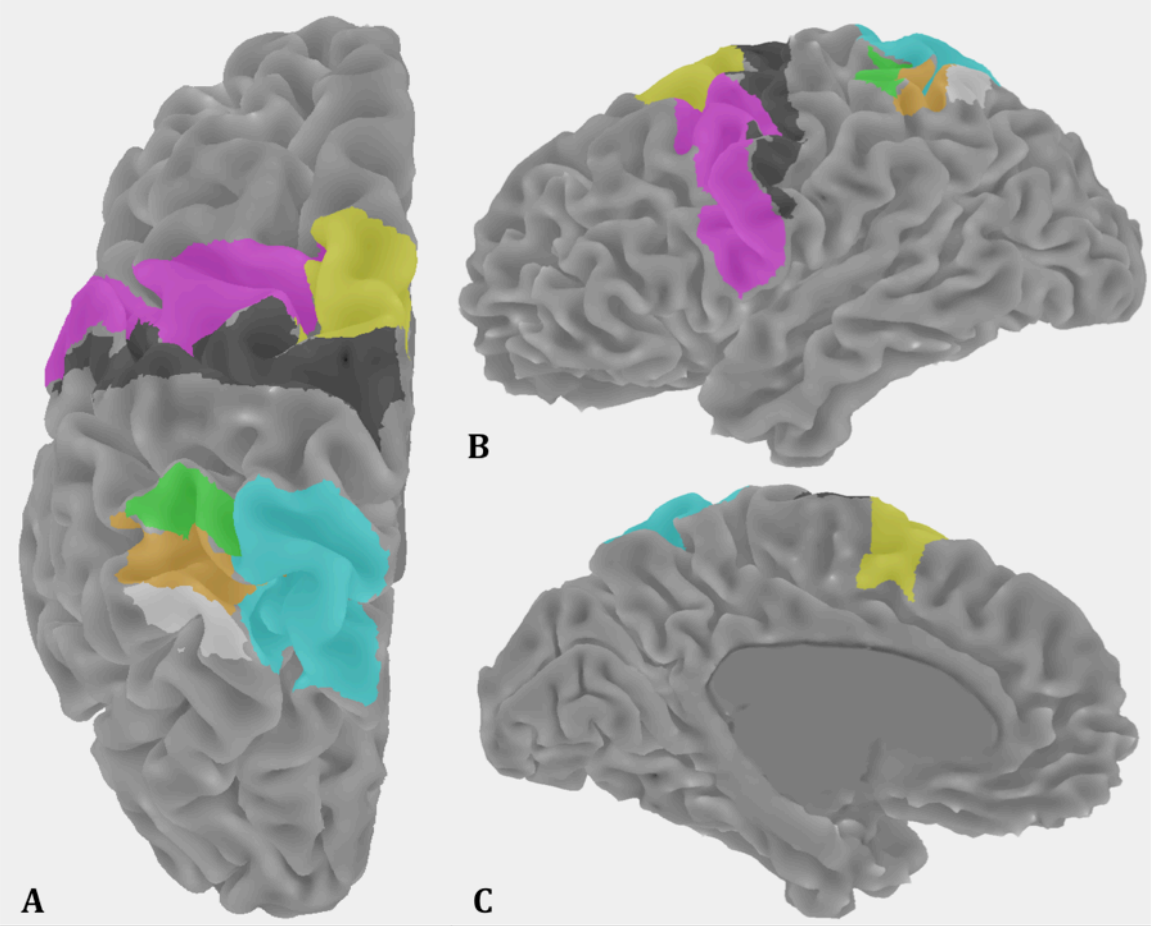

Figure 22. Regions of interest as drawn on the segmented brain surface of one sample participant. The figure shows the seven regions of interest drawn on the segmented brain of one participant viewed from a superior (A), sagittal (B) and medial (C) view. The primary motor cortex (M1) is in dark grey, supplementary motor area (SMA) is in yellow, premotor cortex (PM) in magenta, superior parietal lobule (SPL) in cyan, anterior intraparietal sulcus (aIPS) in green, medial intraparietal sulcus (mIPS) in orange and posterior intraparietal sulcus (pIPS) in light grey.

We defined M1 by using the precentral and central sulcus as upper and lower boundary respectively, and the medial wall and the lateral sulcus as medial and lateral boundary respectively (Puce, Constable, Luby, McCarthy, Nobre, Spencer et al., 1995). SMA was then drawn by locating the area delimited posteriorly by the precentral sulcus, anteriorly by accounting roughly for one third of the superior frontal gyrus, laterally by the superior frontal sulcus and medially by the cingulate sulcus (Picard and Strick, 1996; Chu and Black, 2012). We identified the premotor cortex by selecting the area

delimited medially by the superior frontal sulcus and adjacent to the SMA, laterally by the lateral sulcus and adjacent to M1, anteriorly by the ascending Sylvian fissure and posteriorly by the precentral sulcus (Hoshi and Tanji, 2004). The SPL was defined by the area located posterior to the postcentral sulcus, anterior to the parieto-occipital sulcus, medial to the intraparietal sulcus and lateral to the medial wall (excluded). The segmentation of the intraparietal sulcus was achieved by following an "equidistant procedure" described elsewhere (Connolly, Vuong and Thiele, 2015).

After drawing the ROIs, we then used the flatmap function of mrTools to create flat patches of our regions of interest thus allowing to fully visualise resulting functional activation within the brains' naturally occurring folds. **Figure 23** shows an example of the functional activity plotted on the 3D anatomical segmentations and on a flat patch of the same ROI. Having functional activation plotted on flat patches also allows for easier access to active voxels used for individual visualisation of the event-related time courses (**Figure 22-23**).

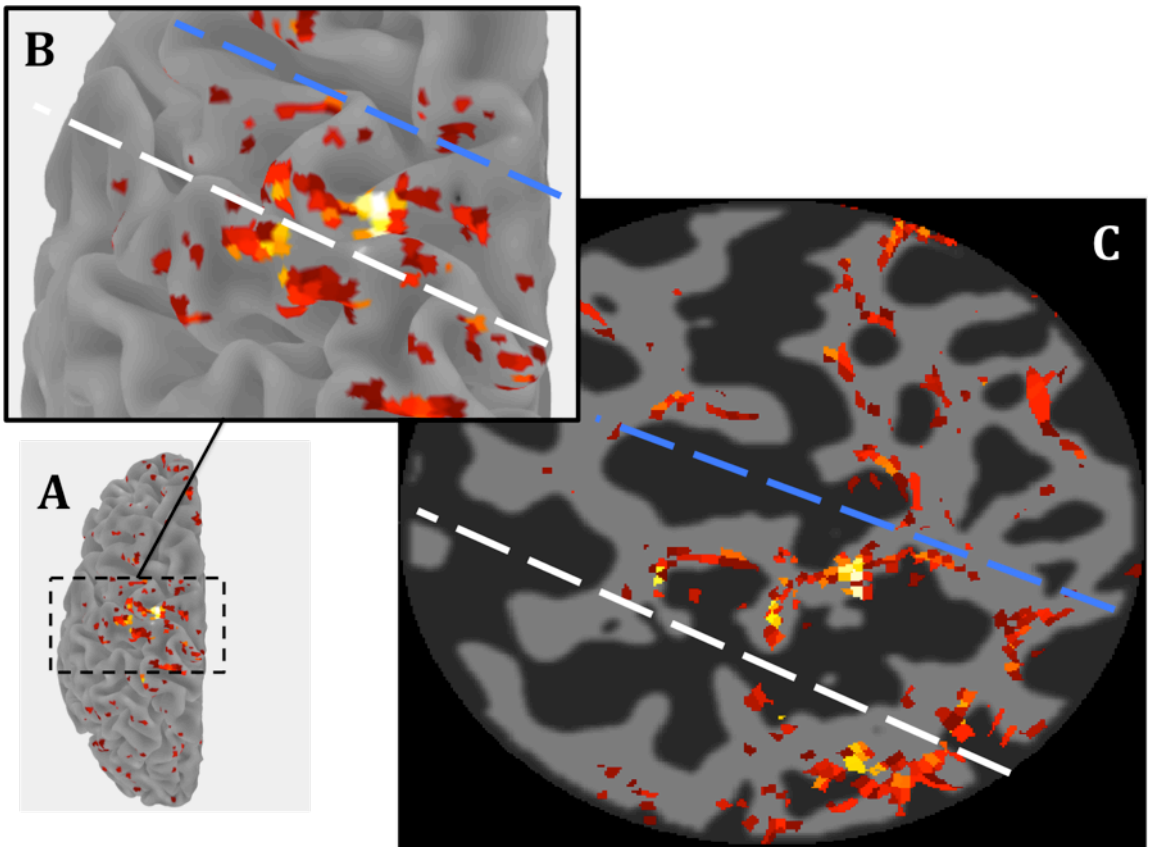

Figure 23. The flatmap function allows for easier and clearer visualisation of each active voxel within the Regions of interest. The figure above depicts the flatmap process for the primary motor cortex (M1) of a participant from the control group performing motor imagery averaged across all 6 runs using an r2 threshold of 0.25. M1 activation is calculated by comparing our two predictors, "target off", corresponding to the cue for participants to perform an action and the "wait" condition where no action is required. The full view of the left hemisphere (A) and the zoomed in panel (B) clearly show a cluster of activation over the M1 area located between the central sulcus (white dotted line) and pre-central sulcus (blue dotted line). Individual voxels within the cluster are much clearer in the flat patch of the same area (C). Please note that both the dotted square in panel A and the dotted lines in panel B and C are for illustration purposes only and do not resemble the ROIs drawn.

An interrogator function can be used in mrTools to plot the haemodynamic response of individual voxels within an ROI as well as an average response of the whole selected ROI. **Figure 24** shows the plots originating from interrogating the voxels on the flat patch in **Figure 23**.

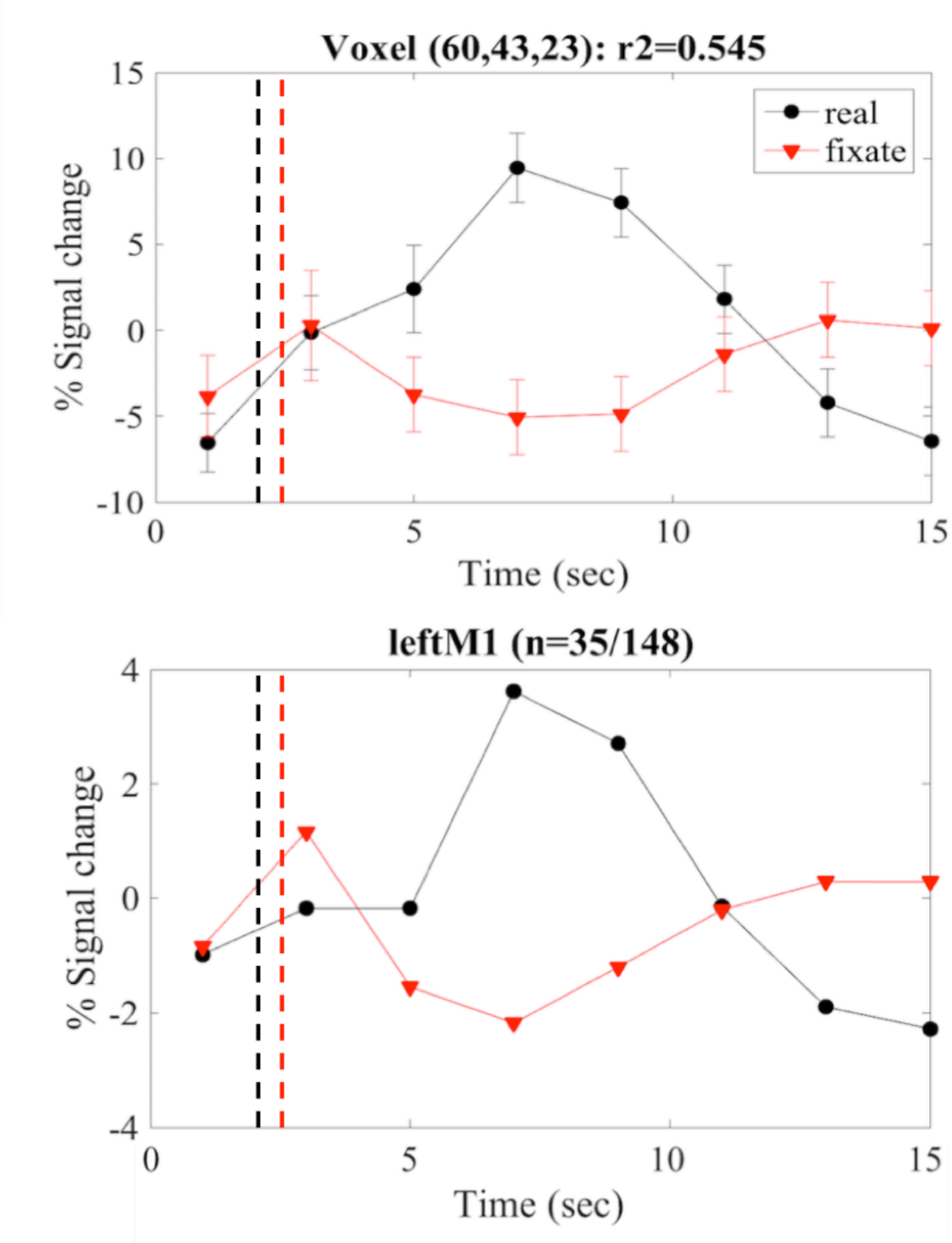

Figure 24. The time course plots originating from the interrogate function of mrTools of the left primary motor cortex (M1) of a control participant during a real reaching task. The time course of the selected voxel is displayed in the top panel. The average activity of a high coherence voxel selected within the region of interest is displayed in the bottom panel. The black and red dashed lines represent the target appearing and disappearing respectively. The solid black line represents the functional

activity of the selected voxel M1 during performance of reaching real movements within one testing session. The solid red line represents the activity of M1 when no action was performed within the same trial. Please note this figure is for visualisation purpose only and aimed to show the relevant step in the analysis using the mrTools software and was not used to compute analytical procedures.

The resulting plots were then saved and used in a custom MATLAB programme to extract time course information specific to each region of interest. The programme also computed averaging and normalising by subtracting the first data point from the cumulative time courses. It is important to note that due to the limited sample size (n=4 for each group) we only computed averages for illustration purposes. We used a MATLAB function called 'ShadedErrorBar' (Campbell, 2011) to produce figures depicting the residual activation of the regions of interest for our SCI and control groups (refer to Results).

3.4 Results

Owing to the small sample size (n=8, divided in two groups) we will only be able to report descriptive information of the brain activation during the imagined movement, real movement and fixation conditions. We will also report the results of the motor imagery questionnaires administered before and after the brain imaging sessions.

3.4.1 Motor Imagery Questionnaire

An important result that emerged after administering the MIQ-RS II to the SCI group is that individuals with long term paralysis seem to prefer visual motor imagery rather than kinaesthetic imagery. Participants verbally reported, in most cases, that trying to imagine the feel of a movement, especially of the lower limbs, was quite difficult whereas they all felt considerably more comfortable imagining the visual components of the movement. They all seemed confident in imagining themselves moving, in a first-

person perspective rather than imagining watching someone else moving. This is of importance given that ambiguity is found when searching the literature on which brain areas might be involved when performing kinaesthetic or visual imagery as well as if the imagery is performed in a first- or third-person perspective.

No difference in the magnitude of brain activation is reported when investigating visual and kinaesthetic imagery (Fourkas, Avenanti, Urgesi and Aglioti, 2006). Most importantly, similar and overlapping brain areas are reported to be active during kinaesthetic and visual imagery but these were not identical (Guillot, Collet, Nguyen, Malouin, Richards and Doyon, 2008).

For these reasons, we instructed participants in both groups to perform the same kind of visual imagery. Owing to the visual preference of the SCI group, we decided to instruct participants to only perform visual and first person motor imagery.

A summary of the individual scores for the MIQ-RS II is shown in **Table 5**. As previously noted, participants from the SCI group appeared to be more comfortable performing visual motor imagery rather than kinaesthetic whereas a clear preference is not visible in the control group. Comparison of the scores before and after the scanning session do not seem to differ greatly although a small degree of improvement was reported in some of the participants (S2, S3, S4, S2*, S3*, S4*).

Table 3

*Results for the MIQ-RS II for our participants. The * identifies control group*

	MIQ-RS II Score (Kinaesthetic) 1	MIQ-RS II Score (Visual) 1	MIQ- RS II Score (Kinaesthetic) 2	MIQ-RS II Score (Visual) 2
S1	26	40	26	40
S2	23	39	24	39
S3	22	37	22	39
S4	30	37	33	37
S1*	42	42	42	42
S2*	33	29	35	32
S3*	33	26	33	28
S4*	35	34	35	35

3.4.2 Brain activation during visual motor imagery

Via the interrogation function of mrTools, we were able to investigate exactly how many voxels were active during each run for the different ROIs. **Table 6** summarises the average number of voxels active for each ROI for our participants in the Spinal Cord Injury group (SCI) and the Control Group (CG) in the visual motor imagery condition.

Table 6

Number of voxels active during visual motor imagery in Spinal Cord Injury (SCI) and Control (CG) Groups in each region of interest.

	M1	SMA	PM	SPL	aIPS	mIPS	pIPS
SCI	34	65	42	74	44	16	26
CG	115	82	81	78	49	32	49

As demonstrated in **Table 6**, the superior parietal lobule (SPL) and the supplementary motor area (SMA) present the highest number of voxels active during visual motor imagery in the SCI group. Additionally, Medial- and Posterior- intraparietal sulcus (mIPS and pIPS) show the lowest number of active voxels. In the control group (CG), the highest number is detected in M1, followed by SMA and premotor cortex (PM) whereas the lowest activation is detected in the mIPS. Comparing the means across the two groups, we note that there are a similar number of active voxels in SPL and anterior- intraparietal sulcus (aIPS). The highest difference in active voxels is reported within M1 with the SCI group exhibiting 34 active voxels on average against the 115 of the control group. A chi-squared test of independence was calculated to compare the activation of the 7 different ROIs of the two groups. A significant inteaction was found, $\chi^2(6) = 26.681$, $p<.0001$.

A result of the event-related activation during visual motor imagery is displayed in **Figure 25** on whole-brain surfaces. Generally, we observed considerable noise in both groups and this is visible here. However, some clusters of activation are noticeable. Group S1 demonstrates activation in motor and premotor areas in both the SCI participant (left) and control (right) with the control also showing a cluster of activation in the SPL of the posterior parietal cortex. For group S2, we can see mainly scattered activation around motor and premotor areas for the control participant (right), whereas activation is predominantly visible along the posterior parietal cortex and occipital cortex of the SCI participant (left). Clusters of activation are not visible in this configuration for group S3. Finally, group S4 shows several activation clusters around the premotor and motor areas as well as posterior parietal cortex of the control participant (right).

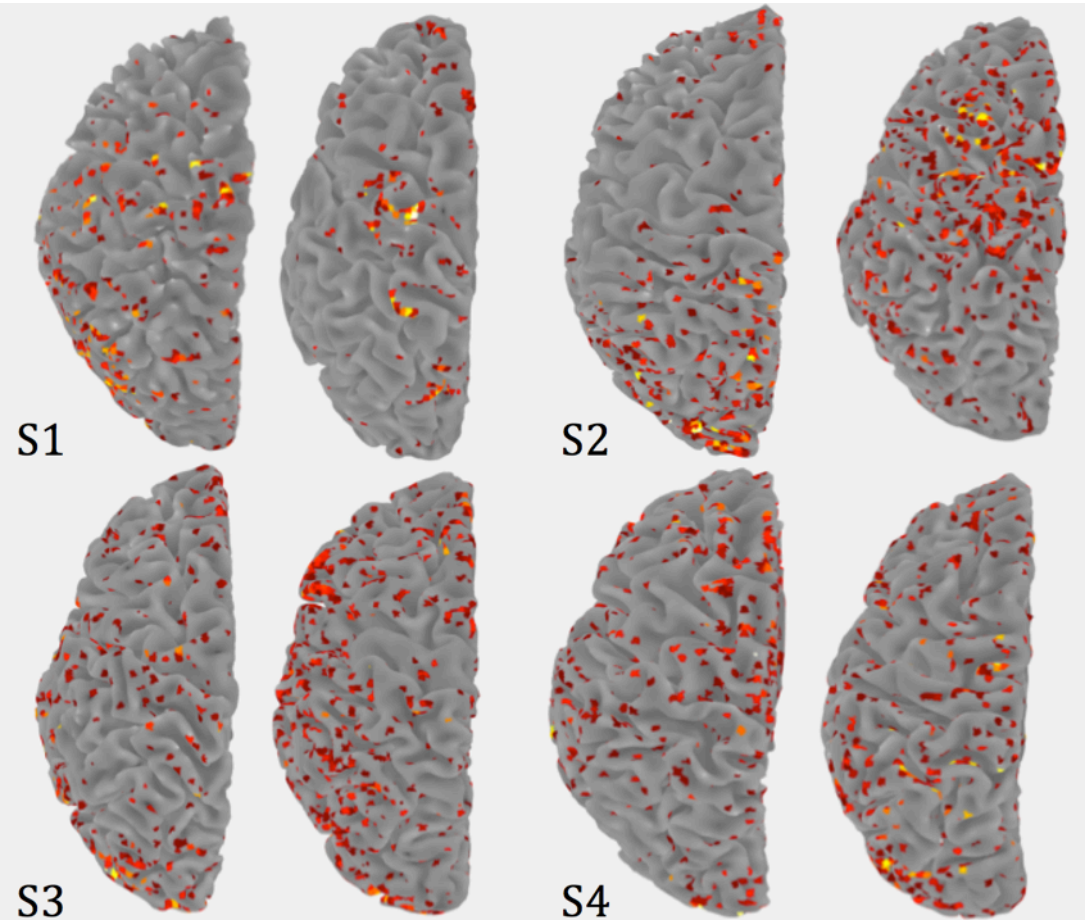

Figure 25. 3D anatomical segmented images of the left hemisphere during visual motor imagery. The figure shows brain activation during visually imagined movements to the 2D light targets displayed during trials. In each group, S1-4, participants from the spinal cord injury group are on the left and their matched control is on the right. The correlation coefficient used to produced these maps was in all cases c = 0.035.

Data obtained by calculating the time course information for each ROI were used to compute averages of the MRI BOLD response for each group and are summarised in **Figures 26-29**. Generally, M1 is inactive in all of our participants from the SCI group whereas the opposite is visible for the matched controls. Additionally, SPL and aIPS are consistently active in the SCI group and in 3 out of 4 occasions this activation is higher than those reported in the matched controls. SMA, although consistently active in our control group, appears quite variable in the SCI group with 2 out of 4 participants

showing little to no activation (group S2-3) and 1 participant showing de-activation instead (group S4).

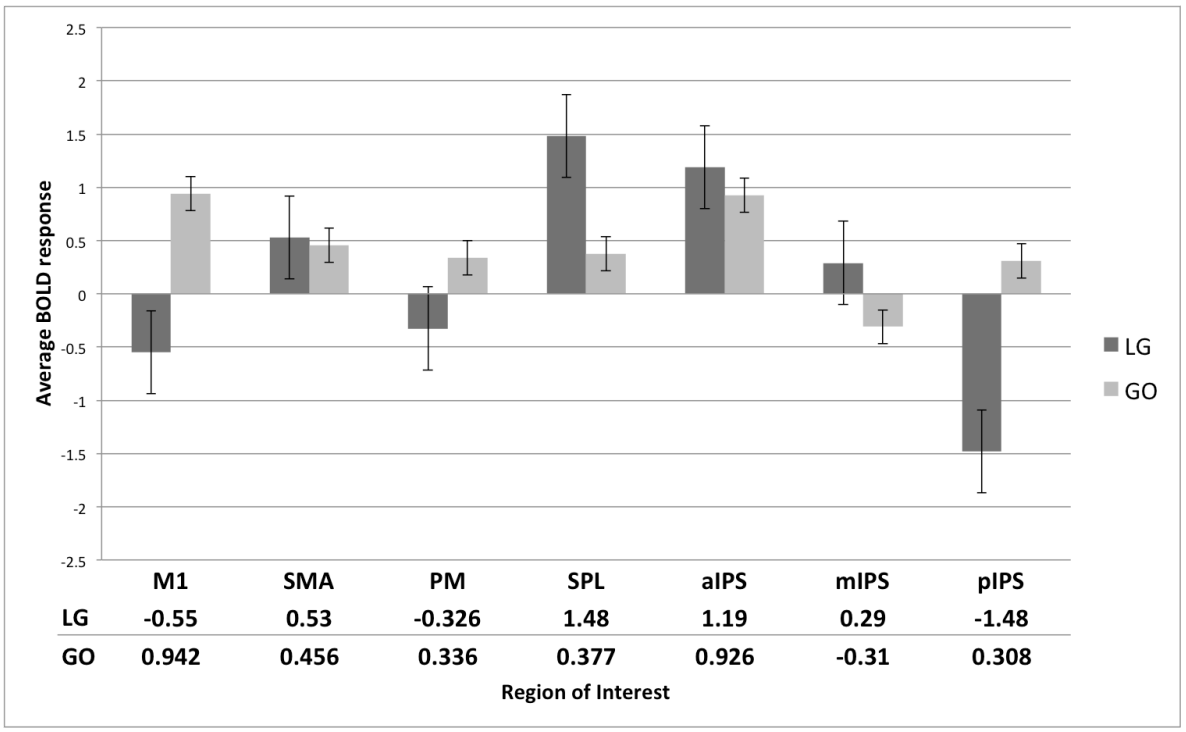

Figure 26. Average BOLD response of visual motor imagery of group S1. This graph shows the average activation during visual motor imagery to the flashed 2D light targets. Results are shown in blue for the participant of the spinal cord injury group (LG) and green for the matched control (GO). Error bars represent the Standard Error.

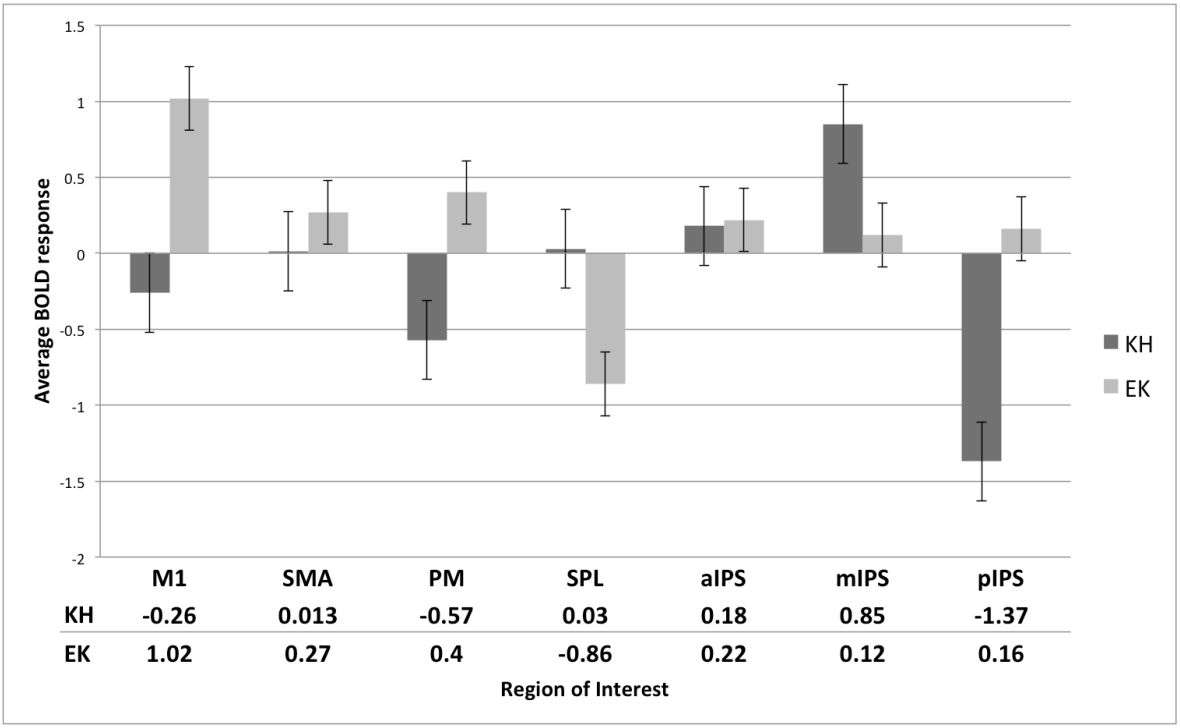

Figure 27. Average BOLD response of visual motor imagery of group S2. The graph above shows the average activation during visual motor imagery to the 2D light targets for a participant from the SCI group (KH) in blue and the matched control (EK) in green. Error bars represent the Standard Error.

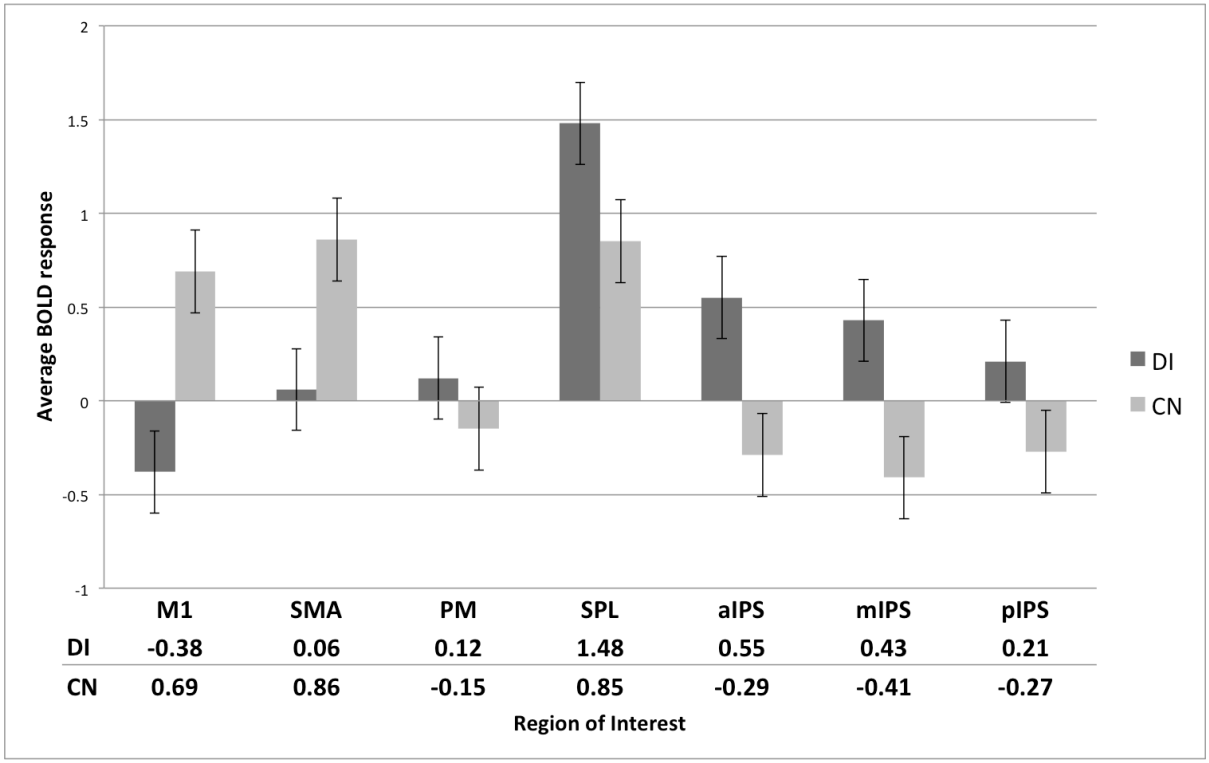

Figure 28. Average BOLD response of visual motor imagery of group S3. The graph shows the brain activation of visual motor imagery to 2D light targets for a participant of the SCI group (DI) in blue and the matched control (CN) in green. Error bars represent the Standard Error.

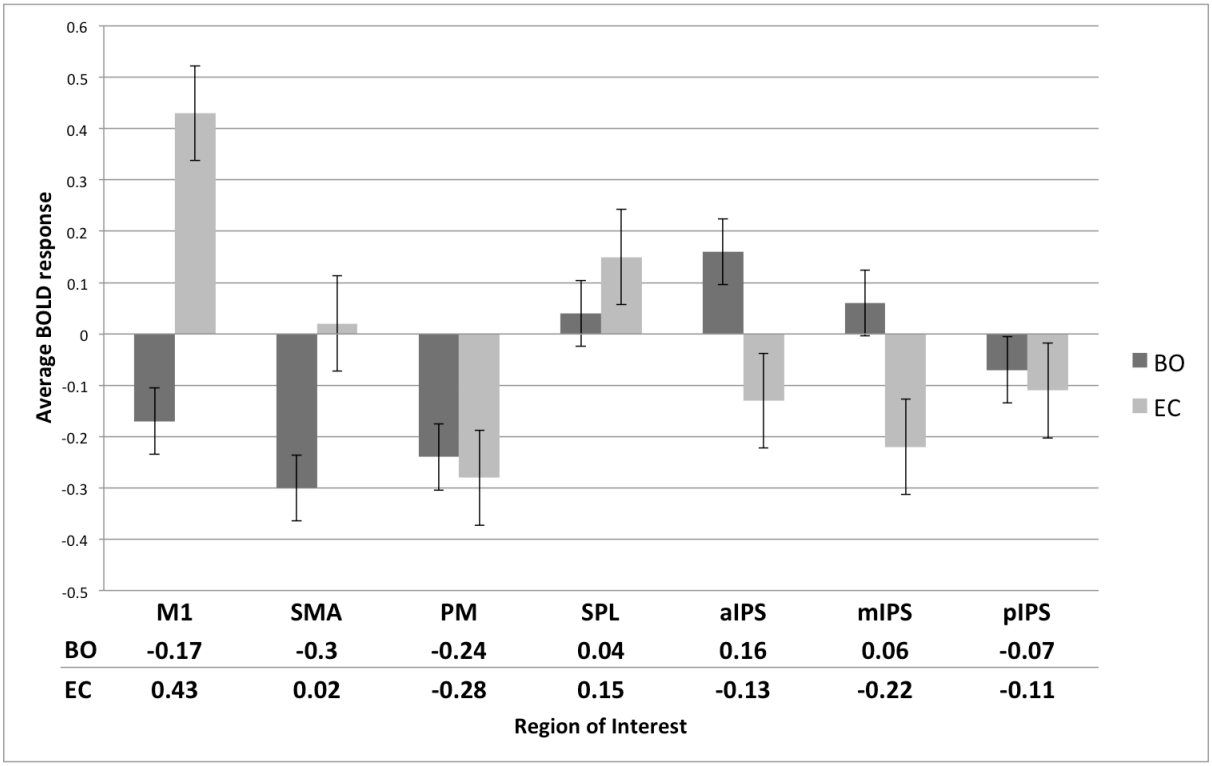

Figure 29. Average BOLD response of visual motor imagery of group S4. The graph shows the brain activation of visual motor imagery to 2D light targets for a participant of the SCI group (BO) in blue and the matched control (EC) in green. Error bars represent the Standard Error.

Figure 30 shows a comparison between activation during real reaches and motor imagery in the control group. Although higher in magnitude when performing real movements, similar activity is reported within the regions of interest investigated.

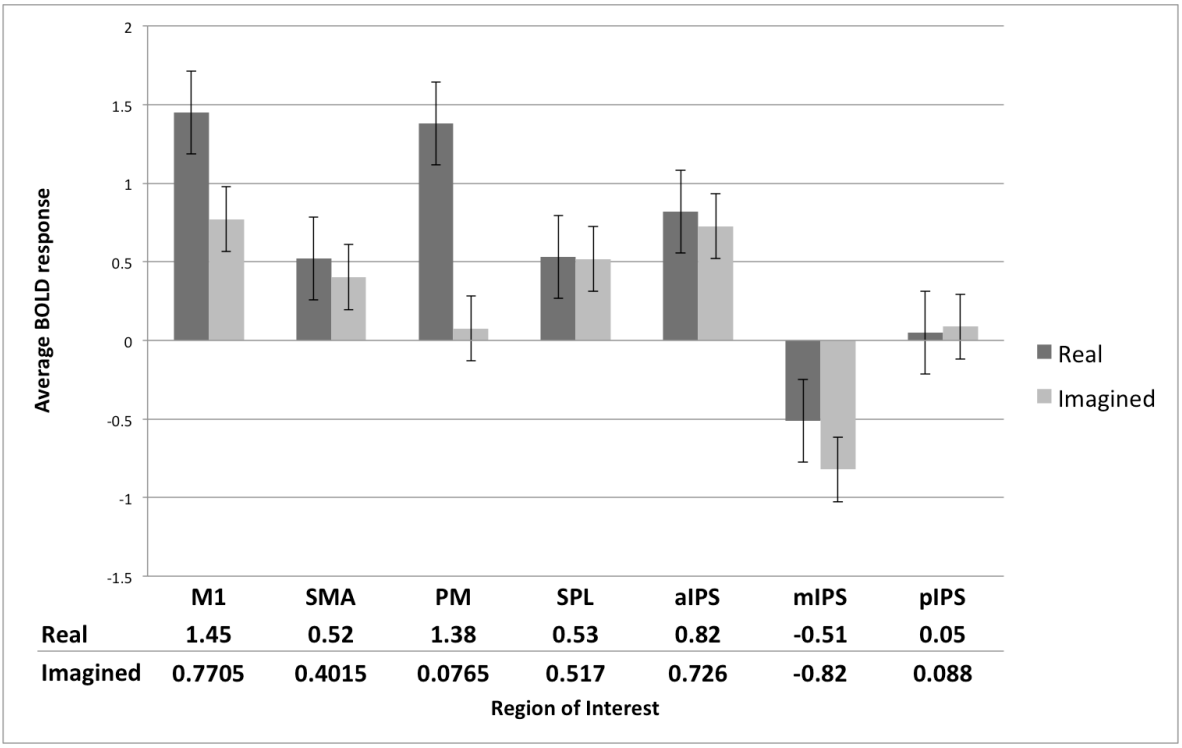

	M1	SMA	PM	SPL	aIPS	mIPS	pIPS
Real	1.45	0.52	1.38	0.53	0.82	-0.51	0.05
Imagined	0.7705	0.4015	0.0765	0.517	0.726	-0.82	0.088

Figure 30. A comparison of real reaches and motor imagery in the control group. The graph above depicts activation registered when controls were performing real reaching movements to 2D targets (blue) and motor imagery (green). Activity has higher magnitude in M1 and PM when a real reach is performed. Same pattern of activity is reported for the remaining regions of interest across the two conditions. Error bars represent the Standard Error.

We then computed group averages of the residual activation for all the trials in which participants performed visual motor imagery, for the seven regions of interest. **Figure 31** demonstrates the activation of motor and premotor areas (M1, SMA and PM) between the SCI group (in red) and the control group (in blue). In line with the single subject level results, M1 appears inactive throughout the trial in the SCI group as activation stays in the negative domain. A rise in the BOLD response is reported at 2 seconds for SMA and this is consistent with the time the 2D target disappeared, cueing for the participant's imagined action. An earlier increase is instead noted for PM peaking at the presentation of the target (1750 ms). Looking at the control group (blue), an increase of activation is visible for all three motor areas with M1 showing the greatest

degree of activation as compared to SMA and PM. SMA demonstrates a similar response to that of the SCI group, with a rise in the fMRI-BOLD response visible after second 2, corresponding to the disappearance of the target and cue for the participant's response. Although enhanced in magnitude, M1 shows a response that closely resembles that of SMA. Similarly to the SCI group, PM of controls also shows an earlier response compared to that of M1 and SMA.

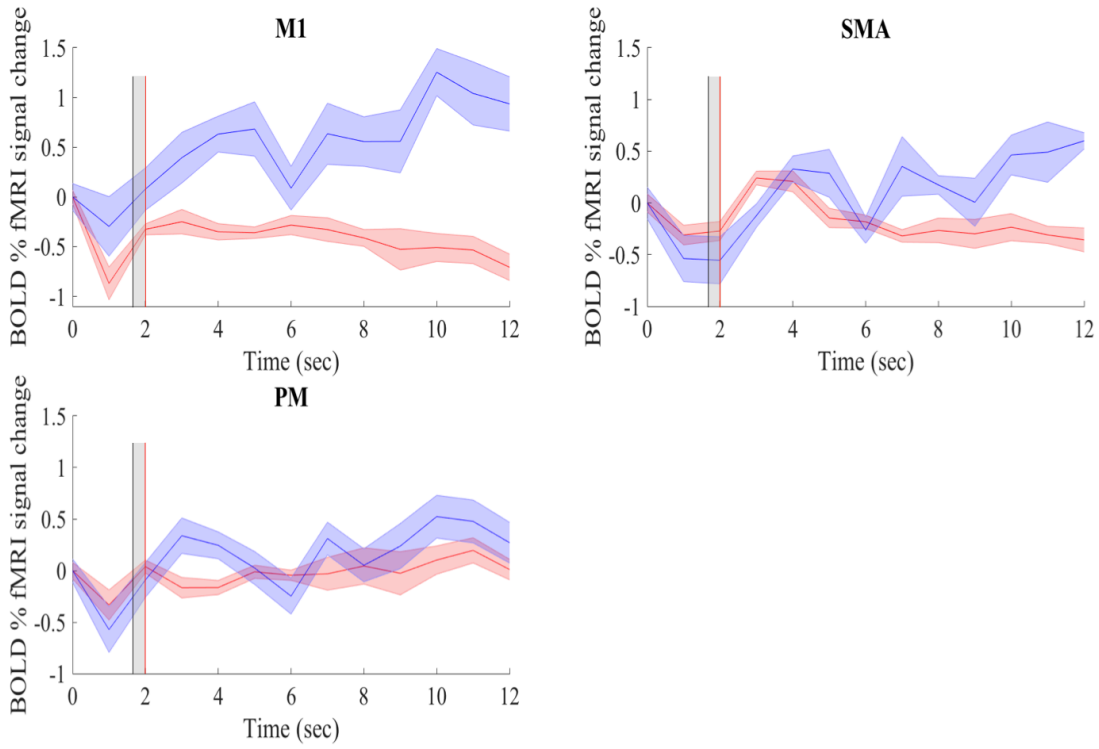

Figure 31. Comparison of the time course of the BOLD fMRI response of M1, SMA and PM between the SCI group and controls. The graph above depicts the average fMRI activation during visual motor imagery of the four participants of the SCI group (red) and the matched controls (blue) in primary motor cortex, supplementary motor area and premotor cortex. The grey shaded area indicates the window in which the visual target is displayed, appearing at 750ms (black line) and disappearing at 1sec (red line).

The average activation for posteriorly located ROIs is depicted in **Figure 32**. Here, positive activity is visible for three of the four parietal in the SCI group (red). SPL, aIPS and mIPS all show a rise in activation consistent with the presentation of the 2D

targets. pIPS shows no activation, on average, during visual motor imagery in this group. Finally, activation of posterior areas in the control group (blue) is generally low but higher for SPL when compared to aIPS and pIPS. mIPS shows small to no activation during visual motor imagery in this group.

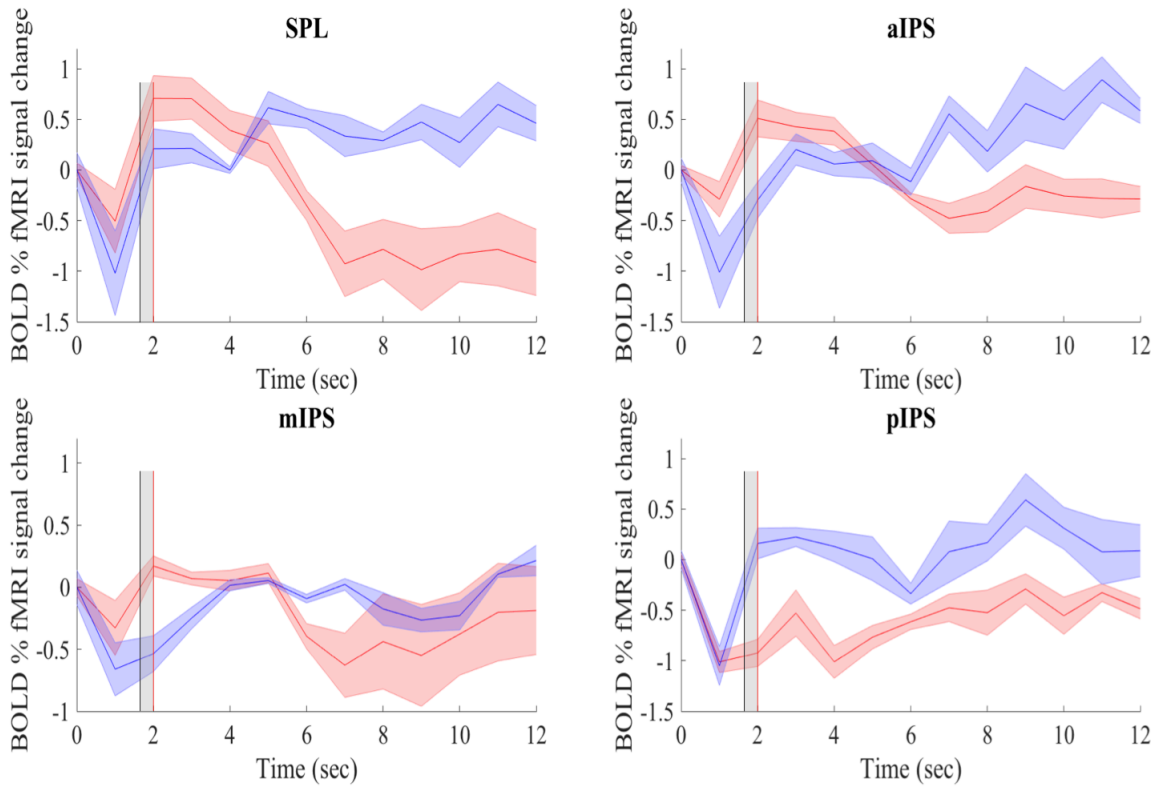

Figure 32. Comparison of the time course of the BOLD fMRI response of SPL, aIPS, mIPS and pIPS between the SCI group and controls. The graph above depicts the average fMRI activation during visual motor imagery of the four participants of the SCI group (red) and the matched controls (blue) in superior parietal lobule, anterior-, medial and posterior intraparietal sulci. The grey shaded area indicates the window in which the visual target is displayed, appearing at 750ms (black line) and disappearing at 1sec (red line).

Further comparison of the overall activation across the two conditions of imagined movement performance and fixation was computed. This is to ensure the activity reported above is not simply a response to the presentation of the visual stimuli participants were required to attend to. **Figures 33-34** show the activation during

performance of imagined movements to the visual targets in motor and premotor areas (**Figure 33**), and posterior areas (**Figure 34**) in both control (blue) and SCI group (red). As visible in both figures, all ROIs show no activation during the trials where participants were instructed to simply maintain fixation.

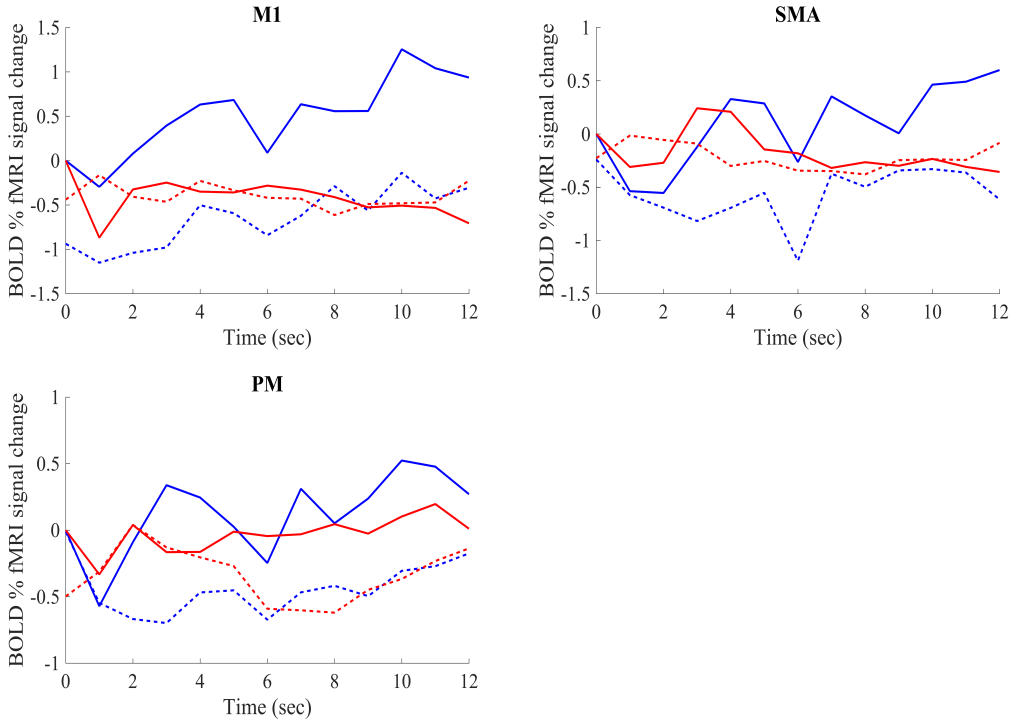

Figure 33. Comparison of the time course of the BOLD fMRI response during Imagined Movements and Fixation conditions in M1, SMA and PM. The graph above depicts the average fMRI activation during the performance of visual motor imagery (solid lines) and fixation (dashed lines) in the control group (blue lines) and the SCI group (red lines). During the fixation condition, participants were instructed to keep their gaze focused on the fixation point whilst visual stimuli where presented in their peripheral visual field in the same way as during the visual motor imagery task. As visible from the graph above, despite the stimuli being consistent, motor and premotor areas show no activation during the fixation condition.

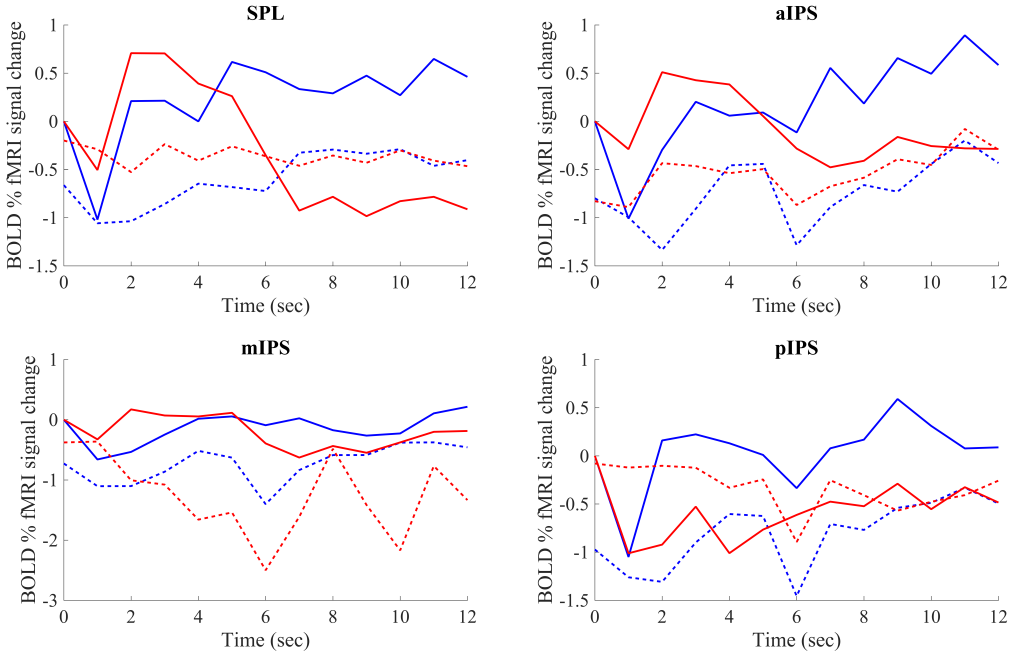

Figure 34. Comparison of the time course of the BOLD fMRI response during Imagined Movements and Fixation conditions in SPL, aIPS, mIPS, and pIPS. The graph above depicts the average fMRI activation during the performance of visual motor imagery (solid lines) and fixation (dashed lines) in the control group (blue lines) and the SCI group (red lines) in posteriorly located regions of interest. During the fixation condition, participants were instructed to keep their gaze focused on the fixation point whilst visual stimuli where presented in their peripheral visual field in the same way as during the visual motor imagery task. As visible from the graph above, despite the stimuli being consistent, these posterior areas show no activation during the fixation condition.

3.5 Discussion

In the current experiment, when comparing brain functional activity during hand motor imagery of individuals with high-level SCI to that of matched controls, we report no to very low fMRI-BOLD responses in the motor cortex and associated frontal areas, which do exhibit high level fMRI-BOLD responses in the control group. Chi-squared comparisons highlight significant differences across the two groups suggesting

activation levels incur changes following a long term SCI (p<0.0001). Furthermore, activation has also been compared to a control condition where participants in both groups were asked to maintain fixation to the centre of the reaching board whilst visual stimuli were presented. This condition was added to account for the possible effect passive visual stimulation could have on the target brain areas when participants were not performing motor imagery. Comparison of brain activity during performance of motor imagery and exclusive fixation showed a general de-activation of all motor, premotor and posterior regions of interest during the control fixation trials (**Figures 33-34**). This suggests that the activity reported in this manuscript during the active tasks is likely related to the visual motor imagery perfomance rather than passive visual stimulation.

During the performance of the imagined reaching task, activation is reported in all participants with SCI in more posteriorly located areas. More specifically, the primary motor cortex (M1) appears to be inactive in all four participants from the SCI group. The premotor cortex (PM) is inactive in three out of four participants in the same group. The Supplementary Motor Area (SMA) is active in three out of four participants with SCI. Furthermore, the number of active voxels in these areas is on average lower than that of controls. This is consistent with previous findings in the literature highlighting a decrease in activation of motor and premotor areas during the first year following SCI paralysis (Jurkiewicz, Mikulis, Fehlings and Verrier, 2010). Although initial activity volume information of our four participants was not investigated on this occasion, we suggest that the lower activity and overall number of active voxels hereby reported could be the result of the same progressive process reported by Jurkiewicz et al. (2010). A longitudinal study to follow individuals diagnosed with SCI for a period of time longer than one year is needed to confirm this, and could be highly beneficial in

understanding the development of brain reorganisation following paralysis. This is especially relevant for those individuals with high-level injuries that retain voluntary motor control over very few areas, i.e. face muscles, eyes and mouth.

Investigating activity within relatively posteriorly located regions of interest, we report that the posterior intraparietal sulcus is relatively inactive in our participants from the SCI group. The superior parietal lobule (SPL) and the anterior- and medial-intraparietal sulci (aIPS and mIPS), however, all show activity that is at times higher than that of controls. These results are also consistent with previous findings in lower-level SCI (Kokotilo, Eng and Curt, 2009). This could be due to the peculiar functional role of the posterior parietal cortex (PPC), reported to be involved in a wide array of motor-related functions such as sensorimotor integration, planning of movements, movement intention, and visual representation of space (Desmurget, Epstein, Turner, Prablanc, Alexander and Grafton, 1999; Snyder, Batista and Andersen, 1997; Wolpert, Goodbody and Husain, 1998; Cohen and Andersen, 2002), all of which are still possible actions in SCI. In other words, the integrative role of the PPC might prevent this area from incurring the same level of functional activation loss as that reported in M1 and the premotor cortex following paralysis (Jurkiewicz et al, 2007; Cramer, Lastra, Lacourse and Cohen, 2005). However, longitudinal studies are needed to establish whether a loss of motor imagery-related activation or overall volume is encountered in PPC over a longer period of time.

However, it is important to also note that one substantial limitation to this study is the use of visual motor imagery as opposed to kinaestetic. Although existing literature reports related brain activity to be similar in magnitude and location (Fourkas, et al., 2006; Guillot, et al., 2008), future experiments should compare activity during performance of both visual and kinaestetic motor imagery in long-term SCI. This could

aid evaluating whether the lack of activity hereby reported in motor and premotor areas is consistent when performing kinaestetic motor imagery instead of visual. Longitudinal approaches could also address the possiblity of the brain response to kinaestetic motor imagery being negatively affected sooner than visual thus strenghtening the need for promt implementation of motor imagery based rehabilitation to preserve adequate brain functional connectivity.

One aspect to note is that the structural volume of brain areas following SCI, including M1, shows no significant differences as compared to the healthy population (Crawley, Jurkiewicz, Yim, Heyn, Verrier, et al., 2004). This suggests that the loss of volume of activity reported in SCI might not be due to atrophy of the motor areas but rather a functional reorganisation following paralysis, whereby M1 adapts to a new internal body representation that is based on the remaining body efferent information (Lotze, Laubis-Hermann, Topka, Erb and Grodd, 1998; Mikulis, Jurkiewicz, McIlroy, Staines, Rickards et al., 2002; Bruehlmeier, Dietz, Leenders, Roelcke, Missimer and Curt, 2001). In other words, the primary motor cortex might repurpose areas dedicated to the functional representation of body parts located below the injury, and therefore no longer connected to M1, for those areas that still are under direct control of the affected individual. This view is further supported by the observation that where initial loss of M1 connectivity was reported following acute states of SCI, a partial degree of motor recovery meant a proportionate increase of movement-related M1 activation (Jurkiewicz, Mikulis, McIlroy, Fehlings and Verrier, 2007). In this context, investigation of the patterns of activation in a larger sample of individuals affected by a long-term SCI may aid in further our understanding of both the progression of the potential loss of activation of motor areas and fine motor control and the nature of the shift toward more posteriorly located areas. Future studies will benefit from overall wider recruitment

and resources allowing for investigating the functional distribution of motor imagery related activity over time.

Where physical rehabilitation has been attempted with limited success and motor functions fail to be restored, motor imagery could contribute to maintain healthy levels of functional connectivity and brain representation (Decety and Boisson, 1990). The performance of mental representations of actions has been linked to the recruitment of brain areas, such as M1, SMA and SPL, which are also active during actual execution of the same actions in the healthy population (Ruby and Decety, 2001; Lotze and Halsband, 2006). A similar distribution of brain activation during real and imagined reaches in the control group is also reported in the current experiment (**Figure 30**).

Looking at the results for the Motor Imagery Questionnaire (MIQ-RS II), we noted that participants of our SCI group naive to motor imagery, appeared more comfortable in performing visual than kinaesthetic motor imagery. Participants stated that they could not clearly mentally rehears the feeling of movement and imagining visually was much more natural to them. Although not possible within this study due to the limited sample size, future research might look at the correlation between residual activation within the Primary Motor Cortex and kinaesthetic motor imagery proficiency. In SCI, the performance of motor imagery has been linked to improved motor recovery and promotion of adaptive plasticity, as well as reinforcing movement-related brain activity in different levels of cervical injury (Grangeon, Revol, Guillot and Collet, 2012).

The introduction of motor imagery training in standard rehabilitation could therefore help maintain healthy brain connectivity and prevent M1 functional disconnection over time (Mateo, Di Rienzo, Bergeron, Guillot, Collet and Rode, 2015). This could be extremely beneficial to those individuals with lower-level cervical SCI who

still maintain some gross control over shoulder and arm movement. Additionally, in the case of high-level SCI, motor imagery training could maximise the individual's suitability to access assistive Brain-Computer Interface by preventing the loss of functional connectivity of motor areas that are commonly recruited when implementing these techniques (Mateo et al., 2015).

However, in our sample of naïve individuals never before formally trained in motor imagery, the primary motor cortex shows no activity and a lower number of active voxels on average as compared to the matched controls. In contrast, areas of the PPC appear to still be active and, in some cases, activity is higher than that reported for controls. BCI relying on posteriorly located extraction sites (i.e. Aflalo et al., 2015) might augment feasibility and effectiveness of these rehabilitative techniques by being able to reach a larger number of individuals within the affected population, including those who sustained the injury farther in the past and might have already incurred in a loss of M1 activation. However, further research with a significantly larger sample size is needed to establish the effects of long-term and high-level SCI on the functional connectivity of the posterior parietal cortex.

Gathering more information will benefit not only the general understanding of brain reorganisation following paralysis but will also support the development of BCI assistive options that are more affordable and inclusive.

4 Secondment

In previous chapters we investigated the interaction between proprioceptive feedback originating within the body and central representation of space as well as eye movement performance. We discussed how this interaction could be potentially detrimental to the efficient use and application of BCI assistive techniques and could contribute to limit their introduction to a standard rehabilitation setting. One of the most compelling aspects of BCI techniques is the possibility to restore lost independence by allowing the user to interact with their environment (i.e. wheelchair, tablets, smart home devices) without external assistance. This ability, however, generates a substantial amount of movement-related noise that needs to be controlled for (Minguillon, Lopez-Gordo and Pelayo, 2017) and this is especially true for head movements where most of the current BCI signal extraction devices are placed (Ramoser, Muller-Gerking and Pfurtscheller, 2000; Hamedi, Salleh and Noor, 2016; Bamdad, Zarshenas and Auais, 2014; Vaid, Singh and Kaur, 2015). In a project carried out at the Netherlands Organisation for Applied Scientific Research (Nederlandse Organisatie voor Toegepast Natuurwetenschappelijk Onderzoek, TNO), we investigate the possibility of early detection of head movements to improve real-time BCI signal acquisition through electroencephalography (EEG). If we are able to detect planned head movements before their actual execution, computations can be made in advance to adjust and control for the movement-related noise. We were able to detect self-generated head rotations as early as 300ms before actual movement execution. The signal was extracted from channels CP1 and CP2, corresponding roughly to the primary motor cortex (M1). More interestingly, the signal detected was clear enough to also distinguish the direction of the movement (left or right) and whether movements occurred at all (no movement). Implications for BCI application are discussed in the

context of real-time applications that would benefit from early detection of self-paced, exploratory head movements. A successful application of the design hereby presented can be found in later work by the same research group (Brouwer, van der Waa and Stokking, 2018).

4.1 A Feasible BCI in Real Life: Using Predicted Head Rotation to Improve HMD Imaging

Brouwer, A.M., van der Waa, J.S., Hogervorst, M.A., Cacace, A., Stokking, H.

Accepted: March 2017

4.1.1 Abstract

While brain signals potentially provide us with valuable information about a user, it is not straightforward to derive and use this information to smooth man-machine interaction in a real life setting. We here propose to predict head rotation on the basis of brain signals in order to improve images presented in a Head Mounted Display (HMD). Previous studies based on arm and leg movements suggest that this could be possible, and a pilot study showed promising results. From the perspective of the field of Brain-Computer Interfaces (BCI), this application provides a good case to put the field's achievements to the test and to further develop in the context of a real life application. The main reason for this is that within the proposed application, acquiring accurately labelled training data (whether and which head movement took place) and monitoring of the quality of the predictive model can happen on the fly. From the perspective of

HMD technology and Intelligent User Interfaces, the proposed BCI potentially improves user experience and enables new types of immersive applications.

Author Keywords

EEG; passive BCI; movement; HMD; Virtual Reality

ACM Classification Keywords

H.1.2 User/Machine Systems, H.5.2 User Interfaces

4.1.2 Predicting head rotation: background and application

Monitoring cognitive and affective state using brain signals could be potentially useful in a range of applications such as real time adaptation of automated systems to fit the affective state of a particular individual. While impressive progress has been made in the field, it is still difficult to pinpoint 'killer applications' where these estimates from brain signals could, in the near term, support the user enough to justify wearing electrodes. There are several reasons for this (Brouwer, Zander, Korteling and Bronkhorst, 2015). One is that in many cases, there are other, more reliable measures of cognitive and affective state available (like user performance, behavioural measures and explicit user input). Perhaps even more important is the problem of acquiring data to train the BCI system. Training data should preferably be collected for the same individual and in the same conditions as those where the BCI system is to be used, and updated regularly. Correct labels (i.e., the 'true' cognitive or affective state that goes with a data interval) are, especially under those conditions, often difficult to acquire.

We here present a possible BCI application that can be envisioned to provide added value relatively soon, based on currently existing methods and equipment, since it is a system that automatically collects correctly labelled data without user effort, it can validate itself on the fly and gradually improve the man-machine interaction even when the accuracy of its predictions is limited. Also, it is likely that at least in some applications, brain signals are more informative than other possible sources of information. The proposed BCI application is the prediction of head movements in order to reduce delays in images presented in HMDs. For certain HMD displays, especially those presenting streamed video data, choices in usage of bandwidth have to be such that image resolution is sacrificed to reducing delays in the viewed image when the head moves. This trade-off could be chosen more optimally if we would know whether it is likely the head is going to rotate, and if so, in which direction.

EEG signals preceding movement

Before a body movement takes place, several processes have occurred in the brain. Depending on what elicited the movement, or what is its goal, attention has been drawn, a decision has been made, and the movement has been planned by the brain. After planning, signals are sent to the muscles to contract, and only then the movement starts. This means that we can potentially use brain signals to shorten the time of reliably detecting that the head started to move compared to conventional methods, or to even predict head movements.

The literature reports two general signals related to movement planning than can be captured by EEG. One is the readiness potential (cf. lateralized readiness potential, contingent negative variation or CNV, bereitschaftspotential (Coles, 1989;, Guggisberg and Mottaz, 2013;,Kornhuber and Deecke, 1965; Leuthold, Sommer and Ulrich, 2004;,

Walter, Cooper, Aldridge, McCallum and Winter, 1964), and the other is (lateralized) event related desynchronization (Pfurtscheller, 2001). The first type of signal has been observed at the motor cortex (e.g. at electrodes CP1, CP2) when signals are synchronized on (hand) movement onsets. Depending on the exact research paradigm, voltage starts to go down already 2s before movement onset. This slow negativity effect has been attributed to non-specific (attention related) preparation for action. Around 400 ms before movement onset the signals become asymmetric according to whether the movement is left or right (the 'lateralized' part). For the desynchronization type of signal, power in the 10-12 Hz (alpha or mu) frequency band is investigated. A desynchronized signal, represented by a low power in the 10-12 Hz band, roughly corresponds to a high level of activation of that area. Left hand movement imaging, planning and execution corresponds to a relatively low power in the right hemisphere, and vice versa.

EEG signals preceding head rotation

Studies on the signals described above usually employ hand or arm movements. In the literature, we could not find specific information about EEG and head rotation. Still, we know the approximate location of the neck muscles at the motor cortex. We also expect the two hemispheres to be active in 'mirror image' when left and right movement are contrasted given the global organization of the brain that the left part controls the right side of the body and vice versa. In addition to the markers mentioned above, other markers such as those related to visual attention (expected in the occipital cortex) or higher order attention and planning (decision making; expected in the frontal cortex) may be used.

Predicting single movements

The common approach in research such as cited above is to look at signals averaged across many instances of, for instance, left-, right-, and no movements. This is done in order to average out noise. However, in order to be able to use brain signals to predict a single movement as would be required for our type of application, we need to extract information reliably from single, short intervals of brain data. This is routinely being done in the field of Brain-Computer Interfaces. The approach taken in this field is to train classification models (such as Support Vector Machines) on samples of labelled data: intervals of EEG data that are known to belong to class A (e.g. 'preceded a movement of the left hand') and intervals that are known to belong to class B (e.g. 'preceded a right hand movement'). These models try to find how to best separate the classes A and B in multidimensional feature space, where features can be voltages at different times as recorded by different electrodes, power in certain EEG frequency bands or other variables that are expected to contribute to the distinction between classes. The performance of the trained model can be evaluated by checking how well it can distinguish between the two ('left hand' and 'right hand') classes for new, unseen EEG data.

There has been successful work in this area with respect to (offline) predicting single movements in the case of emergency braking in virtual or real driving (i.e., predicting movement of the foot or leg before it is detectable from letting go of the gas pedal; (Haufe, Kim, Sunnleitner, Schrauf, Curio and Blankertz, 2014; Haufe, Treder, Gugler, Sagebaum, Curio and Blankertz, 2011; Kim, Kim, Haufe and Lee, 2015); steering a steering wheel in virtual driving (Gheorghe, Chavarriaga and Millan, 2014) and self-paced reaching movements (Lew, Chavarriaga, Silvoni and Millan, 2012). These studies show that EEG allows to predict movement onset up to 500 or 800 ms before it is

detected using conventional measures (and/or electrical signals from the muscles). We have not been able to find such studies for the case of head rotation. Predicting voluntary head rotation represents a different, relatively hard case. This is because rotating the head involves many muscles on both sides of the body and a relatively small amount of motor cortex is dedicated to the neck. In addition, when voluntary movements are considered that are not clearly associated with sensory events in the outside world, we cannot make use of brain processes associated with processing sensory signals (as perceiving braking lights in the case of the emergence braking study referred to above).

We did a small pilot study in order to test whether predicting of head movement on the basis of EEG is feasible.

4.1.3 Pilot study

We asked a participant (25 years old, male, right-handed, normal vision) to wear an oculus rift and make self-paced right- and leftward head rotations, starting from and returning to the center at voluntarily chosen times, but leaving about 4 seconds in between movements. This resulted in about 100 left- and 100 rightward movements. EEG was recorded through 32 Biosemi active electrodes. The EEG data was pre-processed (filtered, rereferenced to the common average of all electrodes, baselined, and downsampled). Subsequently, epochs were selected that either preceded a movement or not, where the epochs preceding a movement could be further divided into 'leftward' and 'rightward' movement intervals. We wanted to train classification models to distinguish between those types of epochs. As a first step, we selected epochs of 1s ending at movement onset and other, non-overlapping epochs from intervals preceding the movement intervals (which also did not overlap with the movement itself,

and started at least 1s after a previous movement had ended). The movement onset was determined using sensor data coming from the oculus rift's gyroscope.

Figure 35 shows the voltage of the electrodes averaged across no movement intervals (top panel), leftward rotations (middle panel) and rightward rotation (bottom panel). While there is no distinct activity visible in the no movement intervals, the intervals preceding left and right movement show distinct patterns that are approximate mirror images. The distinguishing information seems to originate mainly from asymmetries in the frontal electrodes, suggesting that the information mostly reflects higher order left- or rightward planning processes.

Starting with the 1s epochs as described above, we explored classification success of a few different (shorter) epochs and times before movement onset. Support vector machine models were used to distinguish between no movement and movement epochs, between no movement and leftward movement, between no movement and rightward movement, and between right- and leftward movements (the latter was only used for intervals preceding a movement). Using epochs of 125 ms of EEG data (all electrodes) coming from around 300 ms before movement onset, these models could correctly classify data that was withheld from training the model with an accuracy of respectively 63% (no movement vs movement), 70% (no vs left), 70% (no vs right) and 76% (left vs right). Overall, it appeared possible to make most of these distinctions across different moments in time before movement onset within the examined second.

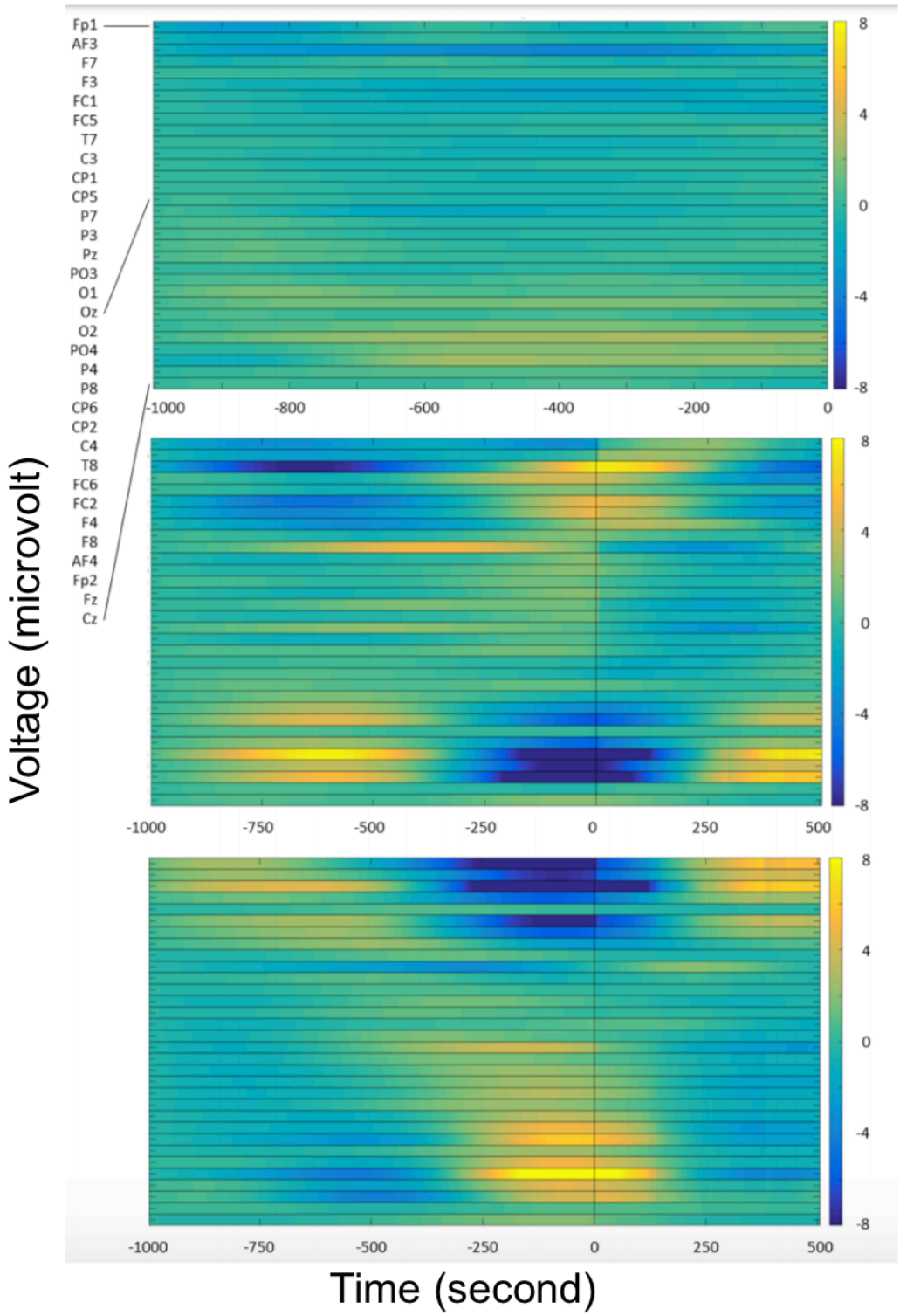

Figure 35. Voltage per EEG electrode (electrode names on the vertical axis) over time (horizontal axis) for no movement epochs (top panel), leftward (middle panel) and rightward (lower panel) movements, where the latter ones are synchronized on movement onset (vertical line).

4.1.4 Implications and next steps

We expect to be able to improve the results as found in the pilot experiment considerably (e.g. by using probabilistic rather than binary classification output) and we still need to explore the timing accuracy that can be reached (e.g. by continuously streaming EEG epochs through a classifier trained on distinguishing 125 ms epochs originating from 300 ms before movement onset). However, we already showed that we can (off-line) predict whether a certain, short interval of EEG data will be followed by a head movement or not, and if so, in which direction the head will move.

For the application we have in mind, this means that we may be able to use EEG signals to optimize the HMD viewing experience of the user. In this study, we used gelled EEG electrodes, meant for laboratory use, but wearable 'dry' or water based EEG electrodes are already available and their quality is improving fast. Such electrodes could be relatively easily integrated in an HMD so that users would not need to wear an extra device. Besides this specific application, more can be envisioned. The HMD case extends to adapting Virtual Reality environments in general, to enhancing movement dependent interfaces (such as cameras mounted on exploration robots that move with a user's head movement) and assistive devices for disabled people.

Within the field of Brain-Computer Interfaces the proposed HMD application surpasses common disadvantages of BCIs. In the proposed application, it can already be useful to detect head rotation with less than 100% accuracy. When we are reasonably sure (as defined by a certain threshold) that a user is going to turn her head leftward, we can sacrifice some of the spatial resolution of the currently displayed image to load the images to the left (cf. D'Acunto, van den Berg, Thomas and Niamut, 2016). If the movement does not occur anyway, this is not an inevitable loss (which contrasts to other potential applications of movement predictions where faulty predictions can lead

to unacceptable situations, such as speeding up emergency braking). Perhaps an even more important feature is that in this HMD case we can train and validate a personalized model on the fly. A user may start wearing the HMD without using the movement predictions. While wearing it, the system collects data on head movement as measured by the motion sensors and EEG, and starts to train (or improve) the movement prediction model. When a certain accuracy is reached (as can be continuously verified without bothering the user), it can start to use the model's predictions to improve user experience. The system can continuously keep track of its own performance without requiring input of the user and if necessary, improve (recalibrate) itself, e.g. by weighing later collected data heavier than earlier collected data.

In future work, we will extend the pilot study to more participants and analyses. In particular, we will examine analyses and approaches that can be applied in real life cases, where we deal with analyzing continuously shifting windows of streaming data.

4.1.5 Acknowledgements

We thank Gert-Jan Schilt for his ideas and support. This research is part of the project Long Term Research on Networked Virtual Reality, TKI (Topconsortium for Knowledge and Innovation), Surcharge Consortium Agreement for PPP projects 0100294530 with KPN as Industrial Partner.

5 Discussion

In the present project the contribution of the Posterior Parietal Cortex (PPC) in the context of rehabilitation of motor control with the aid of Brain-Machine and Brain-Computer Interface (BMI and BCI) techniques was investigated. Given how previous research has highlighted a progressive functional de-activation of the Primary Motor Cortex (M1) in individuals suffering from paralysis one year after sustaining an injury to the spinal cord (Jurkiewicz at el., 2010) and how the PPC has been successfully employed in a tetraplegic human to control a BMI application (Aflalo et al., 2015), this work aims to offer further evidence for the role of this brain area for the benefit of future applications of motor control aids.

This work initially focused on clarifying the way the PPC encodes for space when performing memory-guided saccades. Specifically, we aimed to determine the contribution of the different proprioceptive information originating from subtle postural changes in the encoding of phase maps produced by the PPC when performing a well-established memory-guided saccadotopic task (e.g., Sereno et al., 2001). The findings provided in Chapter 2.1 suggest that body position shifts, as well as subtle hand position changes do interfere with the space encoding process of the Posterior Parietal Cortex. It is also important to note that previous literature has linked changes in the phase maps in PPC during delayed saccade performance to contributions resulting from different retinal stimulation, eye position, and head position (Sereno et al., 2001; Schluppeck et al., 2005; Connolly et al., 2015). In the current studies, care was taken in isolating these possible confounding elements by keeping the head and neck fixed and maintaining both retinal stimulation and eye movements consistent throughout the experimental conditions (see Chapter 2.1.3 Materials and Methods). Based on these methodological criteria, if a change was found in the space encoding of PPC this would

likely be the result of the integration of proprioceptive feedback originating from peripheral areas of the body below the neck and including the dominant hand as all other possible elements were controlled for.

In the control condition, where participants were lying flat on the fMRI scanner bed and no postural alterations were applied, the common contra-lateral bias was found in both fMRI studies from Chapter 2.1 of torso rotation and hand position changes. This means that, when inspecting the phase-encoded maps, an over-representation of the contralateral side of space is visible in each hemisphere. Although not novel, this finding is important in validating overall our experimental condition as it replicates similar findings in the existing literature (Sereno et al., 2001; Konen and Kastner, 2008; Silver and Kastner, 2009).

However, in the active conditions of torso rotated and hand position changed, this effect is lost and the contribution of each hemisphere in the representation of the contra-lateral side of space becomes less defined. In the case of torso rotations, when the body is rotated to the left and right, the right hemisphere continues to show a preference for saccades performed to the contra-lateral side of space. However, the left hemisphere now loses the contra-lateral bias and appears to show a preference to saccades performed toward the left side of space. A cm-test for equal medians confirmed significant differences found across the active, torso rotation conditions, as opposed to the control, torso centre, condition (p<0.05 overall). However when the torso was rotated to the left, the phase-encoded maps of right hemisphere only marginally differ from those reported with the torso in the control condition (p=0.07).

In the case of hand position changes a similar effect was found and the cm-test reports significant differences in the left hemisphere of the PPC phase-maps of right-handed participants (p=0.001) but no significant differences were found within the

right hemisphere (p=0.1774). This finding was expected due to the fact that only the position of the dominant right hand of participants was modified but left the body position otherwise fixed across conditions, only an effect of the left hemisphere was expected, consistent with the contralateral hemispheric control for motor functions (Mattay, Callicott, Bertolino, Santha, Van Horn et al., 1998).

Taken together, the findings of the two fMRI experiments from Chapter 2 suggest that proprioceptive feedback originating from body alterations (full torso rotations in Experiment 1) as well as small position changes of the dominant hand (Experiment 3) is able to affect the resulting phase maps obtained within the PPC. Proprioceptive feedback originating from the body whilst in different positions and the visual stimuli gathered during visual space exploration normally computed at the PPC level (Culham et al., 2006) is likely also used in the process of spatial phase encoding. In other words, the current experiments show that space encoding in the human PPC takes into account body-centred coordinates as overall significant changes were found when manipulating the static torso position (p<0.05) and hand position (p=0.001).

However, it could not be excluded, at this stage, that these findings might have been merely the result of a change in saccade metrics caused by changes in body position. Based on the integrative role of PPC described above, if the final end-points (or accuracy) of saccades changed consistently with body positional changes, so would the phase-maps as these would reflect a change in the eye movements as well as the applied postural changes. For this reason, we ran two control experiments employing eye tracking to ensure that the metrics of the eye-movements performed by our participants did not vary with the same body alterations. There were no significant differences for all metrics suggesting that accuracy and latency of saccades were not affected by torso rotations and hand position changes. This is particularly meaningful as it controls for

the possibility of the phase maps differences being the result of a change in the overall metrics of the recorded eye movements in the scanner.

These results bear clear implications for both future methodological set-ups in research settings as well as the general understanding of spatial coordinate reference frames used by the Posterior Parietal Cortex in humans and these were discussed in previous chapters (see Discussion in Experiment 1). However, if the process of space mapping within the PPC involves and is affected by such subtle position changes of the body, successful applications of PPC-based BCI and BMI techniques should also take such results into account as this can minimise individual differences in the accuracy and overall efficacy of these assistive devices.

The current manuscript previously addressed how assistive and commercial BCI and BMI applications are still far from being introduced in standard practice (see Main Introduction). The ability to obtain clear and rich brain signal (high SNR and ITR) was listed, as well as high individual variability that makes certain users more successful than others in achieving high accuracy levels as some of the determining factors. Evidence that postural changes may produce different phase maps during the process of space mapping could suggest that these postural changes, if not controlled for, might well contribute to the individual and signal quality variability found within previous literature (e.g., Sereno et al., 2001; Konen and Kastner, 2008). Moreover, data processing algorithms may benefit from accounting for postural changes as this may strongly boost data signal quality in real-time and mobile BCI and BMI applications. In the context of Spinal Cord Injury, individual cases should be evaluated in the context of level and completeness of the injury as residual proprioceptive feedback of the areas above the injury or below incomplete injuries may still affect signal quality. Controlling for the body orientation and hand position when driving a BCI or BMI technique could

help reduce this effect and therefore boost data quality and control some of the individual variability found. In other words, when considering the PPC as the main signal extraction site in BCI and BMI applications, findings supporting evidence that proprioceptive feedback influences the nature of the information encoded within this brain area during visual spatial exploration mean data obtained will vary depending on the body position of the end-user operating the device. Additionally, results presented in this manuscript show how even subtle positional changes of individual limbs will produce different phase-encoded maps during delayed-saccade performance. This could pose a significant limitation to the efficacy of novel PPC-based saccade-operated assistive BCI and BMI devices.

Additionally, consistent with previous research in the field (e.g., Rorden, Karnath and Driver, 2001), results obtained from the eye tracking experiments presented here suggest that proprioceptive feedback coming from the periphery of the body does not affect the overall accuracy, end-points and latency of saccadic eye movements with the body and hand in different positions in space. Therefore, in the case of eye movement-based BCI and BMI (e.g., Pfurstscheller et al., 2010; Kishore, Gonzalez-Franco, Hintemuller and Kapeller, 2014; Stawicki, Gembler, Rezeika and Volosyak, 2017), subtle body position changes appear to be less crucial. With exclusive or hybrid eye tracking-based BCI or BMI techniques, good and consistent accuracy levels may be obtained regardless of the position assumed by the end-user during use perhaps making this approach the best suited for commercial applications (Lupu and Ungureanu, 2013; Kim, Kim and Jo, 2015; Thompson, Guis and Huggins, 2013).

Individuals who have compromised sensorimotor functions due to a Spinal Cord Injury (SCI) could benefit highly from the use of assistive BCI and BMI techniques. As more extensively discussed in the Main Introduction and Introduction to Chapter 3,

existing literature offers inspiring examples of successful applications of such devices in this cohort by using both primary motor and posterior parietal cortex (i.e., Hochberg et al., 2006; Aflalo et al., 2015). However, an overall degree of functional reorganisation of the motor and premotor cortices following SCI has been reported and this seems related to the elapsed time following the injury onset (Dahlberg et al., 2018; Sabre et al., 2013;Jurkiewicz et al., 2010). A lack of evidence of the prolonged effects of this reorganisation following paralysis, especially at the PPC level, leaves the open question of how sustainable BCI and BMI applications may be in the case of individuals with a long-term SCI.

To address this question, Chapter 3 investigated the effects that a state of prolonged and stable paralysis can have on the PPC of a cohort of individuals suffering from high-level cervical (C4) SCI. As mentioned above, longitudinal fMRI research highlighted a progressive loss of functional activation during attempted and imagined ankle movements of the primary motor cortex within the first year since the onset of paralysis following SCI (Jurkiewicz et al., 2010). In this study, participants retained control of the body above the waist and the effects were only followed for a total of 12 months since the onset of the condition. The current work specifically investigated brain functional activity during imagined arm movements in a cohort of individuals suffering from quadriplegia following high-level and long-term (>2 years on average) cervical SCI.

Although this project did not follow the participants since the very onset of paralysis, activation of the SCI group during motor imagery performance was found to be significantly different to that of matched controls ($p<0.001$). Specifically, a much lower residual activation of M1 and associated frontal motor areas was found when compared to controls and when compared to areas of the PPC. The average number of

active voxels in M1 was also found to be lower in the SCI group when compared to that of controls. However, comparable activation levels and overall number of active voxels to that of controls was found in the Superior Parietal Lobule, anterior Intraparietal Sulcus (aIPS) and medial Intraparietal Sulcus (mIPS).

These results offer supportive evidence of what has been previously reported by Jurkiewicz and colleagues (2010) in showing an overall loss of functional activation in M1 and associated motor areas. This is possibly due to functional reorganisation of areas of M1 no longer connected to the peripheral body (Curt et al., 2002; Dahlberg et al., 2018).

Although not longitudinal in nature, the current study suggests that if left un-trained, M1 tends to naturally and progressively lose motor imagery-related functional activity. The PPC, however, appears to be overall behaving in a similar manner to that of controls in our cohort. When taken together with evidence such as that presented by Jurkiewicz and colleagues (2010) and the study detailed in Chapter 3, PPC-based BMI might offer a more inclusive option in the ultimate goal of assisting individuals affected by severe paralysis and related loss of independence in daily living activities. In the case of long-term, established paralysis, where the progressive loss of activation of M1 has already taken place, PPC-based BMI might be a more viable option.

There is currently one report of a PPC-based application of an invasive BMI in the existing literature (Aflalo et al., 2015). In this study, researchers were able to successfully decode motor imagery from the aIPS of an individual with quadriplegia following SCI. They used the signal extracted from aIPS to control a computer cursor on a screen showing the feasibility of decoding goal intention as well as trajectory of the intended movement from this area. The inherent importance of this study is that it

shows the possibility of achieving comparable results to that of BMI techniques based on M1 implants.

Additionally, Chapter 3 specifically investigated the brain functional activation during imagined arm movements. This chapter highlighted how, in long-term paralysis following SCI, motor and premotor areas showed overall deactivation during visual motor imagery performance. Activation in PPC, however, remains detectable. These findings may also bear direct implications to non-invasive approaches, especially EEG-based ones where centrally located electrodes are used (Hwang, Kwon and Im, 2009; Townsend, Graimann and Pfurtscheller, 2004). Although successful in healthy controls, some of these techniques using motor imagery might experience loss of accuracy and overall performance if used on individuals with established and long-term paralysis where motor imagery related brain activity might have already shifted to more posteriorly located areas such as PPC.

Future research might benefit from investigating alternative electrode placement sites that best capture residual motor-imagery related potentials of motor impaired individuals to increase the overall efficacy of the technique. Evidence showing the possibility of extracting goal intended behaviour as well as action trajectory from the elements of the PPC, suggests this area might be of aid in EEG-based BCI techniques as well as invasive approaches.

The possible suitability of human PPC in invasive and non-invasive EEG-based BCI techniques applies to the nature of the study summarised in Chapter 4 as well. In summary, we investigated the possibility to detect self-paced head movements before their actual occurrence in a cohort of healthy participants with a standard wet-EEG. The results show that it is possible to extract head-movement related potentials as early as 300ms prior to the action performance and to distinguish the direction of the

movements as well. Electrodes were placed over the central areas of CP1 and CP2, thus corresponding to the Primary Motor Cortex (M1). Although successful in healthy participants and therefore proving suitable for commercial applications of BCI techniques, such methodology should be tested in a cohort of motor impaired individuals prior to introducing it in the context of assistive techniques. Depending on the specific condition inhibiting motor behaviour, related potentials might incur the same functional shifting shown in Chapter 3 thus rendering electrode re-placement necessary to maximise efficacy and feasibility of the technique. Although not specifically tested in the present project, a similar approach shifting toward more posteriorly located areas, such as PPC, might prove beneficial in improving the feasibility of assistive future applications.

Overall, the present project aimed to contribute to the advancement of the use of BCI and BMI approaches in the rehabilitation of motor impairments. Emerging from the pioneering work of Aflalo and colleagues (2015), this work was aimed to further investigate the role the PPC might have in the future development of both BCI and BMI techniques.

Time and monetary constraints account for important limitations on the breath the current manuscript has covered. Given greater resources, this work would have further explored the effects of long-term paralysis after SCI in the functional representation of motor imagery of arm reaching movements. Being able to follow up the development of the motor imagery-related functional activity of the participants from the first months since the onset of paralysis to several years after the condition was stabilised might have offered a better understanding of the processes leading to the results presented in Chapter 3. This could have contributed significantly to the knowledge already shown by previous research in a cohort of low-level SCI during the

first year since the onset of paralysis (Jurkiewicz et al., 2010) and could have confirmed that a similar progressive state of functional reorganisation is visible in high-level, long term SCI as well. The possibility of conducting further testing would have also given the chance to include investigation of the residual motor imagery activity of the lower limbs as well, necessary in the ambulatory process.

Evidence such as this would prove useful in supporting research toward more inclusive and feasible BCI and BMI techniques that can support individuals with different degrees of paralysis, different onset times, and in different environments that go beyond the enclosed laboratory setting.

A higher number of recording sessions would have been of great benefit to most of the research hereby presented but especially so in the investigation of the reference frames of the PPC. Here, the higher number of conditions resulted in a lower number of saccades performed on average for each torso orientation and hand position as compared to those recorded in previous applications of the same experimental design. Existing examples within the literature, in fact, usually employ a higher number of recording sessions and fewer experimental conditions, resulting in a higher number of total saccades performed and thus much clearer phase maps (e.g., Sereno et al., 2001). In both experimental conditions of torso rotations and hand position changes, we reported a significant amount of noise. This might have been reduced if the methodological process used here could have replicated more closely that of previous experiments. Although the data obtained were still able to replicate successfully the established contralateral bias in space encoding representation (i.e., the control conditions), future research from this lab would benefit in extending the number of recording sessions to achieve data quality that is consistent with that shown in existing research in this field.

Recording saccade metrics during the fMRI scanning sessions might also prove useful to further decouple the contribution of body position alterations and eye movement performance in the related space encoded maps of the PPC. Although this was achieved through following control experiments (Chapter 2.1, Experiment 2 and Chapter 2.2), using an MRI-compatible eye-tracker device allowing to record both brain functional activity and saccade metrics at the same time on the same participants would help control for possible environmental changes and individual differences in order to further confirm the results presented here.

In conclusion, the present project provides evidence furthering our knowledge of the Posterior Parietal Cortex and the way this area could prove useful in the context of assistive BCI and BMI techniques. This manuscript presented data supporting the relationship between body proprioceptive feedback and the internal representation of space within this area. This further supports the existing idea that body-centred reference frames exist within the PPC. It was further discussed how in a cohort of individuals suffering from high-level cervical and complete Spinal Cord Injury, the residual level of brain activity following motor imagery of the arm appears to be lower within motor and premotor areas when compared to a group of matched controls. The posterior parietal cortex areas, however, appear to have maintained normal levels of activity during the same motor imagery tasks. Overall, such results can inform future research in continuing to investigate the suitability of PPC-based assistive techniques when other motor-related areas might be substantially impaired due to long-term paralysis. Likewise, in the case of similar reduced activity of motor areas, non-invasive techniques, such as those presented in our collaborative study (Study 4), should also

explore the possibility of implementing decoding algorithms to extract motor signals from posteriorly located areas, such as the PPC.

6 References

Abel, L. A., Troost, B. T., & Dell'osso, L. F. (1983). The effects of age on normal saccadic characteristics and their variability. *Vision Research*, *23*(1), 33–37.

Aflalo, T., Kellis, S., Klaes, C., Lee, B., Shi, Y., Pejsa, K., … Andersen, R. A. (2015). Decoding motor imagery from the posterior parietal cortex of a tetraplegic human. *Science*, *348*(6237), 906–910.

Allison, B. Z., Wolpaw, E. W., & Wolpaw, J. R. (2007). Brain–computer interface systems: Progress and prospects. *Expert Review of Medical Devices*, *4*(4), 463–474.

Andersen, R. A., & Buneo, C. A. (2002). Intentional maps in posterior parietal cortex. *Annual review of neuroscience*, *25*(1), 189-220.

Andersen, R. A., & Mountcastle, V. B. (1983). The influence of the angle of gaze upon the excitability of the light-sensitive neurons of the posterior parietal cortex. *Journal of Neuroscience*, *3*(3), 532-548.

Andersen, R. A., Essick, G. K., & Siegel, R. M. (1985). Encoding of spatial location by posterior parietal neurons. *Science (New York, N.Y.)*, *230*(4724), 456–458.

Andersen, R. A., Musallam, S., & Pesaran, B. (2004). Selecting the signals for a brain–machine interface. *Current Opinion in Neurobiology*, *14*(6), 720–726.

Andersen, R. A., Snyder, L. H., Li, C. S., & Stricanne, B. (1993). Coordinate transformations in the representation of spatial information. *Current opinion in neurobiology*, *3*(2), 171-176.

Anderson, K. D. (2004). Targeting Recovery: Priorities of the Spinal CordInjured Population. *J. Neurotrauma*, 1371–1383.

Aricò, P., Borghini, G., Flumeri, G. D., Sciaraffa, N., & Babiloni, F. (2018). Passive BCI beyond the lab: Current trends and future directions. *Physiological Measurement*, *39*(8), 08TR02.

Arvaneh, M., Guan, C., Ang, K. K., & Quek, C. (2011). Optimizing the Channel Selection and Classification Accuracy in EEG-Based BCI. *IEEE Transactions on Biomedical Engineering*, *58*(6), 1865–1873.

Azom, M. A., Rana, M. M., & Ahmad, M. (2013). Design and implementation of a user independent SSVEP based brain-computer interface with high transfer rates. *2013 International Conference on Informatics, Electronics and Vision (ICIEV)*, 1–6.

Babiloni, F., Cincotti, F., Lazzarini, L., Millan, J., Mourino, J., Varsta, M., … Marciani, M. G. (2000). Linear classification of low-resolution EEG patterns produced by imagined hand movements. *IEEE Transactions on Rehabilitation Engineering*, *8*(2), 186–188.

Baloh, R. W., Sills, A. W., Kumley, W. E., & Honrubia, V. (1975). Quantitative measurement of saccade amplitude, duration, and velocity. *Neurology*, *25*(11), 1065-1065.

Baranauskas, G. (2014a). What limits the performance of current invasive brain machine interfaces? *Frontiers in Systems Neuroscience*, *8*.

Baranauskas, G. (2014b). What limits the performance of current invasive brain machine interfaces? *Frontiers in Systems Neuroscience*, *8*.

Batista, A. P., Buneo, C. A., Snyder, L. H., & Andersen, R. A. (1999). Reach Plans in Eye-Centered Coordinates. *Science*, *285*(5425), 257–260.

Becker, W. (1972a). The control of eye movements in the saccadic system. *Bibliotheca Ophthalmologica: Supplementa Ad Ophthalmologica*, *82*, 233–243.

Becker, W. (1972b). The control of eye movements in the saccadic system. *Bibliotheca Ophthalmologica: Supplementa Ad Ophthalmologica*, *82*, 233–243.

Beenen, N., Büttner, U., & Lange, H. W. (1986). The diagnostic value of eye movement recording in patients with Huntington's disease and their offspring. *Electroencephalography and Clinical Neurophysiology*, *63*(2), 119–127.

Behrman, A. L., Bowden, M. G., & Nair, P. M. (2006). Neuroplasticity After Spinal Cord Injury and Training: An Emerging Paradigm Shift in Rehabilitation and Walking Recovery. *Physical Therapy*, *86*(10), 1406–1425.

Bell, C. J., Shenoy, P., Chalodhorn, R., & Rao, R. P. N. (2008). Control of a humanoid robot by a noninvasive brain–computer interface in humans. *Journal of Neural Engineering*, *5*(2), 214–220.

Belliveau, J. W., Kennedy, D. N., McKinstry, R. C., Buchbinder, B. R., Weisskoff, R., Cohen, M. S., ... & Rosen, B. R. (1991). Functional mapping of the human visual cortex by magnetic resonance imaging. *Science*, *254*(5032), 716-719.

Berens P. (2009). CircStat : A *MATLAB* Toolbox for Circular Statistics. J Stat Softw. 2009;31.

Birman, D., & Gardner, J. L. (2018). A quantitative framework for motion visibility in human cortex. *Journal of Neurophysiology*, *120*(4), 1824–1839.

Blabe, C. H., Gilja, V., Chestek, C. A., Shenoy, K. V., Anderson, K. D., & Henderson, J. M. (2015). Assessment of brain-machine interfaces from the perspective of people with paralysis. *Journal of Neural Engineering*, *12*(4), 043002.

Blondet, M. V. R., Badarinath, A., Khanna, C., & Jin, Z. (2013). A wearable real-time BCI system based on mobile cloud computing. *2013 6th International IEEE/EMBS Conference on Neural Engineering (NER)*, 739–742.

Bonanno, G. A., Kennedy, P., Galatzer-Levy, I. R., Lude, P., & Elfström, M. L. (2012). Trajectories of resilience, depression, and anxiety following spinal cord injury. *Rehabilitation Psychology*, *57*(3), 236–247.

Bosco A, Breveglieri R, Hadjidimitrakis K, Galletti C, Fattori P. Reference frames for reaching when decoupling eye and target position in depth and direction. Sci Rep. 2016;6.

Bourassa, D. C. (1996). Handedness and eye-dominance: a meta-analysis of their relationship. *Laterality: Asymmetries of Body, Brain and Cognition*, *1*(1), 5-34.

Boussaoud D, Bremmer F. Gaze effects in the cerebral cortex: Reference frames for space coding and action. Experimental Brain Research. 1999. pp. 170–180.

Bracken, M. B., Freeman Jr, D. H., & Hellenbrand, K. (1981). Incidence of acute traumatic hospitalized spinal cord injury in the United States, 1970–1977. American Journal of Epidemiology, 113(6), 615-622.

Bradbury, E. J., & McMahon, S. B. (2006). Spinal cord repair strategies: Why do they work? *Nature Reviews Neuroscience*, *7*(8), 644.

Brainard, D. H. (1997) The Psychophysics Toolbox, Spatial Vision 10:433-436.

Bremmer, F., Ilg, U. J., Thiele, A., Distler, C., & Hoffmann, K.-P. (1997). Eye Position Effects in Monkey Cortex. I. Visual and Pursuit-Related Activity in Extrastriate Areas MT and MST. *Journal of Neurophysiology*, *77*(2), 944–961.

Brotchie, P. R., Andersen, R. A., Snyder, L. H., & Goodman, S. J. (1995). Head position signals used by parietal neurons to encode locations of visual stimuli. *Nature*, *375*(6528), 232–235.

Brouwer A-M, Zander TO, van Erp JBF, Korteling JE, Bronkhorst AW (2015) Using neurophysiological signals that reflect cognitive or affective state: six recommendations to avoid common pitfalls. *Front. in Neurosci*. 9:136.

Bruehlmeier, M., Dietz, V., Leenders, K. L., Roelcke, U., Missimer, J., & Curt, A. (1998a). How does the human brain deal with a spinal cord injury? *European Journal of Neuroscience*, *10*(12), 3918–3922.

Bruehlmeier, M., Dietz, V., Leenders, K. L., Roelcke, U., Missimer, J., & Curt, A. (1998b). How does the human brain deal with a spinal cord injury?: Spinal cord injury and brain plasticity. *European Journal of Neuroscience*, *10*(12), 3918–3922.

Burns, A. S., & Ditunno, J. F. (2001). Establishing Prognosis and Maximizing Functional Outcomes After Spinal Cord Injury: A Review of Current and Future Directions in Rehabilitation Management. *Spine*, *26*(24S), S137.

Cao, Y., Chen, Y., & DeVivo, M. (2011). Lifetime Direct Costs After Spinal Cord Injury. *Topics in Spinal Cord Injury Rehabilitation*, *16*(4), 10–16.

Carmena, J. M., Lebedev, M. A., Crist, R. E., O'Doherty, J. E., Santucci, D. M., Dimitrov, D. F., … Nicolelis, M. A. L. (2003). Learning to Control a Brain–Machine Interface for Reaching and Grasping by Primates. *PLOS Biology*, *1*(2), e42.

Cavina-Pratesi, C., Monaco, S., Fattori, P., Galletti, C., McAdam, T. D., Quinlan, D. J., Culham, J. C. (2010). Functional Magnetic Resonance Imaging Reveals the Neural Substrates of Arm Transport and Grip Formation in Reach-to-Grasp Actions in Humans. *Journal of Neuroscience*, *30*(31), 10306–10323.

Chae, J., Kilgore, K., Triolo, R., & Creasey, G. (2000). Functional neuromuscular stimulation in spinal cord injury. *Physical Medicine and Rehabilitation Clinics of North America*, *11*(1), 209–226, x.

Chaudhary, U., Birbaumer, N., & Curado, M. R. (2015a). Brain-Machine Interface (BMI) in paralysis. *Annals of Physical and Rehabilitation Medicine*, *58*(1), 9–13.

Chaudhary, U., Birbaumer, N., & Curado, M. R. (2015b). Brain-Machine Interface (BMI) in paralysis. *Annals of Physical and Rehabilitation Medicine*, *58*(1), 9–13.

Chu, R. M., & Black, K. L. (2012). Chapter 8 - Current Surgical Management of High-Grade Gliomas. In A. Quiñones-Hinojosa (Ed.), *Schmidek and Sweet Operative Neurosurgical Techniques (Sixth Edition)* (pp. 105–110).

Cohen, Y. E., & Andersen, R. A. (2002). A common reference frame for movement plans in the posterior parietal cortex. *Nature Reviews Neuroscience*, *3*(7), 553–562.

Coles MG (1989) Modern mind-brainreading: psychophysiology, physiology, and cognition. *Psychophysiol.* 251–269.

Collinger, J. L., Boninger, M. L., Bruns, T. M., Curley, K., Wang, W., & Weber, D. J. (2013). Functional priorities, assistive technology, and brain-computer interfaces after spinal cord injury. *Journal of Rehabilitation Research and Development*, *50*(2), 145–160.

Connolly, J. D., Vuong, Q. C., & Thiele, A. (2013). Gaze-dependent topography in human posterior parietal cortex. *Cerebral Cortex*, *25*(6), 1519-1526.

Corbetta, M., Burton, H., Sinclair, R. J., Conturo, T. E., Akbudak, E., & McDonald, J. W. (2002). Functional reorganization and stability of somatosensory-motor cortical topography in a tetraplegic subject with late recovery. *Proceedings of the National Academy of Sciences*, *99*(26), 17066–17071.

Craig, A., Tran, Y., & Middleton, J. (2009). Psychological morbidity and spinal cord injury: A systematic review. *Spinal Cord*, *47*(2), 108–114.

Cramer, S. C., Lastra, L., Lacourse, M. G., & Cohen, M. J. (2005). Brain motor system function after chronic, complete spinal cord injury. *Brain*, *128*(12), 2941–2950.

Crawley, A. P., Jurkiewicz, M. T., Yim, A., Heyn, S., Verrier, M. C., Fehlings, M. G., & Mikulis, D. J. (2004). Absence of localized grey matter volume changes in the motor cortex following spinal cord injury. *Brain Research*, *1028*(1), 19–25.

Cripps, R. A., Lee, B. B., Wing, P., Weerts, E., Mackay, J., & Brown, D. (2011). A global map for traumatic spinal cord injury epidemiology: Towards a living data repository for injury prevention. *Spinal Cord*, *49*(4), 493–501.

Culham, J. C., Cavina-Pratesi, C., & Singhal, A. (2006). The role of parietal cortex in visuomotor control: what have we learned from neuroimaging?. *Neuropsychologia*, *44*(13), 2668-2684.

Curt, A., Alkadhi, H., Crelier, G. R., Boendermaker, S. H., Hepp-Reymond, M. C., & Kollias, S. S. (2002). Changes of non-affected upper limb cortical representation in paraplegic patients as assessed by fMRI. *Brain*, *125*(11), 2567-2578.

Curt, A., Bruehlmeier, M., Leenders, K. L., Roelcke, U., & Dietz, V. (2002). Differential effect of spinal cord injury and functional impairment on human brain activation. *Journal of Neurotrauma*, *19*(1), 43–51.

D'Acunto L, van den Berg J, Thomas E, Niamut O (2016, May). Using MPEG DASH SRD for zoomable and navigable video. In Proceedings of the 7th International Conference on Multimedia Systems (p. 34). ACM.

Dahlberg, L. S., Becerra, L., Borsook, D., & Linnman, C. (2018). Brain changes after spinal cord injury, a quantitative meta-analysis and review. *Neuroscience & Biobehavioral Reviews*, *90*, 272-293.

Day, B. L., Steiger, M. J., Thompson, P. D., & Marsden, C. D. (1993). Effect of vision and stance width on human body motion when standing: Implications for afferent control of lateral sway. *The Journal of Physiology*, *469*(1), 479–499.

De Vivo, M. J., Stuart Krause, J., & Lammertse, D. P. (1999). Recent trends in mortality and causes of death among persons with spinal cord injury. *Archives of Physical Medicine and Rehabilitation*, *80*(11), 1411–1419.

Decety, J., & Boisson, D. (1990). Effect of brain and spinal cord injuries on motor imagery. *European Archives of Psychiatry and Clinical Neuroscience*, *240*(1), 39–43.

Desmurget, M., Epstein, C. M., Turner, R. S., Prablanc, C., Alexander, G. E., & Grafton, S. T. (1999). Role of the posterior parietal cortex in updating reaching movements to a visual target. *Nature Neuroscience*, *2*(6), 563.

DeSouza, J. F., Dukelow, S. P., Gati, J. S., Menon, R. S., Andersen, R. A., & Vilis, T. (2000). Eye position signal modulates a human parietal pointing region during memory-guided movements. *Journal of Neuroscience*, *20*(15), 5835-5840.

DeVivo, M. J. (1997). Causes and costs of spinal cord injury in the United States. *Spinal cord*, *35*(12), 809.

Dichgans, J., & Brandt, T. (1978). Visual-Vestibular Interaction: Effects on Self-Motion Perception and Postural Control. In S. M. Anstis, J. Atkinson, C. Blakemore, O. Braddick, T. Brandt, F. W. Campbell, … H.-L. Teuber (Eds.), *Perception* (pp. 755–804).

Dietz, V., & Curt, A. (2006). Neurological aspects of spinal-cord repair: promises and challenges. *The Lancet Neurology*, *5*(8), 688-694.

Dijkerman, H. C., Ietswaart, M., Johnston, M., & MacWalter, R. S. (2004). Does motor imagery training improve hand function in chronic stroke patients? A pilot study. *Clinical Rehabilitation*, *18*(5), 538–549.

Dobkin, B., Barbeau, H., Deforge, D., Ditunno, J., Elashoff, R., Apple, D., … Trial Group, the S. C. I. L. (2007). The Evolution of Walking-Related Outcomes Over the First 12 Weeks of Rehabilitation for Incomplete Traumatic Spinal Cord Injury: The Multicenter Randomized Spinal Cord Injury Locomotor Trial. *Neurorehabilitation and Neural Repair*, *21*(1), 25–35.

Duhamel JR, Bremmer F, BenHamed S, Graf W. Spatial invariance of visual receptive fields in parietal cortex neurons. Nature. 1997;389: 845–848. doi:10.1038/39865

Duhamel, J.-R., Bremmer, F., Hamed, S. B., & Graf, W. (1997). Spatial invariance of visual receptive fields in parietal cortex neurons. *Nature*, *389*(6653), 845.

Edlinger, G., Holzner, C., Guger, C., Groenegress, C., & Slater, M. (2009). Brain-computer interfaces for goal orientated control of a virtual smart home environment. *2009 4th International IEEE/EMBS Conference on Neural Engineering*, 463–465.

Edwards, A. S. (1946). Body sway and vision. *Journal of Experimental Psychology*, *36*(6), 526–535.

Eger E, Sterzer P, Russ MO, Giraud AL, Kleinschmidt A. A supramodal number representation in human intraparietal cortex. Neuron. 2003;37: 719–725.

Ettinger, U., Kumari, V., Crawford, T. J., Davis, R. E., Sharma, T., & Corr, P. J. (2003). Reliability of smooth pursuit, fixation, and saccadic eye movements. *Psychophysiology*, *40*(4), 620–628.

Ferreira, A., Celeste, W. C., Cheein, F. A., Bastos-Filho, T. F., Sarcinelli-Filho, M., & Carelli, R. (2008). Human-machine interfaces based on EMG and EEG applied to robotic systems. *Journal of NeuroEngineering and Rehabilitation*, *5*(1), 10.

Findlay, J. M. (1982). Global visual processing for saccadic eye movements. *Vision Research*, *22*(8), 1033–1045.

Fischer, B., & Ramsperger, E. (1986). Human express saccades: Effects of randomization and daily practice. *Experimental Brain Research*, *64*(3), 569–578.

Fischl, B. (2012). FreeSurfer. *Neuroimage*, *62*(2), 774-781.

Follett, K. A. (2000). The Surgical Treatment of Parkinson's Disease. *Annual Review of Medicine*, *51*(1), 135–147.

Folstein, S. E., Leigh, R. J., Parhad, I. M., & Folstein, M. F. (1986). The diagnosis of Huntington's disease. *Neurology*, *36*(10), 1279–1279.

Fourkas, A. D., Avenanti, A., Urgesi, C., & Aglioti, S. M. (2006). Corticospinal facilitation during first and third person imagery. *Experimental Brain Research*, *168*(1–2), 143–151.

Freehafer, A. A. (1991). Tendon transfers in patients with cervical spinal cord injury. *Journal of Hand Surgery*, *16*(5), 804–809.

Freehafer, A. A., Kelly, C. M., & Peckham, P. H. (1984). Tendon transfer for the restoration of upper limb function after a cervical spinal cord injury. *The Journal of Hand Surgery*, *9*(6), 887–893.

Frost, D., & Pöppel, E. (1976). Different programming modes of human saccadic eye movements as a function of stimulus eccentricity: Indications of a functional subdivision of the visual field. *Biological Cybernetics*, *23*(1), 39-48.

Fuhrer, M. J., Rintala, D. H., Hart, K. A., Clearman, R., & Young, M. E. (1993). Depressive symptomatology in persons with spinal cord injury who reside in the community. *Archives of Physical Medicine and Rehabilitation*, *74*(3), 255–260.

Fukushima, J., Fukushima, K., Chiba, T., Tanaka, S., Yamashita, I., & Kato, M. (1988). Disturbances of voluntary control of saccadic eye movements in schizophrenic patients. *Biological Psychiatry*, *23*(7), 670–677.

Gallivan, J. P., Cavina-Pratesi, C., & Culham, J. C. (2009). Is That within Reach? fMRI Reveals That the Human Superior Parieto-Occipital Cortex Encodes Objects Reachable by the Hand. *Journal of Neuroscience*, *29*(14), 4381–4391.

Gardner JL, Merriam EP, Movshon JA, Heeger DJ. Maps of Visual Space in Human Occipital Cortex Are Retinotopic, Not Spatiotopic. J Neurosci. 2008;28: 3988–3999. doi:10.1523/JNEUROSCI.5476-07.2008

Gardner, J. L., Sun, P., Waggoner, R. A., Ueno, K., Tanaka, K., & Cheng, K. (2005). Contrast Adaptation and Representation in Human Early Visual Cortex. *Neuron*, *47*(4), 607–620.

Gheorghe L, Chavarriaga R, Millán J del R (2013) Steering timing prediction in a driving simulator task. *Conf Proc IEEE Eng Med Biol Soc.* 6913-6.

Giangregorio, L., & McCartney, N. (2006). Bone loss and muscle atrophy in spinal cord injury: epidemiology, fracture prediction, and rehabilitation strategies. *The journal of spinal cord medicine*, *29*(5), 489-500..

Goldberg, J. H., & Wichansky, A. M. (2003). Eye tracking in usability evaluation: A practitioner's guide. In *The Mind's Eye*(pp. 493-516). North-Holland.

Gould, D., Damarjian, N., & Greenleaf, C. (2002). Imagery training for peak performance. In *Exploring sport and exercise psychology, 2nd ed* (pp. 49–74).

Grangeon, M., Revol, P., Guillot, A., Rode, G., & Collet, C. (2012). Could motor imagery be effective in upper limb rehabilitation of individuals with spinal cord injury? A case study. *Spinal Cord*, *50*(10), 766–771.

Graupe, D., & Kohn, K. H. (1997). Transcutaneous functional neuromuscular stimulation of certain traumatic complete thoracic paraplegics for independent short-distance ambulation. *Neurological Research*, *19*(3), 323–333.

Green, J. F., King, D. J., & Trimble, K. M. (2000). Antisaccade and smooth pursuit eye movements in healthy subjects receiving sertraline and lorazepam. *Journal of Psychopharmacology (Oxford, England)*, *14*(1), 30–36.

Gregg, M., Hall, C., & Butler, A. (2010). The MIQ-RS: a suitable option for examining movement imagery ability. *Evidence-Based Complementary and Alternative Medicine*, *7*(2), 249-257.

Grubb JD, Reed CL. Trunk orientation induces neglect-like lateral biases in covert attention. Psychol Sci. 2002;13: 553–556.

Guger, C., Edlinger, G., Harkam, W., Niedermayer, I., & Pfurtscheller, G. (2003). How many people are able to operate an EEG-based brain-computer interface (BCI)?. *IEEE transactions on neural systems and rehabilitation engineering*, *11*(2), 145-147.

Guger, C., Ramoser, H., & Pfurtscheller, G. (2000). Real-time EEG analysis with subject-specific spatial patterns for a brain-computer interface (BCI). *IEEE Transactions on Rehabilitation Engineering*, *8*(4), 447–456.

Guger, C., Daban, S., Sellers, E., Holzner, C., Krausz, G., Carabalona, R., … Edlinger, G. (2009a). How many people are able to control a P300-based brain–computer interface (BCI)? *Neuroscience Letters*, *462*(1), 94–98.

Guggisberg, A. G., & Mottaz, A. (2013). Timing and awareness of movement decisions: does consciousness really come too late?. *Frontiers in human neuroscience*, *7*, 385.

Guillot, A., Collet, C., Nguyen, V. A., Malouin, F., Richards, C., & Doyon, J. (2009). Brain activity during visual versus kinesthetic imagery: An fMRI study. *Human Brain Mapping*, *30*(7), 2157–2172.

Hamid, S., & Hayek, R. (2008). Role of electrical stimulation for rehabilitation and regeneration after spinal cord injury: An overview. *European Spine Journal*, *17*(9), 1256–1269.

Harkema, S. J. (2001). Neural Plasticity after Human Spinal Cord Injury: Application of Locomotor Training to the Rehabilitation of Walking. *The Neuroscientist*, *7*(5), 455–468.

Harkema, S. J., Schmidt-Read, M., Lorenz, D. J., Edgerton, V. R., & Behrman, A. L. (2012). Balance and Ambulation Improvements in Individuals With Chronic Incomplete Spinal Cord Injury Using Locomotor Training–Based Rehabilitation. *Archives of Physical Medicine and Rehabilitation*, *93*(9), 1508–1517.

Harrar, V., & Harris, L. R. (2009). Eye position affects the perceived location of touch. *Experimental Brain Research*, *198*(2), 403–410.

Haufe, S., Kim, J. W., Kim, I. H., Sonnleitner, A., Schrauf, M., Curio, G., & Blankertz, B. (2014). Electrophysiology-based detection of emergency braking intention in real-world driving. *Journal of neural engineering*, *11*(5), 056011.

Haufe, S., Treder, M. S., Gugler, M. F., Sagebaum, M., Curio, G., & Blankertz, B. (2011). EEG potentials predict upcoming emergency brakings during simulated driving. *Journal of neural engineering*, *8*(5), 056001.

Hauschild, M., Mulliken, G. H., Fineman, I., Loeb, G. E., & Andersen, R. A. (2012). Cognitive signals for brain–machine interfaces in posterior parietal cortex include continuous 3D trajectory commands. *Proceedings of the National Academy of Sciences*, *109*(42), 17075–17080.

Hema C., R., Paulraj M., P., S. Yaacob, A. H. Adom, & R. Nagarajan. (2007). Motor Imagery Signal Classification For A Four State Brain Machine Interface. *Zenodo*.

Ho, C. H., Triolo, R. J., Elias, A. L., Kilgore, K. L., DiMarco, A. F., Bogie, K., ... & Chan, K. M. (2014). Functional electrical stimulation and spinal cord injury. *Physical Medicine and Rehabilitation Clinics*, *25*(3), 631-654.

Ho, C. H., Wuermser, L.-A., Priebe, M. M., Chiodo, A. E., Scelza, W. M., & Kirshblum, S. C. (2007). Spinal cord injury medicine. 1. Epidemiology and classification. *Archives of Physical Medicine and Rehabilitation*, *88*(3 Suppl 1), S49-54.

Hochberg, L. R., Serruya, M. D., Friehs, G. M., Mukand, J. A., Saleh, M., Caplan, A. H., … Donoghue, J. P. (2006a). Neuronal ensemble control of prosthetic devices by a human with tetraplegia. *Nature*, *442*(7099), 164.

Hochberg, R., John, & Donoghue, P. (2006). Sensors for braincomputer interfaces: Options for turning thought into action. *IEEE Engineering in Medicine and Biology Magazine*, 32–38.

Holzner, C., Guger, C., Edlinger, G., Gronegress, C., & Slater, M. (2009). Virtual Smart Home Controlled by Thoughts. *2009 18th IEEE International Workshops on Enabling Technologies: Infrastructures for Collaborative Enterprises*, 236–239.

Horki, P., Solis-Escalante, T., Neuper, C., & Müller-Putz, G. (2011). Combined motor imagery and SSVEP based BCI control of a 2 DoF artificial upper limb. *Medical & Biological Engineering & Computing*, *49*(5), 567–577.

Hoshi, E., & Tanji, J. (2004). Functional specialization in dorsal and ventral premotor areas. In *Brain Mechanisms for the Integration of Posture and Movement*: *Vol. 143*. *Progress in Brain Research* (pp. 507–511).

Hotz-Boendermaker, S., Funk, M., Summers, P., Brugger, P., Hepp-Reymond, M.-C., Curt, A., & Kollias, S. S. (2008). Preservation of motor programs in paraplegics as demonstrated by attempted and imagined foot movements. *NeuroImage*, *39*(1), 383–394.

Huang, J., Yu, C., Wang, Y., Zhao, Y., Liu, S., Mo, C., … Shi, Y. (2014). FOCUS: Enhancing Children's Engagement in Reading by Using Contextual BCI Training Sessions. *Proceedings of the SIGCHI Conference on Human Factors in Computing Systems*, 1905–1908.

Husain, M., & Kennard, C. (1997). Distractor-dependent frontal neglect. *Neuropsychologia*, *35*(6), 829–841.

Hwang, H.-J., Kwon, K., & Im, C.-H. (2009). Neurofeedback-based motor imagery training for brain–computer interface (BCI). *Journal of Neuroscience Methods*, *179*(1), 150–156.

Ilg, U. J., Schumann, S., & Thier, P. (2004). Posterior Parietal Cortex Neurons Encode Target Motion in World-Centered Coordinates. *Neuron*, *43*(1), 145–151.

Jeunet, C., Vi, C., Spelmezan, D., N'Kaoua, B., Lotte, F., & Subramanian, S. (2015, September). Continuous tactile feedback for motor-imagery based brain-computer interaction in a multitasking context. In *IFIP Conference on Human-Computer Interaction* (pp. 488-505). Springer, Cham.

Johnson, R. L., Brooks, C. A., & Whiteneck, G. G. (1996). Cost of traumatic spinal cord injury in a population-based registry. *Spinal Cord*, *34*(8), 470.

Johnstone, B. R., Jordan, C. J., & Buntine, J. A. (1988). A review of surgical rehabilitation of the upper limb in quadriplegia. *Spinal Cord*, *26*(5), 317.

Jurkiewicz, M. T., Mikulis, D. J., McIlroy, W. E., Fehlings, M. G., & Verrier, M. C. (2007). Sensorimotor cortical plasticity during recovery following spinal cord injury: A longitudinal fMRI study. *Neurorehabilitation and Neural Repair*, *21*(6), 527–538.

Kapoula, Z., & Robinson, D. A. (1986). Saccadic undershoot is not inevitable: Saccades can be accurate. *Vision Research*, *26*(5), 735–743.

Karnath, H. O. (1996). Optokinetic stimulation influences the disturbed perception of body orientation in spatial neglect. *Journal of Neurology, Neurosurgery & Psychiatry*, *60*(2), 217–220.

Karnath, H. O., Christ, K., & Hartje, W. (1993). Decrease of contralateral neglect by neck muscle vibration and spatial orientation of trunk midline. *Brain: A Journal of Neurology*, *116 (Pt 2)*, 383–396.

Karnath, H. O., Ferber, S., & Himmelbach, M. (2001). Spatial awareness is a function of the temporal not the posterior parietal lobe. *Nature*, *411*(6840), 950–953.

Kastner S, DeSimone K, Konen CS, Szczepanski SM, Weiner KS, Schneider KA. Topographic Maps in Human Frontal Cortex Revealed in Memory-Guided Saccade and Spatial Working-Memory Tasks. J Neurophysiol. 2007;97: 3494–3507.

Keith, M. W., Kilgore, K. L., Hunter Peckham, P., Stroh Wuolle, K., Creasey, G., & Lemay, M. (1996). Tendon transfers and functional electrical stimulation for restoration of hand function in spinal cord injury. *The Journal of Hand Surgery*, *21*(1), 89–99.

Kennedy, P. R., Bakay, R. A. E., Moore, M. M., Adams, K., & Goldwaithe, J. (2000). Direct control of a computer from the human central nervous system. *IEEE Transactions on Rehabilitation Engineering*, *8*(2), 198–202.

Kennedy, P., & Rogers, B. A. (2000). Anxiety and depression after spinal cord injury: A longitudinal analysis. *Archives of Physical Medicine and Rehabilitation*, *81*(7), 932–937.

Kennedy, P., Lude, P., & Taylor, N. (2006). Quality of life, social participation, appraisals and coping post spinal cord injury: A review of four community samples. *Spinal Cord*, *44*(2), 95.

Kernighan, B. W., & Ritchie, D. M. (2006). *The C programming language*.

Kim I-H, Kim J-W, Haufe S, Lee S-W (2015) Detection of braking intention in diverse situations during simulated driving based on feature combination. *J Neural Eng*. 12(1).

Kim, M., Kim, B. H., & Jo, S. (2015). Quantitative Evaluation of a Low-Cost Noninvasive Hybrid Interface Based on EEG and Eye Movement. *IEEE Transactions on Neural Systems and Rehabilitation Engineering*, *23*(2), 159–168.

Kirshblum, S. C., Burns, S. P., Biering-Sorensen, F., Donovan, W., Graves, D. E., Jha, A., … Waring, W. (2011). International standards for neurological classification of spinal cord injury (Revised 2011). *The Journal of Spinal Cord Medicine*, *34*(6), 535–546.

Kishore, S., González-Franco, M., Hintemüller, C., Kapeller, C., Guger, C., Slater, M., & Blom, K. J. (2014). Comparison of SSVEP BCI and Eye Tracking for Controlling a Humanoid Robot in a Social Environment. *Presence: Teleoperators and Virtual Environments*, *23*(3), 242–252.

Konen, C. S., & Kastner, S. (2008). Representation of Eye Movements and Stimulus Motion in Topographically Organized Areas of Human Posterior Parietal Cortex. *Journal of Neuroscience*, *28*(33), 8361–8375.

Kopinska, A., & Harris, L. R. (2003a). Spatial representation in body coordinates: Evidence from errors in remembering positions of visual and auditory targets after active eye, head, and body movements. *Canadian Journal of Experimental Psychology/Revue Canadienne de Psychologie Expérimentale*, *57*(1), 23–37.

Kopinska, A., & Harris, L. R. (2003b). Spatial representation in body coordinates: Evidence from errors in remembering positions of visual and auditory targets after active eye, head, and body movements. *Canadian Journal of Experimental Psychology/Revue Canadienne de Psychologie Expérimentale*, *57*(1), 23–37.

Kornhuber, H.H., & Deecke ,L. (1965) Hirnpotentialänderungen bei Willkürbewegungen und passiven Bewegungen des Menschen: bereitschaftspotential und reafferente Potentiale. *PflugersArch. Gesamte Physiol. Menschen Tiere* 284, 1–17.

Kotchoubey, B., Lang, S., Winter, S., & Birbaumer, N. (2003). Cognitive processing in completely paralyzed patients with amyotrophic lateral sclerosis. *European Journal of Neurology*, *10*(5), 551–558.

Krause, J. S., Kemp, B., & Coker, J. (2000). Depression after spinal cord injury: Relation to gender, ethnicity, aging, and socioeconomic indicators. *Archives of Physical Medicine and Rehabilitation*, *81*(8), 1099–1109.

Krusienski, D. J., Sellers, E. W., McFarland, D. J., Vaughan, T. M., & Wolpaw, J. R. (2008). Toward enhanced P300 speller performance. *Journal of Neuroscience Methods*, *167*(1), 15–21.

Kuo, C.-C., L. Knight, J., A. Dressel, C., & W. L. Chiu, A. (2012). Non-Invasive BCI for the Decoding of Intended Arm Reaching Movement in Prosthetic Limb Control. *American Journal of Biomedical Engineering*, *2*(4), 155–162.

Kwon, B. K., Tetzlaff, W., Grauer, J. N., Beiner, J., & Vaccaro, A. R. (2004). Pathophysiology and pharmacologic treatment of acute spinal cord injury. *The Spine Journal*, *4*(4), 451–464.

Lebedev, M. A., & Nicolelis, M. A. L. (2006a). Brain–machine interfaces: Past, present and future. *Trends in Neurosciences*, *29*(9), 536–546.

Lebedev, M. A., & Nicolelis, M. A. L. (2011a). Chapter 3 - Toward a whole-body neuroprosthetic. In J. Schouenborg, M. Garwicz, & N. Danielsen (Eds.), *Progress in Brain Research* (pp. 47–60).

Lee, H., Bellamkonda, R. V., Sun, W., & Levenston, M. E. (2005). Biomechanical analysis of silicon microelectrode-induced strain in the brain. *Journal of Neural Engineering*, *2*(4), 81–89.

Lee, W. T., Nisar, H., Malik, A. S., & Yeap, K. H. (2013). A brain computer interface for smart home control. *2013 IEEE International Symposium on Consumer Electronics (ISCE)*, 35–36.

Leigh, R. J., & Riley, D. E. (2000). Eye movements in parkinsonism: It's saccadic speed that counts. *Neurology*, *54*(5), 1018–1019.

Leuthold H, Sommer W, Ulrich R (2004) Preparing for Action: Inferences from CNV and LRP. *J. Psychophysiol.* 18, 77–88.

Leveille, A., Kiernan, J., Goodwin, J. A., & Antel, J. (1982). Eye Movements in Amyotrophic Lateral Sclerosis. *Archives of Neurology*, *39*(11), 684–686.

Levy, I., Schluppeck, D,. Heeger, D.J., & Glimcher, P.W. (2007). Specificity of human cortical areas for reaches and saccades*. Journal of Neuroscience*. 27, 4687–96.

Lew E, Chavarriaga R, Silvoni S, Millán J del R (2012) Detection of self-paced reaching movement intention from EEG signals. *Front. Neuroeng*. 5: 13.

Li, Z., He, W., Yang, C., Qiu, S., Zhang, L., & Su, C. (2016). Teleoperation control of an exoskeleton robot using brain machine interface and visual compressive sensing. *2016 12th World Congress on Intelligent Control and Automation (WCICA)*, 1550–1555.

Lin, C.-T., Lin, F.-C., Chen, S.-A., Lu, S.-W., Chen, T.-C., & Ko, L.-W. (2010). EEG-based Brain-computer Interface for Smart Living Environmental Auto-adjustment. *J. Med. Biol. Eng.*, *30*(4), 11.

Loeb, G. E. (1990). Cochlear Prosthetics. *Annual Review of Neuroscience*, *13*(1), 357–371.

Lomber, S. G., Lomber, S., & Eggermont, J. (Eds.). (2006). *Reprogramming the cerebral cortex: Plasticity following central and peripheral lesions*. Oxford University Press.

López-Larraz, E., Trincado-Alonso, F., Rajasekaran, V., Pérez-Nombela, S., del-Ama, A. J., Aranda, J., … Montesano, L. (2016). Control of an Ambulatory Exoskeleton with a Brain–Machine Interface for Spinal Cord Injury Gait Rehabilitation. *Frontiers in Neuroscience*, *10*.

Lotze, M., & Halsband, U. (2006). Motor imagery. *Journal of Physiology-Paris*, *99*(4), 386–395.

Lotze, M., Laubis-Herrmann, U., Topka, H., Erb, M., & Grodd, W. (1999). Reorganization in the primary motor cortex after spinal cord injury - A functional Magnetic Resonance (fMRI) study. *Restorative Neurology and Neuroscience*, *14*(2–3), 183–187.

Luo, Z., Han, S., & Duan, F. (2015). The development of a smart house system based on Brain-Computer Interface. *2015 IEEE International Conference on Robotics and Biomimetics (ROBIO)*, 1012–1017.

Lupu, R. G., & Ungureanu, F. (2013). A survey of eye tracking methods and applications. *Buletinul Institutului Politehnic din Iasi, Automatic Control and Computer Science Section*, *3*, 72-86.

Ma, V. Y., Chan, L., & Carruthers, K. J. (2014). Incidence, Prevalence, Costs, and Impact on Disability of Common Conditions Requiring Rehabilitation in the United States: Stroke, Spinal Cord Injury, Traumatic Brain Injury, Multiple Sclerosis, Osteoarthritis, Rheumatoid Arthritis, Limb Loss, and Back Pain. *Archives of Physical Medicine and Rehabilitation*, *95*(5), 986-995.e1.

Mak, J. N., McFarland, D. J., Vaughan, T. M., McCane, L. M., Tsui, P. Z., Zeitlin, D. J., … Wolpaw, J. R. (2012). EEG correlates of P300-based brain–computer interface (BCI) performance in people with amyotrophic lateral sclerosis. *Journal of Neural Engineering*, *9*(2), 026014.

Marino, R. J., Barros, T., Biering-Sorensen, F., Burns, S. P., Donovan, W. H., Graves, D. E., … Priebe, M. (2003). International Standards For Neurological Classification Of Spinal Cord Injury. *The Journal of Spinal Cord Medicine*, *26*(sup1), S50–S56.

Mastaglia, F. L., Black, J. L., Cala, L. A., & Collins, D. W. (1977). Evoked potentials, saccadic velocities, and computerized tomography in diagnosis of multiple sclerosis. *Br Med J*, *1*(6072), 1315–1317.

Mateo, S., Di Rienzo, F., Bergeron, V., Guillot, A., Collet, C., & Rode, G. (2015). Motor imagery reinforces brain compensation of reach-to-grasp movement after cervical spinal cord injury. *Frontiers in Behavioral Neuroscience*, *9*.

Mattay, V. S., Callicott, J. H., Bertolino, A., Santha, A. K. S., Van Horn, J. D., Tallent, K. A., … Weinberger, D. R. (1998). Hemispheric control of motor function: A whole brain echo planar fMRI study. *Psychiatry Research: Neuroimaging*, *83*(1), 7–22.

Maynard, F. M., Bracken, M. B., Creasey, G., Jr, J. F. D., Donovan, W. H., Ducker, T. B., … Young, W. (1997). International Standards for Neurological and Functional Classification of Spinal Cord Injury. *Spinal Cord*, *35*(5), 266–274.

McDonald, J. W., & Sadowsky, C. (2002). Spinal-cord injury. *The Lancet*, *359*(9304), 417–425.

McFarland, D. J., & Wolpaw, J. R. (2008). Brain-Computer Interface Operation of Robotic and Prosthetic Devices. *Computer*, *41*(10), 52–56.

McManus, I. C. (1999). Eye-dominance, writing hand, and throwing hand. *Laterality: Asymmetries of Body, Brain and Cognition*, *4*(2), 173-192.

Meienberg, O., Harrer, M., & Wehren, C. (1986). Oculographic diagnosis of hemineglect in patients with homonymous hemianopia. *Journal of Neurology*, *233*(2), 97–101.

Meienberg, Otmar, Müri, R., & Rabineau, P. A. (1986). Clinical and Oculographic Examinations of Saccadic Eye Movements in the Diagnosis of Multiple Sclerosis. *Archives of Neurology*, *43*(5), 438–443.

Merriam EP, Gardner JL, Movshon JA, Heeger DJ. Modulation of Visual Responses by Gaze Direction in Human Visual Cortex. J Neurosci. 2013;33: 9879–9889.

Merzenich, M. M. (1983). CODING OF SOUND IN A COCHLEAR PROSTHESIS: SOME THEORETICAL AND PRACTICAL CONSIDERATIONS. *Annals of the New York Academy of Sciences*, *405*(1), 502–508.

Mikulis, D. J., Jurkiewicz, M. T., McIlroy, W. E., Staines, W. R., Rickards, L., Kalsi-Ryan, S., … Verrier, M. C. (2002). Adaptation in the motor cortex following cervical spinal cord injury. *Neurology*, *58*(5), 794–801.

Milan, J. del R., & Carmena, J. M. (2010). Invasive or Noninvasive: Understanding Brain-Machine Interface Technology [Conversations in BME]. *IEEE Engineering in Medicine and Biology Magazine*, *29*(1), 16–22.

Morrow, MarkJ., & Sharpe, JamesA. (1993). The effects of head and trunk position on torsional vestibular and optokinetic eye movements in humans. *Experimental Brain Research*, *95*(1).

Mosimann, U. P., Müri, R. M., Burn, D. J., Felblinger, J., O'Brien, J. T., & McKeith, I. G. (2005). Saccadic eye movement changes in Parkinson's disease dementia and dementia with Lewy bodies. *Brain*, *128*(6), 1267–1276.

Mullette-Gillman OA, Cohen YE, Groh JM. Motor-related signals in the intraparietal cortex encode locations in a hybrid, rather than eye-centered reference frame. Cereb Cortex. 2009;19: 1761–1775.

Mullette-Gillman OA. Eye-Centered, Head-Centered, and Complex Coding of Visual and Auditory Targets in the Intraparietal Sulcus. J Neurophysiol. 2005;94: 2331–2352.

Munoz, D. P., Armstrong, I. T., Hampton, K. A., & Moore, K. D. (2003). Altered Control of Visual Fixation and Saccadic Eye Movements in Attention-Deficit Hyperactivity Disorder. *Journal of Neurophysiology*, *90*(1), 503–514.

Musallam, S., Corneil, B. D., Greger, B., Scherberger, H., & Andersen, R. A. (2004). Cognitive Control Signals for Neural Prosthetics. *Science*, *305*(5681), 258–262.

Myrden, A., & Chau, T. (2015). Effects of user mental state on EEG-BCI performance. *Frontiers in Human Neuroscience*, *9*.

Nestares O, Heeger DJ. Robust multiresolution alignment of MRI brain volumes. Magn Reson Med. 2000;43: 705–715.

NHS Commissioning Board (NHS England). NHS standard contract for spinal cord injuries (all ages) (2013). Retrieved from https://www.england.nhs.uk/commissioning/wp-content/uploads/sites/12/2014/04/d13-spinal-cord-0414.pdf

Nicolelis, M. A. L., Dimitrov, D., Carmena, J. M., Crist, R., Lehew, G., Kralik, J. D., & Wise, S. P. (2003). Chronic, multisite, multielectrode recordings in macaque monkeys. *Proceedings of the National Academy of Sciences*, *100*(19), 11041–11046.

Nijboer, F., Sellers, E. W., Mellinger, J., Jordan, M. A., Matuz, T., Furdea, A., … Kübler, A. (2008). A P300-based brain-computer interface for people with amyotrophic lateral sclerosis. *Clinical Neurophysiology: Official Journal of the International Federation of Clinical Neurophysiology*, *119*(8), 1909–1916.

Nyström, M., Andersson, R., Holmqvist, K., & Van De Weijer, J. (2013). The influence of calibration method and eye physiology on eyetracking data quality. *Behavior research methods*, *45*(1), 272-288.

O'Connor, P. J. (2006). Trends in spinal cord injury. *Accident Analysis & Prevention*, *38*(1), 71–77.

Oldfield, R. C. (1971). The assessment and analysis of handedness: the Edinburgh inventory. *Neuropsychologia*, *9*(1), 97-113.

Ortner, R., Allison, B. Z., Korisek, G., Gaggl, H., & Pfurtscheller, G. (2011). An SSVEP BCI to Control a Hand Orthosis for Persons With Tetraplegia. *IEEE Transactions on Neural Systems and Rehabilitation Engineering*, *19*(1), 1–5.

Page, S. J., Levine, P., Sisto, S. A., & Johnston, M. V. (2001). Mental practice combined with physical practice for upper-limb motor deficit in subacute stroke. *Physical Therapy*, *81*(8), 1455-1462.

Page, S. J., Levine, P., Sisto, S., & Johnston, M. V. (2001). A randomized efficacy and feasibility study of imagery in acute stroke. *Clinical rehabilitation*, *15*(3), 233-240.

Panicker, R. C., Puthusserypady, S., & Sun, Y. (2011). An Asynchronous P300 BCI With SSVEP-Based Control State Detection. *IEEE Transactions on Biomedical Engineering*, *58*(6), 1781–1788.

Park, C., Looney, D., Rehman, N. ur, Ahrabian, A., & Mandic, D. P. (2013). Classification of Motor Imagery BCI Using Multivariate Empirical Mode Decomposition. *IEEE Transactions on Neural Systems and Rehabilitation Engineering*, *21*(1), 10–22.

Parton, A., Malhotra, P., & Husain, M. (2004). Hemispatial neglect. *Journal of Neurology, Neurosurgery & Psychiatry*, *75*(1), 13-21.

Paulus, W., Straube, A., Krafczyk, S., & Brandt, T. (1989). Differential effects of retinal target displacement, changing size and changing disparity in the control of anterior/posterior and lateral body sway. *Experimental Brain Research*, *78*(2), 243–252.

Pavlidis, G. Th. (1985). Eye Movements in Dyslexia: Their Diagnostic Significance. *Journal of Learning Disabilities*, *18*(1), 42–50.

Pelli, D. G. (1997) The VideoToolbox software for visual psychophysics: Transforming numbers into movies, *Spatial Vision 10*:437-442.

Pérez-Marcos, D., Buitrago, J. A., & Velásquez, F. D. G. (2011). Writing through a robot: A proof of concept for a brain–machine interface. *Medical Engineering & Physics*, *33*(10), 1314–1317.

Pertzov, Y., Avidan, G., & Zohary, E. (2011). Multiple reference frames for saccadic planning in the human parietal cortex. *Journal of Neuroscience*, *31*(3), 1059-1068.

Pesaran, B., Nelson, M. J., & Andersen, R. A. (2006). Dorsal Premotor Neurons Encode the Relative Position of the Hand, Eye, and Goal during Reach Planning. *Neuron*, *51*(1), 125–134.

Pfurtscheller G (2001) Functional brain imaging based on ERD/ERS. *Vis. Res.* 41, 10–11,

1257–1260.

Pfurtscheller, G., Allison, B. Z., Bauernfeind, G., Brunner, C., Solis Escalante, T., Scherer, R., … Birbaumer, N. (2010). The hybrid BCI. *Frontiers in Neuroscience*, *4*.

Pfurtscheller, G., Solis-Escalante, T., Ortner, R., Linortner, P., & Muller-Putz, G. R. (2010). Self-Paced Operation of an SSVEP-Based Orthosis With and Without an Imagery-Based "Brain Switch:" A Feasibility Study Towards a Hybrid BCI. *IEEE Transactions on Neural Systems and Rehabilitation Engineering*, *18*(4), 409–414.

Picard, N., & Strick, P. L. (1996). Motor Areas of the Medial Wall: A Review of Their Location and Functional Activation. *Cerebral Cortex*, *6*(3), 342–353.

Pillai, J. J. (2010). The evolution of clinical functional imaging during the past 2 decades and its current impact on neurosurgical planning. American Journal of Neuroradiology, 31(2), 219-225.

Pineda, J. A., Allison, B. Z., & Vankov, A. (2000). The effects of self-movement, observation, and imagination on /spl mu/ rhythms and readiness potentials (RP's): Toward a brain-computer interface (BCI). *IEEE Transactions on Rehabilitation Engineering*, *8*(2), 219–222.

Pirozzolo, F. J., & Rayner, K. (1980). Handedness, hemispheric specialization and saccadic eye movement latencies. *Neuropsychologia*, *18*(2), 225–229.

Pizzamiglio, L., Antonucci, G., Judica, A., Montenero, P., Razzano, C., & Zoccolotti, P. (1992). Cognitive rehabilitation of the hemineglect disorder in chronic patients with unilateral right brain damage. *Journal of Clinical and Experimental Neuropsychology*, *14*(6), 901–923.

Principe, J. C., & McFarland, D. J. (2008). BMI/BCI Modeling and Signal Processing. In T. W. Berger, J. K. Chapin, G. A. Gerhardt, D. J. McFarland, J. C. Principe, W. V. Soussou, … P. A. Tresco (Eds.), *Brain-Computer Interfaces: An International Assessment of Research and Development Trends* (pp. 47–64).

Puce, A., Constable, R. T., Luby, M. L., McCarthy, G., Nobre, A. C., Spencer, D. D., … Allison, T. (1995). Functional magnetic resonance imaging of sensory and motor cortex: Comparison with electrophysiological localization. *Journal of Neurosurgery*, *83*(2), 262–270.

Ragnarsson, K. T. (2008). Functional electrical stimulation after spinal cord injury: Current use, therapeutic effects and future directions. *Spinal Cord*, *46*(4), 255–274.

Ramat, S., Leigh, R. J., Zee, D. S., & Optican, L. M. (2007). What clinical disorders tell us about the neural control of saccadic eye movements. *Brain*, *130*(1), 10–35.

Ramos-Murguialday, A., Broetz, D., Rea, M., Läer, L., Yilmaz, Ö., Brasil, F. L., … Birbaumer, N. (2013). Brain–machine interface in chronic stroke rehabilitation: A controlled study. *Annals of Neurology*, *74*(1), 100–108.

Rennaker, R. L., Miller, J., Tang, H., & Wilson, D. A. (2007). Minocycline increases quality and longevity of chronic neural recordings. *Journal of Neural Engineering*, *4*(2), L1–L5.

Reuter, M., Schmansky, N. J., Rosas, H. D., & Fischl, B. (2012). Within-subject template estimation for unbiased longitudinal image analysis. *Neuroimage*, *61*(4), 1402-1418.

Robinson, D. A. (1973). Models of the saccadic eye movement control system. *Kybernetik*, *14*(2), 71–83.

Roll, J. P., Vedel, J. P., & Roll, R. (1989). Eye, head and skeletal muscle spindle feedback in the elaboration of body references. In *Progress in brain research* (Vol. 80, pp. 113-123). Elsevier.

Rosen, B. R., & Savoy, R. L. (2012). fMRI at 20: has it changed the world?. *Neuroimage*, *62*(2), 1316-1324.

Ross, R. G., Heinlein, S., Zerbe, G. O., & Radant, A. (2005). Saccadic eye movement task identifies cognitive deficits in children with schizophrenia, but not in unaffected child relatives. *Journal of Child Psychology and Psychiatry*, *46*(12), 1354–1362.

Roth, Z. N., Heeger, D. J., & Merriam, E. P. (2018). Stimulus vignetting and orientation selectivity in human visual cortex. *eLife*, *7*, e37241.

Roy, R. N., Bonnet, S., Charbonnier, S., & Campagne, A. (2013). Mental fatigue and working memory load estimation: Interaction and implications for EEG-based passive BCI. *2013 35th Annual International Conference of the IEEE Engineering in Medicine and Biology Society (EMBC)*, 6607–6610.

Rupp, R. (2014). Challenges in clinical applications of brain computer interfaces in individuals with spinal cord injury. *Frontiers in Neuroengineering*, *7*.

Sabbah, P., De Schonen, S., Leveque, C., Gay, S., Pfefer, F., Nioche, C., ... & Cordoliani, Y. S. (2002). Sensorimotor cortical activity in patients with complete spinal cord injury: a functional magnetic resonance imaging study. *Journal of neurotrauma*, *19*(1), 53-60.

Sabre, L., Tomberg, T., Korv, J., Kepler, J., Kepler, K., Linnamägi, Ü., & Asser, T. (2013). Brain activation in the acute phase of traumatic spinal cord injury. *Spinal Cord*, *51*(8), 623-629.

Sakurada, T., Kawase, T. P., Takano, K., Komatsu, T., & Kansaku, K. (2013). A BMI-based occupational therapy assist suit: Asynchronous control by SSVEP. *Frontiers in Neuroscience*, *7*.

Salvucci, D. D., & Goldberg, J. H. (2000). Identifying Fixations and Saccades in Eye-tracking Protocols. *Proceedings of the 2000 Symposium on Eye Tracking Research & Applications*, 71–78.

Schalk, G., McFarland, D. J., Hinterberger, T., Birbaumer, N., & Wolpaw, J. R. (2004). BCI2000: A General-Purpose Brain-Computer Interface (BCI) System. *IEEE Transactions on Biomedical Engineering*, *51*(6), 1034–1043.

Scherberger H, Goodale MA, Andersen RA. Target Selection for Reaching and Saccades Share a Similar Behavioral Reference Frame in the Macaque. J Neurophysiol. 2006; doi:10.1152/jn.00883.2002

Schindler, I. (2002). Neck muscle vibration induces lasting recovery in spatial neglect. *Journal of Neurology, Neurosurgery & Psychiatry*, *73*(4), 412–419.

Schluppeck, D., Glimcher, P., & Heeger, D. J. (2005). Topographic organization for delayed saccades in human posterior parietal cortex. *Journal of neurophysiology*, *94*(2), 1372-1384.

Schmidt, E. M. (1980). Single neuron recording from motor cortex as a possible source of signals for control of external devices. *Annals of Biomedical Engineering*, *8*(4), 339–349.

Schulmann, D. L., Godfrey, B., & Fisher, A. G. (1987). Effect of Eye Movements on Dynamic Equilibrium. *Physical Therapy*, *67*(7), 1054–1057.

Schulz, R., & Decker, S. (1985). Long-term adjustment to physical disability: The role of social support, perceived control, and self-blame. *Journal of Personality and Social Psychology*, *48*(5), 1162–1172.

Schwab, M. E., & Bartholdi, D. (1996). Degeneration and regeneration of axons in the lesioned spinal cord. *Physiological Reviews*, *76*(2), 319–370.

Schwab, Martin E. (2002). Repairing the Injured Spinal Cord. *Science*, *295*(5557), 1029–1031.

Schwartz, A. B., Cui, X. T., Weber, D. J., & Moran, D. W. (2006). Brain-Controlled Interfaces: Movement Restoration with Neural Prosthetics. *Neuron*, *52*(1), 205–220.

Sekhon, L. H. S., & Fehlings, M. G. (2001). Epidemiology, Demographics, and Pathophysiology of Acute Spinal Cord Injury. *Spine*, *26*(24S), S2.

Sellers, E. W., & Donchin, E. (2006). A P300-based brain–computer interface: initial tests by ALS patients. *Clinical neurophysiology*, *117*(3), 538-548.

Sereno, M. I., Pitzalis, S., & Martinez, A. (2001). Mapping of contralateral space in retinotopic coordinates by a parietal cortical area in humans. *Science*, *294*(5545), 1350-1354.

Serruya, M. D., Hatsopoulos, N. G., Paninski, L., Fellows, M. R., & Donoghue, J. P. (2002). Instant neural control of a movement signal. *Nature*, *416*(6877), 141.

Silver, M. A., & Kastner, S. (2009). Topographic maps in human frontal and parietal cortex. *Trends in cognitive sciences*, *13*(11), 488-495.

Simpson, L. A., Eng, J. J., Hsieh, J. T., & Wolfe and the Spinal Cord Injury Rehabilitation Evidence (SCIRE) Research Team, D. L. (2012). The health and life priorities of individuals with spinal cord injury: a systematic review. *Journal of neurotrauma*, *29*(8), 1548-1555.

Snyder, L. H., Batista, A. P., & Andersen, R. A. (1997). Coding of intention in the posterior parietal cortex. *Nature*, *386*(6621), 167.

Soechting, J. F., & Flanders, M. (1992). Moving in three-dimensional space: frames of reference, vectors, and coordinate systems. *Annual review of neuroscience*, *15*(1), 167-191.

Spataro, R., Chella, A., Allison, B., Giardina, M., Sorbello, R., Tramonte, S., … La Bella, V. (2017). Reaching and Grasping a Glass of Water by Locked-In ALS Patients through a BCI-Controlled Humanoid Robot. *Frontiers in Human Neuroscience*, *11*.

Stawicki, P., Gembler, F., Rezeika, A., & Volosyak, I. (2017). A Novel Hybrid Mental Spelling Application Based on Eye Tracking and SSVEP-Based BCI. *Brain Sciences*, *7*(4), 35.

Stevens, J. A., & Stoykov, M. E. P. (2003). Using Motor Imagery in the Rehabilitation of Hemiparesis. *Archives of Physical Medicine and Rehabilitation*, *84*(7), 1090–1092.

Strauss, D. J., Devivo, M. J., Paculdo, D. R., & Shavelle, R. M. (2006). Trends in life expectancy after spinal cord injury. *Archives of Physical Medicine and Rehabilitation*, *87*(8), 1079–1085.

Sykacek, P., Roberts, S., Stokes, M., Curran, E., Gibbs, M., & Pickup, L. (2003). Probabilistic methods in BCI research. *IEEE Transactions on Neural Systems and Rehabilitation Engineering*, *11*(2), 192–194.

Tasiemski, T., Bergström, E., Savic, G., & Gardner, B. (2000). Sports, recreation and employment following spinal cord injury–a pilot study. *Spinal Cord*, *38*(3), 173–184.

Tate, D., Forchheimer, M., Maynard, F., & Dijkers, M. (1994). Predicting depression and psychological distress in persons with spinal cord injury based on indicators of handicap. *American Journal of Physical Medicine & Rehabilitation*, *73*(3), 175–183.

Thompson, D. E., Gruis, K. L., & Huggins, J. E. (2014). A plug-and-play brain-computer interface to operate commercial assistive technology. *Disability and Rehabilitation: Assistive Technology*, *9*(2), 144–150.

Thulasidas, M., Cuntai Guan, & Jiankang Wu. (2006). Robust classification of EEG signal for brain-computer interface. *IEEE Transactions on Neural Systems and Rehabilitation Engineering*, *14*(1), 24–29.

Thuret, S., Moon, L. D. F., & Gage, F. H. (2006). Therapeutic interventions after spinal cord injury. *Nature Reviews Neuroscience*, *7*(8), 628–643.

Toppi, J., Borghini, G., Petti, M., He, E. J., Giusti, V. D., He, B., … Babiloni, F. (2016). Investigating Cooperative Behavior in Ecological Settings: An EEG Hyperscanning Study. *PLOS ONE*, *11*(4), e0154236.

Townsend, G., Graimann, B., & Pfurtscheller, G. (2004). Continuous EEG classification during motor imagery-simulation of an asynchronous BCI. *IEEE Transactions on Neural Systems and Rehabilitation Engineering*, *12*(2), 258–265.

Turner, J. A., Lee, J. S., Martinez, O., Medlin, A. L., Schandler, S. L., & Cohen, M. J. (2001a). Somatotopy of the motor cortex after long-term spinal cord injury or amputation. *IEEE Transactions on Neural Systems and Rehabilitation Engineering*, *9*(2), 154–160.

Vallar, G., & Perani, D. (1986). The anatomy of unilateral neglect after right-hemisphere stroke lesions. A clinical/CT-scan correlation study in man. *Neuropsychologia*, *24*(5), 609–622.

Vallar, G., Rusconi, M. L., Barozzi, S., Bernardini, B., Ovadia, D., Papagno, C., & Cesarani, A. (1995). Improvement of left visuo-spatial hemineglect by left-sided transcutaneous electrical stimulation. *Neuropsychologia*, *33*(1), 73–82.

Van Allen, M. W. (1973). Latency of ocular movement in cerebral disease. *Documenta Ophthalmologica. Advances in Ophthalmology*, *34*(1), 37–40.

Vaughan, T. M., Heetderks, W. J., Trejo, L. J., Rymer, W. Z., Weinrich, M., Moore, M. M., … Wolpaw, J. R. (2003). Brain-computer interface technology: A review of the Second International Meeting. *IEEE Transactions on Neural Systems and Rehabilitation Engineering : A Publication of the IEEE Engineering in Medicine and Biology Society*, *11*(2), 94–109.

Vos, M. D., Kroesen, M., Emkes, R., & Debener, S. (2014). P300 speller BCI with a mobile EEG system: Comparison to a traditional amplifier. *Journal of Neural Engineering*, *11*(3), 036008.

Vourvopoulos, A., & Liarokapis, F. (2014). Evaluation of commercial brain–computer interfaces in real and virtual world environment: A pilot study. *Computers & Electrical Engineering*, *40*(2), 714–729.

Waldert, S. (2016a). Invasive vs. Non-Invasive Neuronal Signals for Brain-Machine Interfaces: Will One Prevail? *Frontiers in Neuroscience*, *10*.

Waldert, S. (2016b). Invasive vs. Non-Invasive Neuronal Signals for Brain-Machine Interfaces: Will One Prevail? *Frontiers in Neuroscience*, *10*.

Wall, P. D., & Egger, M. D. (1971). Formation of new connexions in adult rat brains after partial deafferentation. *Nature*, *232*(5312), 542-545.

Walter, W.G., Cooper, R., Aldridge, V.J., McCallum, W.C., Winter, A.A.L. (1964) Contingent negative variation: An electrical sign of sensorimotor association and expectancy in the human brain. *Nature* 203, 380-384.

Wang, Y., Hong, B., Gao, X., & Gao, S. (2007). Implementation of a Brain-Computer Interface Based on Three States of Motor Imagery. *2007 29th Annual International Conference of the IEEE Engineering in Medicine and Biology Society*, 5059–5062.

Waters, R. L., Adkins, R. H., Yakura, J. S., & Sie, I. (1994). Motor and sensory recovery following incomplete tetraplegia. *Archives of Physical Medicine and Rehabilitation*, *75*(3), 306–311.

Weinberg, J., Diller, L., Gordon, W. A., Gerstman, L. J., Lieberman, A., Lakin, P., … Ezrachi, O. (1977). Visual scanning training effect on reading-related tasks in acquired right brain damage. *Archives of Physical Medicine and Rehabilitation*, *58*(11), 479–486.

Wiart, L., Côme, A. B., Debelleix, X., Petit, H., Joseph, P. A., Mazaux, J. M., & Barat, M. (1997). Unilateral neglect syndrome rehabilitation by trunk rotation and scanning training. *Archives of Physical Medicine and Rehabilitation*, *78*(4), 424–429.

Wilson, S. J., Glue, P., Ball, D., & Nutt, D. J. (1993). Saccadic eye movement parameters in normal subjects. *Electroencephalography and Clinical Neurophysiology*, *86*(1), 69–74.

Wodlinger, B., Downey, J. E., Tyler-Kabara, E. C., Schwartz, A. B., Boninger, M. L., & Collinger, J. L. (2014). Ten-dimensional anthropomorphic arm control in a human brain-machine interface: Difficulties, solutions, and limitations. *Journal of Neural Engineering*, *12*(1), 016011.

Wolpaw, J. R., & McFarland, D. J. (2004). Control of a two-dimensional movement signal by a noninvasive brain-computer interface in humans. *Proceedings of the National Academy of Sciences*, *101*(51), 17849–17854.

Wolpaw, J. R., Birbaumer, N., Heetderks, W. J., McFarland, D. J., Peckham, P. H., Schalk, G., ... & Vaughan, T. M. (2000). Brain-computer interface technology: a review of the first international meeting. *IEEE transactions on rehabilitation engineering*, *8*(2), 164-173.

Wolpaw, J. R., Birbaumer, N., McFarland, D. J., Pfurtscheller, G., & Vaughan, T. M. (2002). Brain-computer interfaces for communication and control. *Clinical Neurophysiology: Official Journal of the International Federation of Clinical Neurophysiology*, *113*(6), 767–791.

Wolpert, D. M., Goodbody, S. J., & Husain, M. (1998). Maintaining internal representations: The role of the human superior parietal lobe. *Nature Neuroscience*, *1*(6), 529.

Wyndaele, M., & Wyndaele, J.-J. (2006a). Incidence, prevalence and epidemiology of spinal cord injury: What learns a worldwide literature survey? *Spinal Cord*, *44*(9), 523.

Wyndaele, M., & Wyndaele, J.-J. (2006b). Incidence, prevalence and epidemiology of spinal cord injury: What learns a worldwide literature survey? *Spinal Cord*, *44*(9), 523–529.

Yarkony, G. M., Roth, E. J., Cybulski, G., & Jaeger, R. J. (1992). Neuromuscular stimulation in spinal cord injury: I: Restoration of functional movement of the extremities. *Archives of physical medicine and rehabilitation*, *73*(1), 78-86.

Yi, W., Qiu, S., Wang, K., Qi, H., Zhao, X., He, F., … Ming, D. (2017). Enhancing performance of a motor imagery based brain–computer interface by incorporating electrical stimulation-induced SSSEP. *Journal of Neural Engineering*, *14*(2), 026002.

Yin, E., Zhou, Z., Jiang, J., Chen, F., Liu, Y., & Hu, D. (2013a). A novel hybrid BCI speller based on the incorporation of SSVEP into the P300 paradigm. *Journal of Neural Engineering*, *10*(2), 026012.

Zhang, B., Jianjun Wang, & Fuhlbrigge, T. (2010). A review of the commercial brain-computer interface technology from perspective of industrial robotics. *2010 IEEE International Conference on Automation and Logistics*, 379–384.

Ziegler, G., Grabher, P., Thompson, A., Altmann, D., Hupp, M., Ashburner, J., … Freund, P. (2018). Progressive neurodegeneration following spinal cord injury: Implications for clinical trials. *Neurology*, *90*(14), e1257–e1266.

7 Appendix

7.1 Appendix A

Full Resolution of Figures 7 and 11

Figure 7

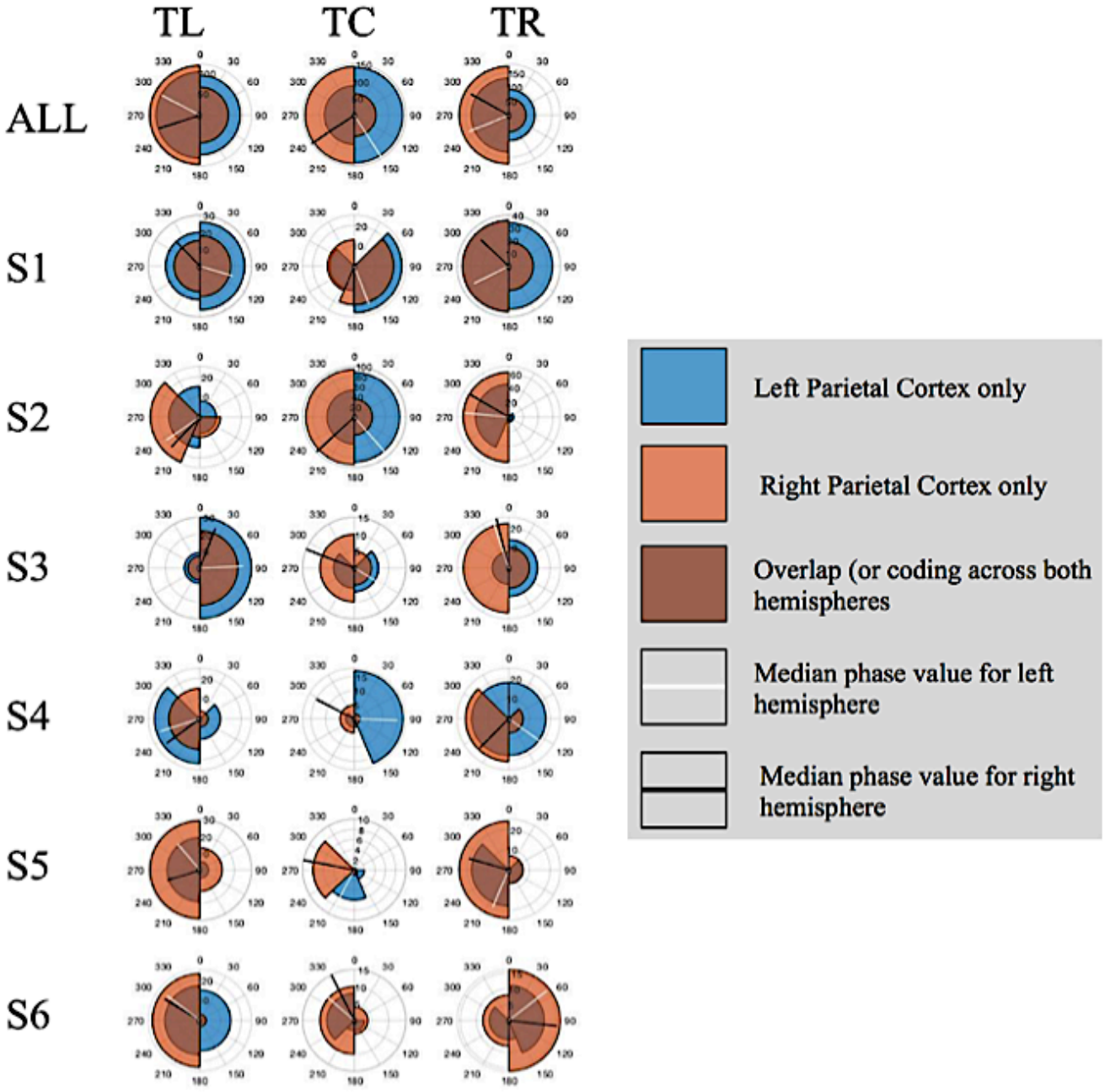

Figure 11

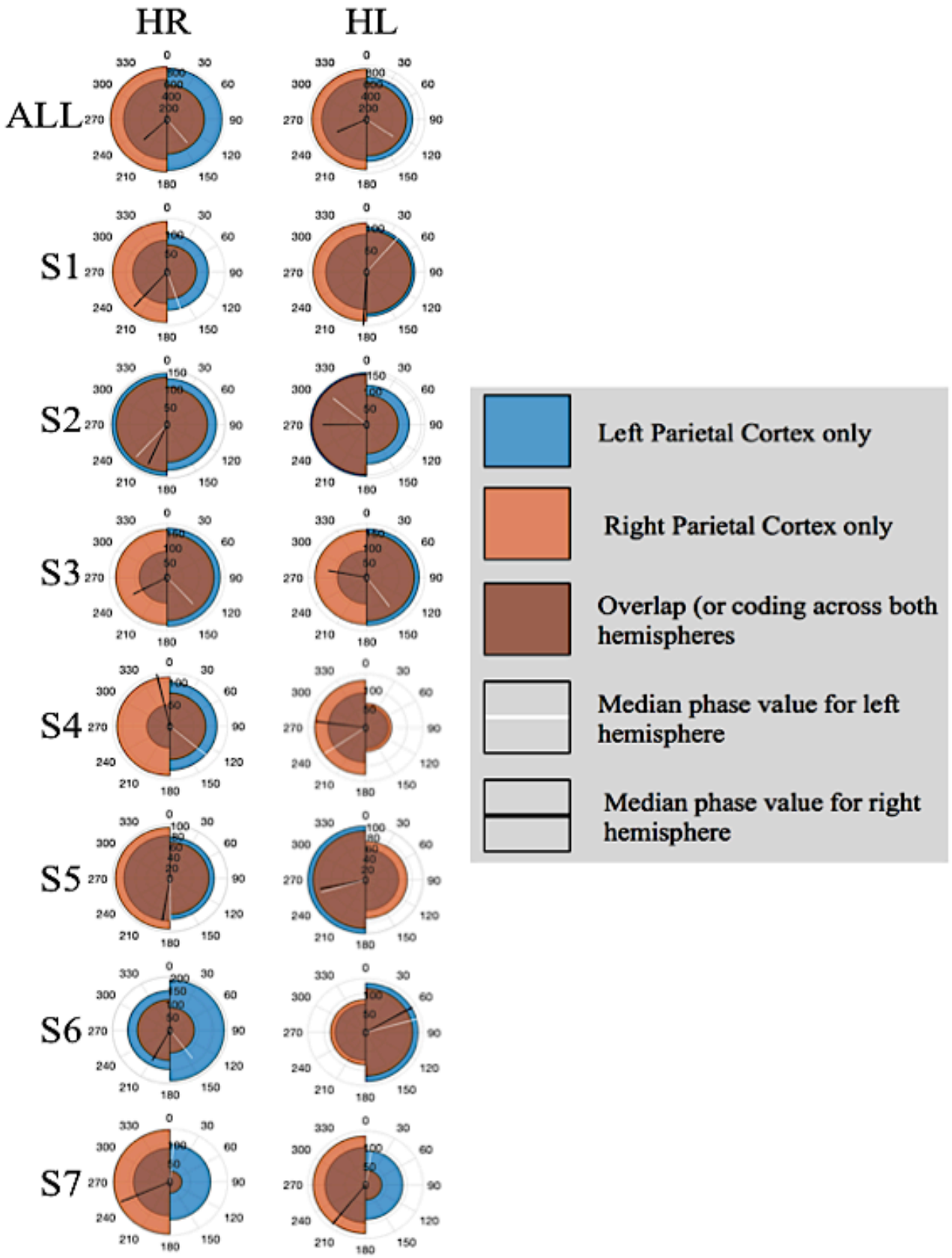
HR
HL
ALL
S1
S2
S3
S4
S5
S6
S7
Left Parietal Cortex only
Right Parietal Cortex only
Overlap (or coding across both hemispheres
Median phase value for left hemisphere
Median phase value for right hemisphere

7.2 Appendix B

Motor Imagery Questionnaire II – Revised

This questionnaire wishes to evaluate your level of confidence in imagining movement. Be as accurate as possible and take as long as you feel necessary to arrive at the proper rating for each movement. You may choose the same rating for any number of movements described and it is not necessary to use the entire length of the scale if it does not feel appropriate.

Visual Imagery Scale

We will start with you attempting to *see* yourself making some movements.

1. **Starting Position:** Sit comfortably on a chair with your arms on your lap and your feet together. Make a fist with one of your hands.

   Action to perform: Raise your hand above your head until your arm is fully extended, keeping your fingers in a fist. Next, lower your hand back to your lap while maintaining a fist.

   Mental Task: Assume the starting position. Attempt to see yourself making the movement just described with as clear and vivid a visual image as possible. Now rate the ease/difficulty with which you were able to do this mental task.

1	2	3	4	5	6	7

Very Hard to see	Hard to see	Somewhat hard to see	Neutral (not easy, not hard)	Somewhat easy to see	Easy to see	Very Easy to see

2. **Starting Position:** Extend your arm straight out to your side so that it is parallel to the ground, with your fingers extended and your palm down.

   Action: Move your arm forward until it is directly in front of your body (still parallel to the ground). Keep your arm extended during the movement and make it slowly. Now move your arm back to the starting position, straight out to your side.

   Mental Task: Assume the starting position. Attempt to see yourself making the movement just described with as clear a visual image as possible and rate below.

1	2	3	4	5	6	7
Very Hard to see	Hard to see	Somewhat hard to see	Neutral (not easy, not hard)	Somewhat easy to see	Easy to see	Very Easy to see

3. **Starting Position:** Sit with your arms fully extended above your head.

   Action: Slowly bend forward at the waist so that your fingertips can touch your toes then return to the starting position with your arms above your head.

Mental Task: Attempt to see yourself making the movement just described then rate below.

1	2	3	4	5	6	7
Very Hard to see	Hard to see	Somewhat hard to see	Neutral (not easy, not hard)	Somewhat easy to see	Easy to see	Very Easy to see

4. **Starting Position:** Put your hand in front of you about shoulder height as if you are about to push open a swinging door. Your fingers should be pointing upwards.

   Action: Extend your arm fully as if you are pushing open the door, keeping your fingers pointing upwards. Now let the swinging door close by returning your hand and arm to the starting position.

   Mental Task: Attempt to see yourself making the movement and rate the ease/difficulty below.

1	2	3	4	5	6	7
Very Hard to see	Hard to see	Somewhat hard to see	Neutral (not easy, not hard)	Somewhat easy to see	Easy to see	Very Easy to see

5. **Starting Position:** While sitting with your hands on your lap, pretend you see a drinking glass on the table in front of you.

   Action: Reach forward, grasp the glass and lift it off the table to take a sip. Put the glass down and return your hand to the starting position.

   Mental Task: Attempt to see yourself making the movement and rate the ease/difficulty below.

1	2	3	4	5	6	7
Very Hard to see	Hard to see	Somewhat hard to see	Neutral (not easy, not hard)	Somewhat easy to see	Easy to see	Very Easy to see

6. **Starting Position:** You are standing with the hands on your side. Imagine there is a closed door in front of you.

   Action: Reach forward, grasp the door handle and pull open the door. Then let go of the handle and return your arm to your side.

   Mental Task: Assume the starting position then imagine seeing yourself opening the same door. Rate below.

1	2	3	4	5	6	7

Very Hard to see	Hard to see	Somewhat hard to see	Neutral (not easy, not hard)	Somewhat easy to see	Easy to see	Very Easy to see

Kinaesthetic Imagery Scale

We will now move on to let you *feel* rather than seeing yourself making the movement.

7. **Starting Position:** Sit comfortably on a chair with your arms on your lap and your feet together. Make a fist with one of your hands.

   Action: Raise your hand above your head until your arm is fully extended, keeping your fingers in a fist. Next, lower your hand back to your lap while maintaining a fist.

   Mental Task: Assume the starting position. Attempt to see yourself making the movement just described with as clear and vivid a visual image as possible. Now rate the ease/difficulty with which you were able to do this mental task.

1	2	3	4	5	6	7
Very Hard to feel	Hard to feel	Somewhat hard to feel	Neutral (not easy, not hard)	Somewhat easy to feel	Easy to feel	Very Easy to feel

8. **Starting Position:** Extend your arm straight out to your side so that it is parallel to the ground, with your fingers extended and your palm down.

   Action: Move your arm forward until it is directly in front of your body (still parallel to the ground). Keep your arm extended during the movement and make it slowly. Now move your arm back to the starting position, straight out to your side.

   Mental Task: Assume the starting position. Attempt to see yourself making the movement just described with as clear a visual image as possible and rate below.

1	2	3	4	5	6	7
Very Hard to feel	Hard to feel	Somewhat hard to feel	Neutral (not easy, not hard)	Somewhat easy to feel	Easy to feel	Very Easy to feel

9. **Starting Position:** Sit with your arms fully extended above your head.

   Action: Slowly bend forward at the waist so that your fingertips can touch your toes then return to the starting position with your arms above your head.

   Mental Task: Attempt to see yourself making the movement just described then rate below.

1	2	3	4	5	6	7

Very Hard to feel	Hard to feel	Somewhat hard to feel	Neutral (not easy, not hard)	Somewhat easy to feel	Easy to feel	Very Easy to feel

10. **Starting Position:** Put your hand in front of you about shoulder height as if you are about to push open a swinging door. Your fingers should be pointing upwards.

    Action: Extend your arm fully as if you are pushing open the door, keeping your fingers pointing upwards. Now let the swinging door close by returning your hand and arm to the starting position.

    Mental Task: Attempt to see yourself making the movement and rate the ease/difficulty below.

1	2	3	4	5	6	7
Very Hard to feel	Hard to feel	Somewhat hard to feel	Neutral (not easy, not hard)	Somewhat easy to feel	Easy to feel	Very Easy to feel

11. **Starting Position:** While sitting with your hands on your lap, pretend you see a drinking glass on the table in front of you.

    Action: Reach forward, grasp the glass and lift it off the table to take a sip. Put the glass down and return your hand to the starting position.

Mental Task: Attempt to see yourself making the movement and rate the ease/difficulty below.

1	2	3	4	5	6	7
Very Hard to feel	Hard to feel	Somewhat hard to feel	Neutral (not easy, not hard)	Somewhat easy to feel	Easy to feel	Very Easy to feel

12. **Starting Position:** You are standing with the hands on your side. Imagine there is a closed door in front of you.

Action: Reach forward, grasp the door handle and pull open the door. Then let go of the handle and return your arm to your side.

Mental Task: Assume the starting position then imagine seeing yourself opening the same door. Rate below.

1	2	3	4	5	6	7
Very Hard to feel	Hard to feel	Somewhat hard to feel	Neutral (not easy, not hard)	Somewhat easy to feel	Easy to feel	Very Easy to feel